universität
wien

DIPLOMARBEIT

Titel der Diplomarbeit

Characterization of Cellular Membranes under Conditions of Ether Lipid Deficiency

Verfasser

Fabian Dorninger

angestrebter akademischer Grad

Magister der Naturwissenschaften (Mag.rer.nat.)

Wien, 2011

Abstract

Ether lipids form a specialized class of lipids that are characterized by an O-alkyl bond at the sn-1 position of their glycerol backbone. The initial steps of their biosynthesis take place in the peroxisome. Among ether lipids, plasmalogens take on a dominant role. They perform important physiological functions, for example as constituents of cellular membranes or as scavengers of radicals. In humans, the lack of ether lipids, evoked by genetic defects concerning peroxisomal enzymes crucial for their biosynthesis, causes a fatal disease, rhizomelic chondrodysplasia punctata (RCDP). Recent research has also identified a subpopulation of glycosylphosphatidylinositol (GPI) anchors, a posttranslational modification that targets proteins to the outer surface of the cell membrane, as an ether lipid. Proteins associated with the membrane by GPI anchorage are recruited to specialized domains called membrane rafts, tightly packed assemblies, which are also enriched in plasmalogens. These microdomains constitute important platforms for various cellular processes like signal transduction or membrane trafficking. Thus, ether lipids might in many respects be essential for membrane composition. However, the exact role of these lipids in membranes and membrane subdomains has not yet been elucidated.

In the present study, the use of human RCDP fibroblasts with major and minor amounts of residual plasmalogens allows for a comprehensive description of cellular responses to complete or partial depletion of ether lipids. Nano-electrospray ionization mass spectrometric analysis of these primary cultured human fibroblasts (performed in cooperation with the Heidelberg University Biochemistry Center) shows that the cells compensate for the loss of plasmalogens by increasing the synthesis of other phospholipids, namely phosphatidylethanolamines, which share the head group (ethanolamine) with the majority of plasmalogens. Supplementation of ether lipid-deficient cultures with plasmalogen precursors that already contain an ether linkage circumvents the peroxisomal steps of ether lipid synthesis. Interestingly, the resulting rescue of plasmalogen levels causes a corresponding decline in phosphatidylethanolamines, so that the amount of total ethanolamine phospholipids is kept constant in every circumstance. In addition, using immunofluorescence microscopy, the present study offers the proof that an O-alkyl chain is not necessarily required for the membrane anchoring of Thy-1, a GPI-anchored protein. However, sucrose density gradient centrifugation suggests a reorganization of membrane rafts upon depletion of ether lipids. Furthermore, some raft proteins, amongst others GPI-anchored proteins, exhibit changed amounts in western blot analysis and show an altered floating behavior in a density gradient. Additionally, preliminary experiments in murine myoblast cultures derived from ether lipid-deficient mice point to differences in the formation of the neuromuscular junction under conditions of ether lipid deficiency, which might also be a result of changed membrane properties.

Summarizing, in spite of compensatory mechanisms employed by human fibroblasts in response to ether lipid deficiency, a variety of changes, especially concerning cellular membranes, can be detected under these conditions. Owing to the importance of raft domains in several cellular activities, changed rafts might cause severe impairments in a multicellular organism, one of which could be the altered formation of the neuromuscular junction. Thus, the present findings suggest a crucial role of ether lipids in membrane raft composition and offer first insights into serious functional consequences in response to the depletion of these molecules.

Kurzfassung

Etherlipide bilden eine Klasse von Lipiden, die sich durch ihre O-Alkyl-Bindung an der sn-1-Position ihres Glycerin-Rückgrats auszeichnen und deren erste Biosyntheseschritte im Peroxisom ablaufen. Plasmalogene, die wichtigsten Etherlipide, haben große physiologische Bedeutung, zum Beispiel als strukturgebende Moleküle in der Zellmembran oder als Radikalfänger. Ein Mangel an Etherlipiden, der durch Mutationen in den entsprechenden peroxisomalen Enzymen hervorgerufen wird, führt im Menschen zu einer schweren Krankheit, rhizomelischer Chondrodysplasia punctata (RCDP). Neueste Forschungsarbeiten zeigten, dass auch eine Untergruppe der GPI-Anker, einer posttranslationalen Modifikation, die Proteine an der Außenseite der Zellmembran verankert, eine Etherbindung beinhaltet und damit vom peroxisomalen Biosyntheseweg abhängig ist. GPI-verankerte Proteine werden innerhalb der Membran in kleine Subdomänen, so genannte „membrane rafts", dirigiert. Letztere sind dicht gepackte Membranabschnitte, die auch besonders reich an Plasmalogenen sind und die eine entscheidende Rolle zum Beispiel in der Signaltransduktion spielen. Etherlipide dürften daher in mehrerlei Hinsicht entscheidend für den Aufbau von zellulären Membranen sein, jedoch sind ihre genaue Aufgabe und Wirkung noch unbekannt.

In der vorliegenden Arbeit werden unter Verwendung modernster Techniken primäre Hautfibroblasten von RCDP-Patienten mit größeren und kleinen Plasmalogen-Restmengen auf ihre Reaktion auf die Etherlipiddefizienz untersucht. Mittels Nano-Elektrospray-Ionisierungs-Massenspektrometrie (nano-ESI-MS) kann gezeigt werden, dass das Fehlen der Plasmalogene durch die erhöhte Synthese anderer Phospholipide, der Phosphatidylethanolamine, die die gleiche Kopfgruppe (Ethanolamin) wie ein Großteil der Plasmalogene besitzen, kompensiert wird. In Zellkultur kann der Defekt in der peroxisomalen Etherlipid-Biosynthese umgangen werden, indem Vorläufermoleküle mit bereits vorhandener Etherbindung dem Medium beigemengt werden. Interessanterweise reagieren Fibroblasten auf die vermehrte Bildung von Plasmalogenen bei Verfügbarkeit einer solchen Substanz mit einer Reduktion von Phosphatidylethanolaminen. Das weist darauf hin, dass die insgesamte Menge an Ethanolamin-Phospholipiden unter allen Umständen konstant gehalten wird. Weiters wird in dieser Arbeit mit Hilfe von Immunfluoreszenzmikroskopie bewiesen, dass – zumindest im Falle des GPI-verankerten Proteins Thy-1 – eine O-Alkyl-Kette in GPI-Ankern nicht zwingend für deren Membranassoziation erforderlich ist. Hingegen zeigt sich, dass die Menge an einzelnen Raft-Proteinen, unter anderem auch GPI-verankerten Proteinen, in Etherlipid-defizienten Zellen verändert ist. Die Rafts weisen zusätzlich ein im Vergleich zu Kontrollzellen verändertes Flotationsverhalten in einem Saccharose-Dichtegradienten auf. Als mögliche funktionelle Konsequenz dieser Veränderungen können leicht verkleinerte Acetylcholinrezeptor-Cluster bei der Enstehung der neuromuskulären Synapse in vitro an Hand von Myotuben, isoliert aus Etherlipid-defizienten Mäusen, nachgewiesen werden.

Alles in allem werden von Etherlipid-defizienten Zellen zwar kompensatorische Mechanismen eingesetzt; diese können aber Veränderungen der Zellmembran, besonders der „membrane rafts", nicht verhindern. Aufgrund der großen Bedeutung dieser Subdomänen ist es naheliegend, dass ihre Veränderung auch für den gesamten Organismus schwere Konsequenzen (wie vielleicht eine geänderte Bildung der neuromuskulären Synapse) nach sich zieht, was in dieser Arbeit gezeigt werden kann.

TABLE OF CONTENTS

ABBREVIATIONS

AA	Arachidonic acid
AChR	Acetylcholine receptor
AGMO	Alkylglycerol monooxygenase
AGPAT	Alkylglycerol-3-phosphate acyltransferase
AGPS	Alkylglycerone phosphate synthase
ANOVA	Analysis of variance
APC	Antigen-presenting cell
BA	Batyl alcohol
BSA	Bovine serum albumin
CD	Cluster of differentiation
CDP	Cytidine diphosphate
CHO	Chinese hamster ovary
CoA	Coenzyme A
Cx	Connexin
DAG	Diacylglycerol
DAPAT	Dihydroxyacetone phosphate acyltransferase (systematic name: GNPAT)
DHA	Docosahexaenoic acid
DHAP	Dihydroxyacetone phosphate
DMEM	Dulbecco's Modified Eagle Medium
dNTP	Deoxynucleotide triphosphate
DRM	Detergent-resistant membrane
ER	Endoplasmic reticulum
ESI	Electrospray ionization
EtOH	Ethanol
FBS	Fetal bovine serum
Flot	Flotillin
FUDR	Fluorodeoxyuridine
GlcNAc	N-Acetylglucosamine
GNPAT	Glyceronephosphate O-acyltransferase (alternative name of DAPAT)
GPI	Glycosylphosphatidylinositol
HDG	1-O-Hexadecyl-sn-glycerol
HDG-P	1-O-Hexadecyl-2-hydroxy-sn-glycero-3-phosphate
HRP	Horseradish peroxidase
HS	Horse serum
HPLC	High performance liquid chromatography
ko	knockout
MEF	Mouse embryonic fibroblast
MHC	Major histocompatibility complex
MuSK	Muscle specific kinase
NAD	Nicotinamide adenine dinucleotide
NADP	Nicotinamide adenine dinucleotide phosphate
NCAM	Neural cell adhesion molecule
NMJ	Neuromuscular junction
PAF	Platelet-activating factor

PBD	Peroxisome biogenesis disorder
PBS	Phosphate buffered saline
PC	Phosphatidylcholine
PCR	Polymerase chain reaction
PE	Phosphatidylethanolamine
PEX	Peroxin
PI	Phosphatidylinositol
PKC	Protein kinase C
PL-PC	Plasmenylcholine
PL-PE	Plasmenylethanolamine
PM	Plasmalogen
PS	Phosphatidylserine
PTS	Peroxisomal targeting signal
PUFA	Polyunsaturated fatty acid
RBC	Red blood cell
RCDP	Rhizomelic chondrodysplasia punctata
SDS	Sodium dodecyl sulfate
S.E.M.	Standard error of the mean
SM	Sphingomyelin
SNP	Single nucleotide polymorphism
TBST	Tris-buffered saline/Tween
TCR	T-cell receptor
TfR	Transferrin receptor
Thy-1	Thymus cell antigen 1
TOF	Tetralogy of Fallot
wt	Wild type

CHAPTER 1

INTRODUCTION

1.1 Peroxisomes

1.1.1 General Background

Peroxisomes are single-membrane-bound organelles that fulfill a large variety of functions in nearly all eukaryotic cells. Originally being described as "microbodies" in electron micrograph pictures (Rhodin, 1958), their importance in various metabolic processes was soon discovered: Peroxisomes play major roles in the metabolism of reactive nitrogen and oxygen species, which includes the detoxification of hydrogen peroxide, the biosynthesis of ether phospholipids, bile acids and docosahexaenoic acid, and the degradation of pipecolic, phytanic and very long-chain fatty acids. In addition, they are – to a certain extent – also involved in the metabolism of glyoxylate, amino acids and isoprenoids as well as the pentose phosphate pathway (Wanders and Waterham, 2006a). Not only have there been metabolic functions assigned to peroxisomes, very recently they have also been shown to offer signaling platforms for innate immune responses (Dixit et al., 2010).

The manifold functional importance of the peroxisome is additionally underlined by the fact that peroxisomal dysfunctions lead to severe inherited human disorders, which can be grouped into the peroxisome biogenesis disorders (PBDs) and the single peroxisomal enzyme/transporter deficiencies. PBDs involve 13 complementation groups with defects in different PEX genes[1], the best-studied one being Zellweger (or cerebrohepatorenal) syndrome, which is characterized by complete absence of peroxisomes leading to severe symptoms like craniofacial and eye abnormalities, neuronal migration defects and hepatomegaly. The disease inhibits normal development and affected children usually die within the first year of life (Steinberg et al., 2006; Wilson et al., 1986).
In patients suffering from peroxisomal single enzyme/transporter deficiencies, one of the metabolic pathways in the peroxisome is disrupted. Disorders range from defects in ether lipid biosynthesis (see chapter 1.2) or peroxisomal alpha- and beta-oxidation, for example X-linked adrenoleukodystrophy, the most common monogenetic peroxisomal disorder, to dysfunctions of glyoxylate metabolism (Wanders and Waterham, 2006b).

1.1.2 Peroxisomal Import

As peroxisomes do not contain any DNA themselves, proteins have to be imported post-translationally into the pre-existing organelle (Lazarow and Fujiki, 1985). The import of peroxisomal matrix proteins is a complex process; currently, two different peroxisomal targeting signals (PTS), utilizing distinct pathways, are known to enable the uptake of matrix proteins into the organelle:

---

[1] PEX genes encode peroxins, proteins that are essential for peroxisome biogenesis (Distel et al., 1996)

Introduction

In order for a protein to be imported into the peroxisome, a PTS motif has to be recognized by a soluble receptor protein in the cytosol.

Ø The most prevalent targeting sequence, the PTS1, consists of the tripeptide -SKL at the very carboxy terminus of a peroxisomal protein (Gould et al., 1989). In addition, many functional variants of this sequence exist (Brocard and Hartig, 2006).
PTS1 is recognized by its cytosolic receptor Pex5p[2], which is able to interact with the sequence via its six tetratricopeptide repeats in the C-terminal segment (Brocard et al., 1994).

Ø A comparably minor part of proteins utilizes the PTS2 pathway to be imported into peroxisomes. PTS2 has been identified as a conserved nonapeptide of the consensus sequence [R/K]-[L/V/I]-X_5-[H/Q]-[L/A]. It is located near the N-terminus of certain peroxisomal matrix proteins and – in contrast to PTS1 – is cleaved from the cargo protein after import (Swinkels et al., 1991).
The receptor for PTS2 is Pex7p, a member of the WD-40[3] protein family (Marzioch et al., 1994), which unlike Pex5p cannot act autonomously, but instead interacts with auxiliary proteins as for example PEX5L, the long variant of PEX5, in mammals (Braverman et al., 1998).

The two pathways converge at the outer face of the peroxisomal membrane, where the receptor-cargo complexes bind to a docking machinery consisting of Pex13p and Pex14p (and Pex17p in yeasts), which themselves form a complex with other peroxins (Pex8p, Pex2p, Pex10p, Pex12p), jointly constituting the "importomer" (Agne et al., 2003; Rayapuram and Subramani, 2006). Receptor and cargo are then translocated across the membrane in a fashion that has not been fully elucidated, and the matrix protein is released from its receptor (Lanyon-Hogg et al., 2010). The latter is then recycled back into the cytosol or destined for degradation by the proteasome through polyubiquitination (Platta et al., 2004). A summary of this complex process is depicted in Figure 1.

In addition to these two pathways, peroxisomal membrane proteins are imported by a different strategy, whose exact mechanism is currently still under debate (Ma and Subramani, 2009).

---

[2] This annotation refers to yeast proteins. The process, however, is accomplished in a similar fashion by mammalian homologs.
[3] This name indicates the length of approximately 40 amino acids and the terminating dipeptide consisting of tryptophan (W) and aspartic acid (D).
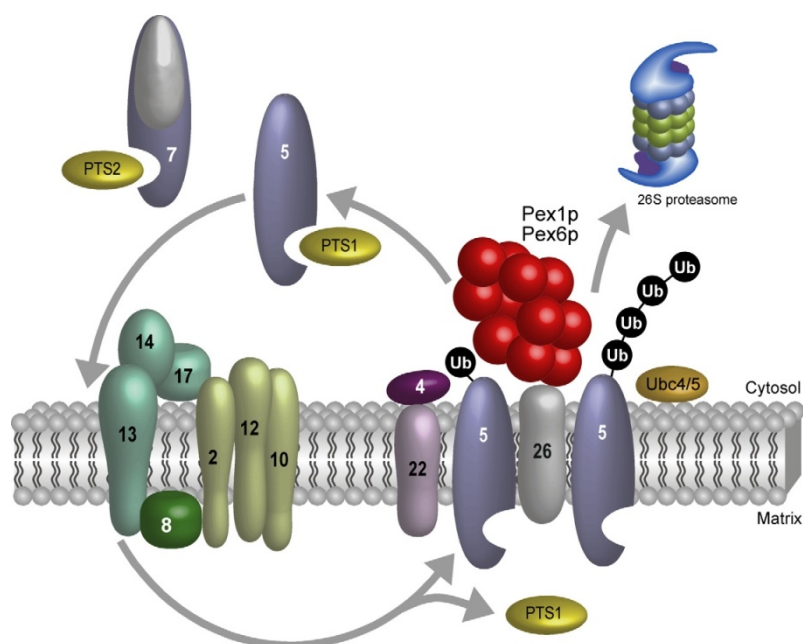
Figure 1: Import of proteins into the peroxisomal matrix (adapted from: Platta and Erdmann, 2007). PTS motifs in peroxisomal matrix proteins are recognized by the respective receptors (Pex5p for PTS1, Pex7p for PTS2) and the receptor-cargo complex is shuttled across the peroxisomal membrane. In the peroxisome lumen (= matrix), the cargo protein is released from its receptor. The latter is then ubiquitinated and recycled into the cytosol (in case of monoubiquitination) or degraded by the proteasome (in case of polyubiquitination).

1.2 Plasmalogens and the Group of Ether Lipids

One of the most important pathways taking place in the peroxisome is the biosynthesis of ether phospholipids, of which plasmalogens constitute by far the largest group.

Plasmalogens carry a glycerol backbone like other phospholipids (phosphatidylserine, -choline, -ethanolamine, etc.) and are characterized by a vinyl ether bond[4] – in contrast to the ester bond found in diacylglycerophospholipids – at the sn-1 position (for the structure of a classical plasmalogen species see Figure 2). The aliphatic moieties at the sn-1 position normally consist of C16:0, C18:0 or C18:1. In contrast, the sn-2 position is – especially in neurons – usually occupied by a polyunsaturated fatty acid (PUFA) of the n-6 or n-3 class (Han, 2005). At the sn-3 position, the glycerol backbone is linked via a phosphodiester bond to a head group, mainly ethanolamine or choline, although in rare cases also other species like inositol or serine have been described. Plasmalogens are therefore referred to as plasmenylethanolamines (PL-PE) or plasmenylcholines (PL-PC), respectively, whereas their ether linked counterparts, which do not harbor the characteristic vinyl bond, are named plasmanylethanolamines and -cholines. Plasmalogens have quite an unusual distribution in living organisms, as their existence has been shown in strictly anaerobic bacteria, but not in aerobic bacteria or fungi. However, in vertebrate and invertebrate animal species, plasmalogens are very common. The following paragraphs will focus on characteristics of plasmalogens and ether lipids in mammals, though keeping in mind that their biosynthetic pathway in bacteria differs from the one in animals (Goldfine, 2010).

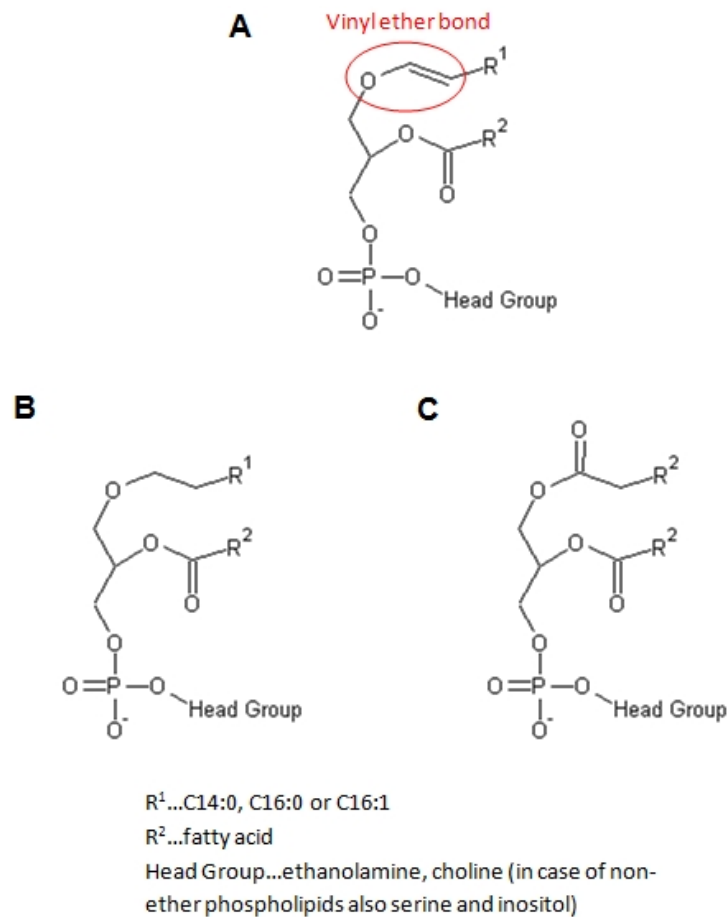[4] A cis double bond adjacent to the ether linkage

Introduction

Figure 2: Examples of phospholipid structures. (A) Plasmalogen (Plasmenyl-) (B) Non-plasmalogen ether phospholipid (Plasmanyl-) (C) Non-ether phospholipid (Phosphatidyl-). The vinyl ether bond is the main characteristic of plasmalogens.

The abundance of plasmalogens varies strongly between different tissues and cell types with the highest amounts being present in brain, heart, spleen, lymphocytes, macrophages and polymorphonuclear leukocytes as opposed to the liver, in which only 5% of the ethanolamine phospholipids are plasmalogens. The distribution of head groups differs as well: brain myelin is highly enriched in ethanolamine plasmalogens, whereas cardiac muscle has a high content of choline plasmalogens (Nagan and Zoeller, 2001).

Biosynthesis of plasmalogens involves several organelles and comprises a series of steps (for an overview see Figure 3), the first of which take place in the peroxisome. In the initial reaction catalyzed by the peroxisomal matrix protein dihydroxyacetone phosphate acyltransferase (DAPAT, DHAPAT; encoded by the GNPAT gene), dihydroxyacetone phosphate (DHAP) is esterified with a fatty acid supplied by acyl-CoA, thereby generating acyl-DHAP. Whether the substrates for the DAPAT-reaction, DHAP and acyl-CoA, are produced inside the peroxisome or shuttled into the organelle from the cytosol, is still unknown (Wanders and Brites, 2010). DAPAT is exclusively localized and stable within peroxisomes and is – as most other matrix proteins – targeted to the organelle by a PTS1 sequence (Jones and Hajra, 1977; Thai et al., 1997). In the subsequent biosynthetic step, the ether bond is introduced by the second enzyme in the pathway, alkylglycerone phosphate synthase (AGPS; also known as: alkyl-dihydroxyacetone phosphate synthase, ADHAPS; encoded by the AGPS gene) (Brown and Snyder, 1982; Hajra et al., 1988), using a long-chain fatty alcohol derived from dietary intake or generated at the outer face of the peroxisomal membrane (Burdett et al., 1991). AGPS has

been shown to be exclusively peroxisomal as well (Singh et al., 1993), forming a 210 kDa heterotrimeric complex with DAPAT in the peroxisomal matrix, which is essential for DAPAT stability (de Vet et al., 1999; Thai et al., 1997). In contrast to DAPAT, AGPS harbors a PTS2 guiding it to the peroxisome (de Vet et al., 1997). The last contribution of peroxisomes to the generation of ether lipids is the enzyme acyl/alkyl-dihydroxyacetone phosphate reductase, which can be bound either to the peroxisomal membrane or the endoplasmic reticulum (ER) facing the cytosol and catalyzes the reduction of the keto group at the sn-2 position (Datta et al., 1990). All subsequent biosynthetic steps take place in the ER: a fatty acid is esterified with the sn-2 position by alkylglycerol-3-phosphate acyltransferase (AGPAT), the ethanolamine head group is introduced by the sequential activity of a phosphohydrolase and an ethanolamine phosphotransferase and finally the vinyl ether bond is formed by the action of Δ1-alkyl desaturase (Brites et al., 2004). Plasmenylcholine is thought to be synthesized from plasmenylethanolamine via sn-2 and polar head group modifications (Lee et al., 1991).

As plasmalogens account for ~18% of the human phospholipid mass (Nagan and Zoeller, 2001), they have to be of great importance for the individual. However, the functions of these molecules have not yet been fully elucidated:

Ø As plasmalogens contain very high levels of PUFAs compared with their diacyl phospholipid counterparts, they can be seen as storage depots of docosahexaenoic acid (DHA) or arachidonic acid (AA) (Ford and Gross, 1989; Gaposchkin and Zoeller, 1999), which can only to a low extent be synthesized de novo by humans and are essential for brain development and cognitive function. The storage function of plasmalogens is underlined by the fact that DHA levels are reduced in patients lacking ether lipids (Martinez, 1992).

Ø Plasmalogens are involved in several signal transduction processes: A plasmalogen-selective phospholipase A_2 degrades plasmalogens (Hazen et al., 1990) releasing bioactive compounds like lysoplasmalogens, DHA and AA, the latter two being metabolized to eicosanoids, which serve as second messengers (Di Marzo, 1995; Yang et al., 1996). A role of plasmalogens in the regulation of protein kinase C (PKC) signaling has been proposed, as well (Nagan and Zoeller, 2001).

Ø Initially, protection from reactive oxygen species was thought to be the main task accomplished by plasmalogens (Zoeller et al., 1988). This antioxidative function is demonstrated by the fact that the vinyl ether bond is able to scavenge oxygen radicals (Reiss et al., 1997); protection against iron-induced peroxidation is conferred by plasmalogens, too (Sindelar et al., 1999). In addition, enhanced lipid peroxidation in membranes was observed in cells with reduced plasmalogen biosynthesis. However, data are conflicting, as the opinion has emerged that plasmalogen oxidation might also be harmful to the organism by creating highly reactive compounds itself (Felde and Spiteller, 1995). Lessig and Fuchs therefore suggest that "the description of plasmalogens as "antioxidants" should be treated with care" (Lessig and Fuchs, 2009).

Ø Plasmalogens serve as mediators of membrane dynamics and as important structural molecules of the plasma membrane (see also chapter 1.4). They have been shown to have a pronounced effect on membrane fluidity in a way that plasmalogen-containing membranes are less fluid and more ordered than membranes of plasmalogen-deficient cells (Hermetter et al., 1989). Besides, there is evidence for the fusogenic activity of plasmalogens (Glaser and Gross, 1994) suggesting a role of these molecules in membrane dynamics, e.g. in the course

of signal transduction or of synaptic transmission (Gorgas et al., 2006). This is also corroborated by the observation that human fibroblasts defective in ether lipid synthesis show impairments in the endocytotic cycle as well as changes in intracellular cholesterol homeostasis (Thai et al., 2001).
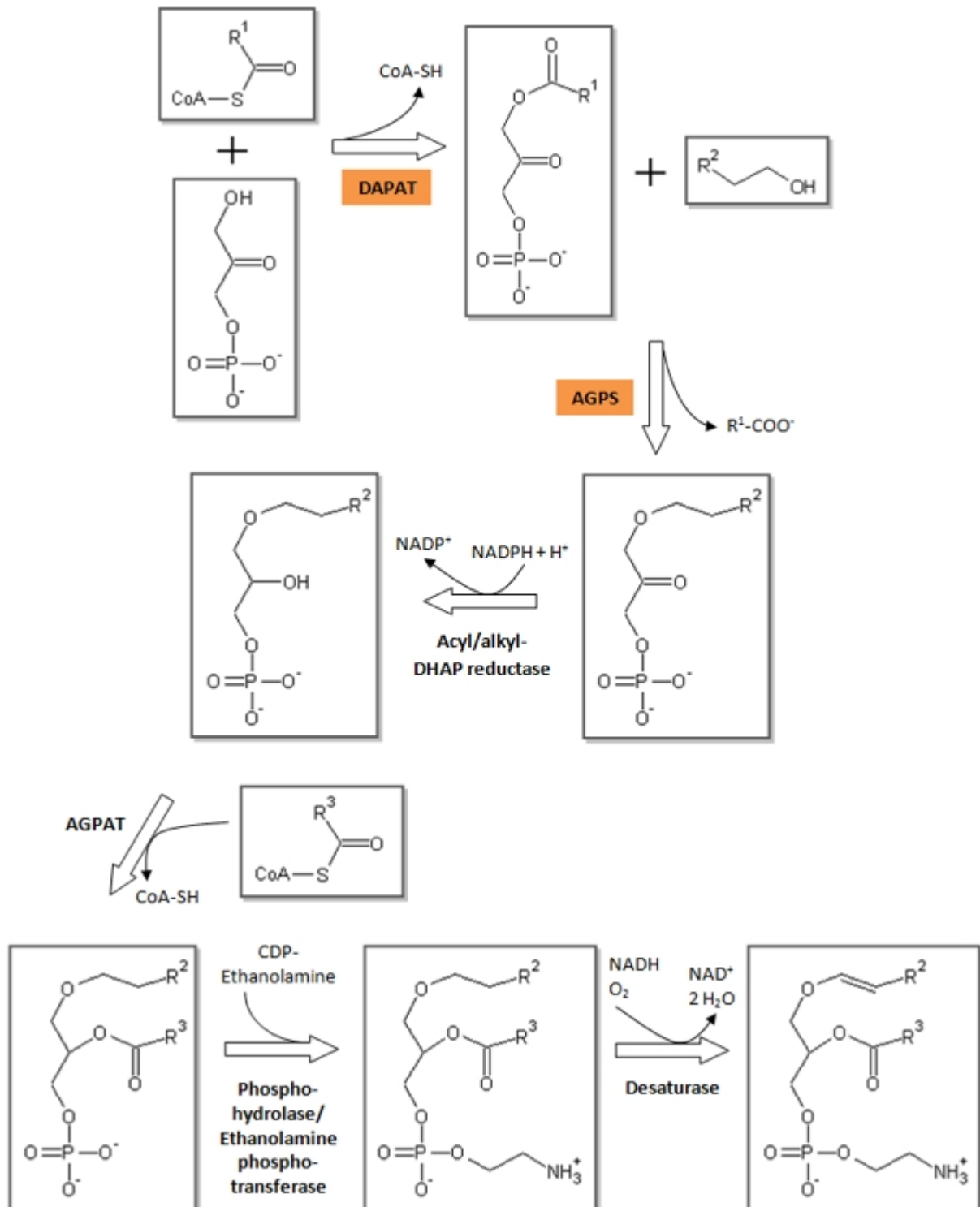
Figure 3: Biosynthesis of plasmalogens. The first two steps take place in the peroxisome, the corresponding enzymes are highlighted. Biosynthesis further proceeds at the outer peroxisomal or ER membrane and is finalized in the ER. DAPAT, dihydroxyacetone phosphate acyltransferase; AGPS, alkyl-dihydroxyacetone phosphate synthase; AGPAT, alkylglycerol-3-phosphate acyltransferase; CDP, cytidine diphosphate; NAD(P), nicotinamide adenine dinucleotide (phosphate); DHAP, dihydroxyacetone phosphate

Although plasmalogens constitute, by far, the most abundant group of ether lipids, there are other ether lipid molecules that follow the same biosynthetic pathway as plasmalogens:

Ø Platelet-activating factor (PAF; 1-O-alkyl-2-acetyl-sn-glycero-3-phosphocholine) is an important signaling molecule in inflammatory reactions and, additionally, serves as mediator in many further physiological as well as pathological processes (Prescott et al., 2000; Stafforini et al., 2003).

Ø Seminolipid, a sulfoglycolipid, makes up more than 90% of glycolipid in the testis and is a crucial factor in the process of spermatogenesis (Honke et al., 2004).

Ø Very recently, the lipid moiety of the GPI anchor was shown to be – at least in some proteins – an ether lipid as well (see chapter 1.3) (Kanzawa et al., 2009).

A role of ether lipids, especially plasmalogens, has been implicated in a variety of human diseases, mainly because of the fact that changes in plasmalogen levels have been reported e.g. in Alzheimer's disease (Han et al., 2001), Down syndrome (Murphy et al., 2000a), Niemann-Pick disease type C (Schedin et al., 1997) or ischemia (Ford et al., 1991). Not surprisingly, deficiency in ether lipid synthesis also accounts for some of the symptoms in various peroxisome biogenesis disorders. In addition, rhizomelic chondrodysplasia puncatata is a group of diseases that are mainly characterized by the loss of ether lipids and therefore highlight the importance of these lipids in the human body.

1.2.1 Rhizomelic Chondrodysplasia Punctata (RCDP)

Rhizomelic chondrodysplasia punctata is a rare, but very severe autosomal recessive disorder of peroxisome metabolism that affects around 1 in 100 000 individuals (Stoll et al., 1989). The clinical hallmarks of the disease include severe symmetrical shortening of proximal long bones (rhizomelia), bilateral cataracts, disturbed endochondral bone formation (chondrodysplasia punctata), severe contractures, cranial facial abnormalities as well as mental and growth retardation (Purdue et al., 1999; Steinberg et al., 2006). Death of affected infants usually occurs in childhood (mainly because of respiratory failure) with many children dying in the first year of life and only 50% of patients or even less surviving to the age of 6 years (Moser et al., 1996; White et al., 2003). The course of the disease can be heterogeneous; some RCDP patients with mild phenotypes have been reported (Braverman et al., 2002; Motley et al., 2002; Nuoffer et al., 1994).

All RCDP patients share a common biochemical feature, which is a defect in ether lipid biosynthesis, but can be grouped on a genetic basis as follows:

Ø RCDP type I, the most common subgroup, is caused by mutations in the PEX7 gene encoding peroxin 7 (PEX7, see chapter 1.1.2), which is the receptor for PTS2 containing proteins in humans (Braverman et al., 1997; Motley et al., 1997; Purdue et al., 1997). As a consequence of the genetic defect, proteins with a PTS2 – for example AGPS, one of the crucial enzymes in ether lipid biosynthesis – cannot be delivered to the peroxisome resulting in defects in ether lipid biosynthesis and the α-oxidation of phytanic acid and a mild impairment in the degradation of very long-chain fatty acids (Hoefler et al., 1988; Schutgens et al., 1993).

Ø Patients suffering from RCDP type II have a defect in DAPAT, the first enzyme in the ether lipid biosynthetic pathway, which leads to a complete inability to synthesize ether phospholipids. Phytanic acid levels were shown to be normal (Wanders et al., 1992).

> Ø RCDP type III is evoked by an isolated AGPS deficiency, due to which affected individuals cannot synthesize plasmalogens and other ether lipids (Wanders et al., 1994).

RCDP types II and III are extremely rare with only a few patients reported. However, the fact that they share all the clinical symptoms with RCDP type I points towards ether lipids as being fully responsible for the severe disease course in all subgroups.

1.2.2 Mouse Models of Ether Lipid Deficiency

Several mouse models have been generated that resemble human RCDP and are, therefore, valuable tools in the elucidation of the molecular mechanisms, in which plasmalogens and ether lipids are involved.

In 2003, the characterization of a DAPAT knockout (ko) mouse model was reported by Rodemer and collaborators (Rodemer et al., 2003). This mouse is viable, but it exhibits a striking phenotype due to its inability to synthesize ether lipids. Males are infertile because of an impairment in blood-testis barrier formation (Komljenovic et al., 2009). The mice show growth reduction and a high variability in lifespan with about 40% of pups dying within their first weeks of life. Other symptoms include ocular abnormalities with cataracts similar to those observed in RCDP, changes in membrane structure, and myelination defects in the cerebellum (Rodemer et al., 2003; Teigler et al., 2009).

In addition to the DAPAT knockout mouse, two different Pex7 mouse models have been established representing the severe and mild form of RCDP type I, respectively. The Pex7 knockout mouse is very severely affected with only 30% of pups surviving past the weaning period. Dwarfism, hypotonia, cataracts, neuronal migration defects and delayed endochondral ossification can be observed and adult mice are infertile (Brites et al., 2003).

The Pex7 hypomorphic mouse created by Braverman and collaborators produces residual levels of Pex7 transcript. These mice have a normal lifespan and are fertile, although plasmalogen levels are markedly reduced and the animals develop cataracts and dwarfism as observed in the complete knockout models of DAPAT and Pex7 deficiency (Braverman et al., 2010).

Several mouse models also of Zellweger syndrome exist (Baes et al., 1997; Faust and Hatten, 1997; Maxwell et al., 2003), in which plasmalogen deficiency definitely accounts for some of the observed defects. However, as individual symptoms cannot be assigned to the lack of ether lipids in these Zellweger mice, the mouse models described above constitute better tools to study plasmalogen and ether lipid functions.

1.3 GPI Anchor

1.3.1 General Background

In eukaryotic cells, there are many ways to modify proteins post-translationally. Several of these modifications, for example the addition of isoprenoids, fatty acids or cholesterol, aim at the attachment of proteins to membranes. Another type of lipid modification tethers proteins exclusively to the outer leaflet of the plasma membrane: the glycosylphosphatidylinositol (GPI) anchor. About 1% of all eukaryotic proteins and 10-20% of membrane proteins that enter the secretory pathway, have been reported to be attached to the membrane by a GPI anchor (Orlean and Menon, 2007).

However, this number is still increasing, as additional GPI-anchored proteins are identified. A wide variety of functions is fulfilled by these proteins, as for example cellular adhesion (by NCAM), signal transduction (by CD14) or intracellular protein sorting. Prominent examples of GPI-anchored proteins include the prion protein being famous as a trigger of Creutzfeldt-Jakob disease in humans, the complement regulators CD55 (decay-accelerating factor) and CD59, and a specific isoform of acetylcholinesterase, which plays an important role in synaptic transmission. The great importance of these proteins is further supported by the fact that an inability to synthesize GPI anchors is embryonically lethal in mammals (Kawagoe et al., 1996) and conditionally lethal in yeast (Leidich et al., 1994).

The structure of the GPI anchor is extraordinarily complex and diverse given that its only confirmed biological function is membrane attachment (Paulick and Bertozzi, 2008). Nevertheless, all anchors so far investigated share the following core structure (for illustration see Figure 4): An ethanolamine links the anchor via an amide bond to the C-terminus of the protein. Further elements of the core structure include a certain sequence of sugar residues and phosphatidylinositol (Ikezawa, 2002).
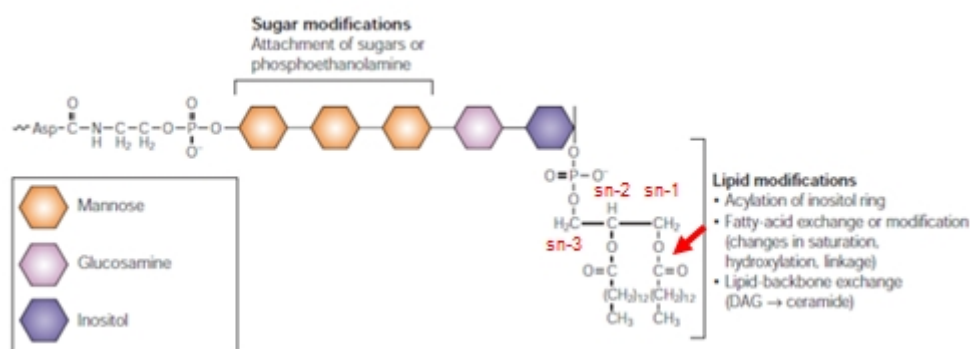

Figure 4: Core structure of the GPI anchor (adapted from: Mayor & Riezman, 2004). Potential sites of lipid and sugar modifications are displayed; the lipid moiety can consist of diacyl- (as depicted here) or alkylacylglycerol. The position of a possible ether bond (instead of the ester bond in the picture) is indicated by a red arrow. DAG, diacylgylcerol

Apart from this core structure, GPI anchors differ strongly from species to species according to their sugar modifications or lipid moieties (Fujita and Kinoshita, 2010). Although anchor structure has been extensively studied in S. cerevisiae or T. brucei as well, the work in the present thesis will exclusively focus on the mammalian GPI anchor.

Sugar modifications in mammals usually have a characteristic pattern and will not be discussed in this context. The lipid moiety, however, can appear in two different shapes; these are either diacylglycerol or 1-alkyl-2-acylglycerol (alkylacylglycerol). In the former case, the sn-1 and sn-2 positions of glycerol are occupied by, usually saturated, fatty acids (C16 or C18 at sn-1; C18 at sn-2) (Kinoshita et al., 2008) except in erythrocytes, where fatty acids of the 20:4 type have been reported at sn-2 (Deeg et al., 1992; Rudd et al., 1997). In the latter case, the sn-1 position is connected via an ether bond to the saturated carbon chain; hence, this molecule is a classical ether lipid. At the sn-3 position, a phosphate group links the lipid moiety to inositol and the residual anchor.

Although the existence of an ether bond in some GPI anchors has been known for quite a long time and the only known pathway of ether lipid biosynthesis involves the peroxisome (see chapter 1.2), the peroxisome dependency of GPI anchor biosynthesis has been under debate until 2009, when the absence of alkylacylglycerol containing GPI anchors in DAPAT-deficient CHO cells was shown

Introduction

(Kanzawa et al., 2009). The latter finding led to a revision of the model for biosynthesis of GPI anchors (cf. Figure 5):

The first steps of the pathway take place at the cytoplasmic face of the ER membrane, where N-acetylglucosamine (GlcNAc) is added to the starting product phosphatidylinositol (PI) and later de-N-acetylated. By a not clearly defined mechanism, the resulting GlcN-PI flips to the luminal side of the ER membrane, where a palmitoyl chain is esterified with the inositol part. This is, where peroxisomes and the ether lipid synthesis pathway come into play: The lipid moiety of the GPI-precursor, which is almost exclusively diacylglycerol (Houjou et al., 2007), is then hypothesized to be exchanged to diradyl-PI[5] consisting of a mixture of alkylacyl-PI and diacyl-PI. The alkylacyl moiety of GPI anchors has been proven to be derived from the peroxisomal ether lipid pathway (Fujita and Kinoshita, 2010; Kanzawa et al., 2009). After this lipid substitution, which is thought to be mediated by a phospholipase C or D member (Kanzawa et al., 2009), different sugar moieties and phosphatidylethanolamine side chains are added to the precursor in a sequential manner. At this point, the immature GPI anchor is transferred to the protein, which is destined for GPI-anchoring by the presence of a certain signal peptide (Caras et al., 1987). Directly thereafter, GPI biosynthesis is finalized by some remodeling steps partly in the ER, partly after transport of the GPI-protein to the trans-Golgi network: The acyl chain is removed from the inositol ring, a process that has been shown to be crucial for GPI anchor functioning and therefore survival in mammals (Ueda et al., 2007). In addition, the glycan moiety is slightly modified and the unsaturated fatty acid at the sn-2 position of glycerol, which is derived from the original PI molecule, exchanged for a saturated one (Fujita and Kinoshita, 2010).

So far, the biological significance of the ether bond in the GPI lipid moiety is not known. However, many mammalian GPI-anchored proteins analyzed show a considerable proportion of alkylacylglycerol in their lipid moiety (Redman et al., 1994; Roberts et al., 1988; Rudd et al., 1997; Walter et al., 1990). From this, the justified question arises, why the cell would involve an additional organelle, namely the peroxisome, in the complex process of GPI biosynthesis, if it was not of utmost importance.

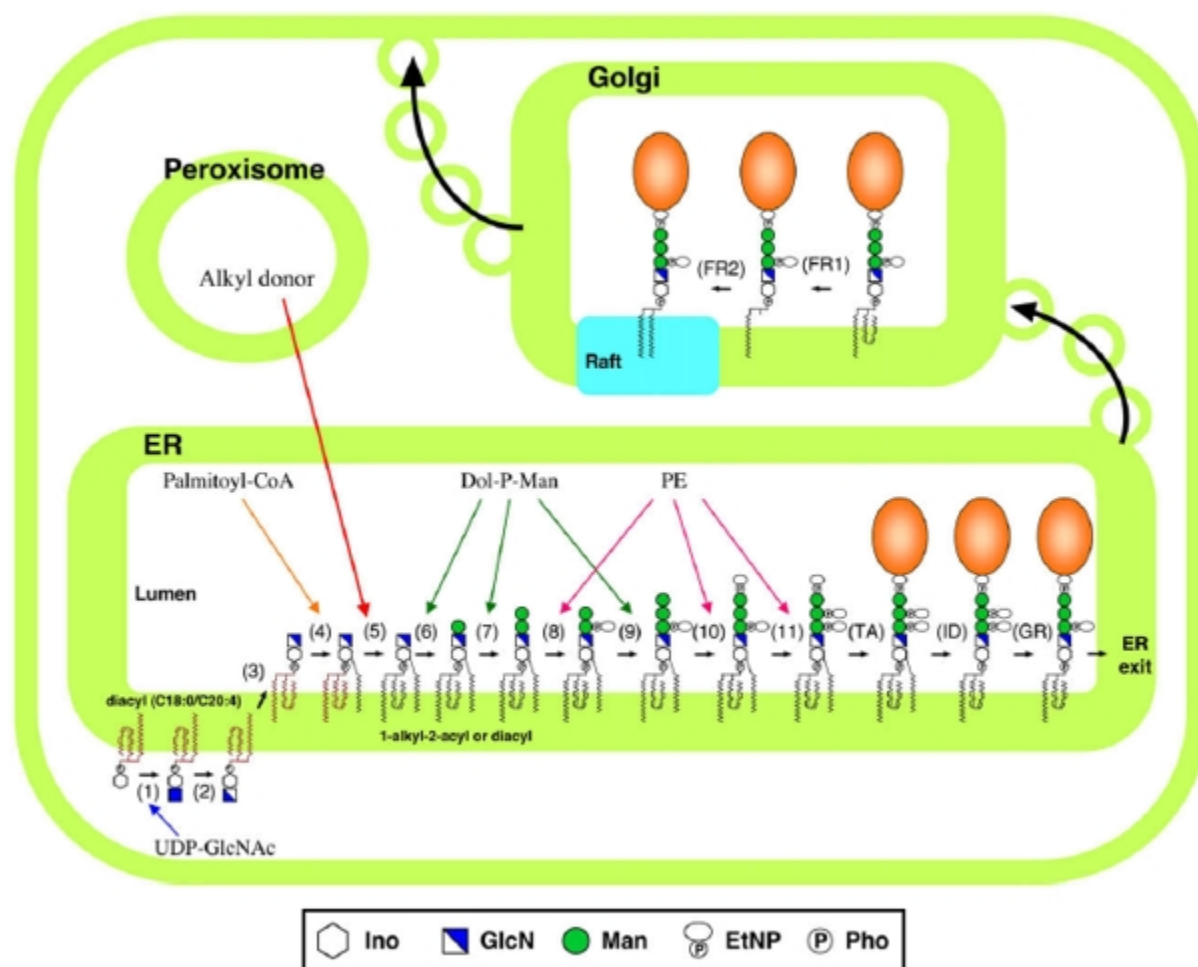[5] Radyl- indicates any acyl-, alkyl- or alkenyl- group.

Figure 5: Biosynthesis of a GPI anchor. Step (5) constitutes the potential insertion of the ether lipid derived from a peroxisomal precursor. TA, transamidation; ID, inositol deacylation; GR, glycan remodeling; FR, fatty acid remodeling; EtNP, ethanolamine phosphate; GlcN, glucosamine; GlcNAc, N-acetylglucosamine; Dol-P-Man, dolichol-phosphate-mannose; PE, phosphatidylethanolamine (adapted from: Fujita and Kinoshita, 2010)

1.3.2 Thy-1 (CD90)

Thymus cell antigen 1 (Thy-1, CD90), a small member of the immunoglobulin superfamily, was used as a "reference" GPI-anchored protein in the course of this study. It is expressed in a variety of different cell types including fibroblasts and (in humans preferentially adult) neurons as well as murine, but not human, T lymphocytes (Pont, 1987), where it is the most abundant glycoprotein (Haeryfar and Hoskin, 2004). As the latter term indicates, Thy-1 is heavily glycosylated with a carbohydrate content of up to 30% of its molecular mass in mice (Pont, 1987). The GPI anchor of the protein has been reported to contain alkylacylglycerol in its lipid moiety in rat brain (Homans et al., 1988).

In mice, important immunological functions are attributed to Thy-1; upon formation of the immunological synapse it can, by binding to a ligand on the surface of an antigen-presenting cell (APC), provide a costimulatory signal for T cell activation in the presence of a T cell-receptor (TCR)/MHC complex. Alternatively, in the absence of TCR, Thy-1 can itself induce T cell activation, even though these activated T cells do not exhibit any cytotoxic effector function (Haeryfar and Hoskin, 2004). In humans, Thy-1 is involved in widespread non-immunological processes like neurite

outgrowth, apoptotic signaling, cell adhesion and migration, tumor suppression and fibroblast proliferation. From a clinical point of view, the manifold regulatory and signaling functions of Thy-1 render it an interesting molecule in disease-related pathways as for example wound healing, cancer metastasis or nerve regeneration (Rege and Hagood, 2006).

1.4 Membrane Rafts

1.4.1 General Background

Cellular membranes are generally known to form liquid-disordered bilayers, in which proteins and lipids are able to move freely and lipids mainly serve as solvent for membrane proteins (Singer and Nicolson, 1972). However, already more than ten years ago, the existence of more ordered, tightly packed and highly dynamic membrane assemblies of specific lipid composition was described (Simons and Ikonen, 1997). The presence of these domains, which were originally named "lipid rafts", has been questioned for a long time (Munro, 2003), but now strong support has emerged for the concept and the existence of "membrane rafts" – as they are termed now – is generally accepted. Many attempts had been made to characterize and define membrane rafts, until, in 2006, the following definition was agreed upon by the experts in the field: "Membrane rafts are small (10-200 nm), heterogeneous, highly dynamic, sterol- and sphingolipid-enriched domains that compartmentalize cellular processes. Small rafts can sometimes be stabilized to form larger platforms through protein-protein and protein-lipid interactions." (Pike, 2006)
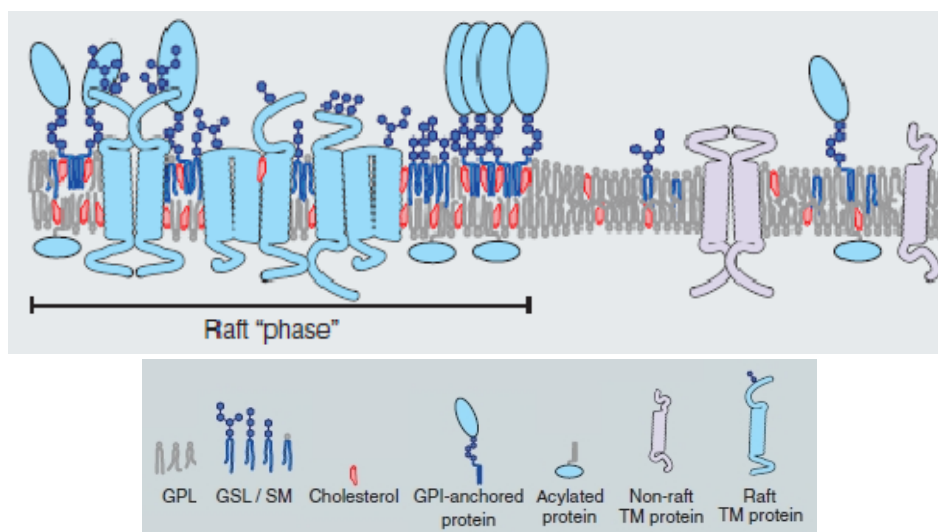
Figure 6: Model of the ordered structure of a membrane raft. GPL, glycerophospholipid; GSL, glycosphingolipid; SM, sphingomyelin; TM, transmembrane (adapted from: Lingwood and Simons, 2010)

As already indicated by the definition, membrane rafts exhibit a lipid and protein composition that distinguishes them from the liquid-disordered phase. Regarding lipids, the outer raft leaflet is mainly made up of sphingolipids and cholesterol, while the cytoplasmic leaflet contains mostly cholesterol and phospholipids (see Figure 6). In addition, also arachidonic acid and plasmenylethanolamine (see chapter 1.2) are enriched in membrane rafts isolated from human epidermal carcinoma cells (Pike et al., 2002). Generally, saturation level and chain length in lipid molecules are said to be higher in rafts compared with non-raft membranes, which accounts for the tight packing of the domains (Brown

and London, 1998). Similar to lipids, proteins are not equally distributed in the plasma membrane, either. Although some membrane spanning proteins, which are preferentially targeted to membrane rafts, have been identified – as for example members of the connexin family (Schubert et al., 2002) –, the hypothesis has arisen that mainly proteins with specific lipid modifications associate with rafts (Leventhal et al., 2010). Among these molecules, GPI-anchored proteins (see chapter 1.3) hold a dominant position; the GPI anchor is presumed to constitute a sorting determinant already in the Golgi network (Brown and Rose, 1992). The length of the anchor has been shown to be critical for protein association with membrane rafts (Benting et al., 1999). Additional lipid modifications conferring raft preference to proteins include N-terminal myristoylation, cysteine acylations, isoprenylations and C-terminal sterol moieties (Leventhal et al., 2010).

Generally, membrane rafts are thought to compartmentalize biological processes at the plasma membrane (and possibly also at other cellular membranes). More precisely, important cellular activities are mediated by these domains such as signal transduction, membrane trafficking and protein sorting (Jacobson et al., 2007; Mayor and Rao, 2004). From a disease-relevant point of view, rafts serve as platforms that enable virus entry, assembly and budding (Chazal and Gerlier, 2003).

One reason, why the existence of membrane rafts was denied by many researchers for a long time, is the fact that they cannot be visualized by classical microscopy techniques. Due to their small size and their high turnover rate, advances have to be made to enable the examination of rafts with microscopic tools (Jacobson et al., 2007). However, other concepts and methods, one of which is introduced in the following chapter, have been developed to study raft biochemistry and functioning.

1.4.2 Detergent-Resistant Membranes (DRMs)

A key feature of membrane rafts is their detergent insolubility, which is a consequence of the interactions of saturated acyl chains (Schroeder et al., 1994). Upon exposure to Triton X-100 at 4 °C, rafts do not solubilize and float to a characteristic density following equilibrium density gradient centrifugation (see also Figure 7) (Lingwood and Simons, 2007). According to the biological question to be answered, variable detergents with different solubilization properties are used (Schuck et al., 2003). Although the isolation of detergent-resistant membranes (DRMs) is still the method of choice for determining affinity of lipids or proteins for membrane rafts, concerns have emerged about the artifacts produced by this method: First of all, DRM isolation is usually done at 4 °C, which might provoke lipid-protein associations that do not take place in vivo at growth temperature. Additionally, detergent treatment itself could induce – to a certain extent – membrane rearrangement or solubilize lipids that are known parts of membrane rafts (Quinn, 2010).

In spite of these drawbacks, DRM isolation is a widely accepted tool to study raft biology. Detergent-free raft isolation procedures have been proposed (Shah and Sehgal, 2007; Smart et al., 1995), but never became the method of choice for most research questions. Furthermore, many of the major breakthroughs in the raft field originated from observations of changes in DRM association (Lingwood and Simons, 2007). However, one should always keep in mind that DRMs cannot be equated with membrane rafts and results of DRM isolation experiments have to be interpreted with caution, although important hints can be gained by these efforts.

1.5 Aims of the Study

As can be deduced from the introduction of this work, ether lipids constitute an essential part of mammalian cells. Many functions have been assigned to them, but still the involvement of these phospholipids in various cellular processes has to be elucidated. Additionally, lack of ether lipids causes the severe human disease RCDP, for which – at the moment – there is no cure. Accordingly, the main focus of this thesis was on ether lipid functions in mammalian, more precisely, in murine and human, tissue.

Depletion of plasmalogens constitutes a major problem for mammalian cells. Therefore, my thesis should clarify how cells react to such conditions and how they can compensate for the loss of these lipids. Another major goal was the evaluation of substances proposed for treatment of RCDP in cell culture and the response of plasmalogen-deficient cells to these compounds.

Ether lipids form important constituents of cellular membranes, especially of small subdomains called membrane rafts (Pike et al., 2002). The latter should be hit by ether lipid deficiency from two different sides: Firstly, membrane rafts contain high amounts of plasmalogens, the major class of ether lipids; and secondly, GPI-anchored proteins, a main protein species in rafts, cannot incorporate alkylacylglycerol into their lipid moiety under conditions of ether lipid deficiency. Therefore, my thesis was intended to shed light on the consequences of ether lipid absence for rafts and GPI-anchored proteins. Furthermore, the role and importance of ether lipids in cellular membranes should be elucidated.

Finally, RCDP patients as well as ether lipid-deficient mice exhibit severe motor deficiency, the origin of which is not clearly defined. With the help of the DAPAT ko mouse, a part of my diploma thesis was designed to study whether a defect in neuromuscular junction formation could account for the observed motor symptoms.

Summarized, the present study was conceptualized to expand the current understanding of the functions and the role of ether lipids in mammals, eventually aiming at clarifying the molecular basis of the symptoms seen in RCDP and on possible treatment strategies for this disease.

CHAPTER 2
MATERIALS AND METHODS

2.1 Materials

2.1.1 Chemicals

Standard chemicals were purchased from Merck or Sigma-Aldrich.

Acrylamide 4X, Gerbu Biochemicals
Ammonium persulfate, Merck
DL-Batyl alcohol (99%), Sigma-Aldrich
Bisacrylamide 4k, Gerbu Biochemicals
Bovine serum albumin (BSA), Sigma-Aldrich
1-O-Hexadecyl-sn-glycerol (1-O-Palmityl-sn-glycerol), Alexis
1-O-Hexadecyl-2-hydroxy-sn-glycero-3-phosphate (ammonium salt), Avanti Polar Lipids Inc.
EDTA (ethylene diamine tetraacetic acid) disodium salt dihydrate, AppliChem
EGTA (ethylene glycol tetraacetic acid), Sigma-Aldrich
Ethidium bromide, Bio-Rad
5-Fluoro-2′-deoxyuridine, Sigma-Aldrich
Formaldehyde 37%, Merck
Gelatin from porcine skin type A, Sigma-Aldrich
Imidazole, Sigma-Aldrich
β-Mercaptoethanol, AppliChem
Mowiol, Carl Roth
NP-40, Calbiochem
Paraformaldehyde, Merck
Ponceau S, Fluka
Sodium deoxycholate, Merck
Sodium dodecyl sulfate (SDS), Sigma-Aldrich
Sucrose, Sigma-Aldrich
N,N,N′,N′-Tetramethylethylenediamine (TEMED), Merck
Tris(hydroxymethyl)-aminomethane (Tris), Merck
Triton® X-100, Promega
Tween® 20, Merck
Urea, AppliChem
Uridine, Sigma-Aldrich

2.1.2 Enzymes, Kits and Special Materials

Amersham Hyperfilm™ ECL, GE Healthcare
cOmplete Protease Inhibitor Cocktail Tablets, Roche

Materials and Methods

Deoxyribonuclease II (DNAse II) from bovine spleen, Sigma-Aldrich
dNTPs (deoxynucleotide triphosphates), Peqlab
DirectPCR® Lysis Reagent (Tail), Peqlab
GoTaq® DNA Polymerase and Buffer, Promega
Immobilon™ Western Chemiluminescent HRP Substrate, Millipore
Kodak® GBX Fixer/Replenisher, Sigma-Aldrich
Kodak® GBX Developer/Replenisher, Sigma-Aldrich
Oligonucleotides, custom-made by Eurofins MWG Operon
PageRuler™ Prestained Protein Ladder, Fermentas
Protein Assay, Bio-Rad
Proteinase K, Peqlab
Protran® Nitrocellulose Transfer Membrane, Whatman
Recombinant Murine Interferon-gamma, PeproTech
Trypsin from bovine pancreas, Sigma-Aldrich
Whatman® Filter Papers, Whatman

2.1.3 Expendables

Corning® Bottle-Top Vacuum Filters, Sigma-Aldrich
Cover Slips 21x26 mm, Carl Roth
Falcon™ Cell Strainers, BD Biosciences
Injekt®-F Single Use Syringes, Braun
Microscope Slides 76x26 mm, Carl Roth
PrecisionGlide® Sterile Needles, BD Biosciences
Serological Pipettes, Sarstedt
Sterican® Hypodermic Needles, Braun
Tissue Culture Cell Scrapers, Sarstedt
Ultra-Clear™ Centrifuge Tubes, Beckman

2.1.4 Antibodies and Probes

Primary:
Monoclonal mouse anti-actin (clone C4), Chemicon®, Millipore
α-Bungarotoxin-Alexa Fluor® 594 conjugate, Molecular Probes™, Invitrogen
Polyclonal rabbit anti-CD55, GeneTex
Polyclonal rabbit anti-connexin 43/GJA1, Abcam
Monoclonal mouse anti-flotillin-1, BD Transduction Laboratories™, BD Biosciences
Polyclonal rabbit anti-Thy-1 (CD90), Epitomics
Monoclonal rat anti-Thy-1.2 (CD90) (clone 30-H12), Leinco Technologies
Monoclonal mouse anti-transferrin receptor (clone H68.4), Zymed®, Invitrogen

Secondary:
Goat anti-rabbit IgG (H+L) HRP (horseradish peroxidase) conjugate, Bio-Rad
Goat anti-mouse immunoglobulins (polyclonal) HRP conjugate, Dako
Goat anti-rat IgG (H+L) Cy3 conjugate, Amersham®, GE Healthcare
Donkey anti-rabbit IgG (H+L) Cy3 conjugate, Jackson ImmunoResearch

2.1.5   Laboratory Equipment

Casy®1 Cell Counter, Schärfe System
Cell Culture Incubators, Heraeus
Centrifuge 5415D, Eppendorf
DM IRB Inverted Microscope, Leica
Electrophoresis Power Supply E425, Consort
Fluovert Microscope, Leitz
Gel Doc™ 2000, Bio-Rad
GeneAmp 2400 PCR System, Perkin Elmer
Gene Power Supply GPS 200/400, Pharmacia
IX71 Inverse Fluorescence Microscope, Olympus
MAC-5000 Controller System, Visitron Systems
Megafuge 1.0, Heraeus
Mini-PROTEAN® 3 Electrophoresis System, Bio-Rad
MyCycler™ Thermal Cycler, Bio-Rad
Optima™ LE-80k Ultracentrifuge, Beckman
PHM92 Lab pH Meter, Radiometer Analytical
PowerPac™ 3000 Power Supply, Bio-Rad
PowerPac™ HC Power Supply, Bio-Rad
PowerShot SX20 IS Digital Camera, Canon
Quattro II Triple Quadrupole Mass Spectrometer, Micromass
Refrigerated Centrifuge 4K15, Sigma
Rota-Rod Treadmill for Mice No. 7650, Ugo Basile
Spot Xplorer™ Digital Camera, Diagnostic Instruments
Thermomixer comfort, Eppendorf
Trans-Blot® Semi-dry Electrophoretic Transfer Cell, Bio-Rad
UV-Visible Spectrophotometer U-2001, Hitachi
VBH Compact C2 Cell Culture Lamina Hood, Steril Manufacturing Division
Vortex-Genie™, Scientific Industries
Water Bath No. 1003, GFL
XM10 Digital Camera, Olympus

2.1.6   Software

ACD/ChemSketch 12.0, ACDLabs
Acrobat 9 Professional, Adobe
Cell^M Imaging Software, Olympus
CorelDraw Graphics Suite X4, Corel
EndNote X3, Thomson Reuters
MetaMorph Microscopy Automation & Image Analysis Software 7.0, Molecular Devices
Office 2007, Microsoft
Photoshop CS4, Adobe
PASW Statistics 17, SPSS Inc.
Quantity One 4.2.3, Bio-Rad
SigmaPlot 11.0, Systat Software

2.1.7 Cell Culture

DMEM (Dulbecco's Modified Eagle Medium) (with 4,5 g/l glucose; without L-glutamine), BioWhittaker®, Lonza
Fetal Bovine Serum (FBS), PAA
Fungizone, Gibco®, Invitrogen
L-Glutamine (in NaCl solution), BioWhittaker®, Lonza
Horse Serum (HS), PAA
PenStrep (10 000 U/ml penicillin, 10 000 µg/ml streptomycin), Gibco®, Invitrogen
Phosphate Buffered Saline (PBS), BioWhittaker®, Lonza
RPMI 1640 (without L-glutamine), BioWhittaker®, Lonza
Trypsin EDTA, BioWhittaker®, Lonza

CELLSTAR® Cell Culture Dishes and Flasks, Greiner Bio-One

2.1.8 Cells

Human RCDP fibroblast cell lines were obtained from Dr. Nancy Braverman (McGill University, Montreal) in the course of a collaboration. Control fibroblast lines were already available in the lab. DAPAT knockout and corresponding wild type mouse fibroblast cell lines were received from Prof. Dr. Wilhelm Just (Heidelberg University Biochemistry Center).

Human fibroblast cell lines were cultivated in RPMI 1640 medium supplemented with 10% FBS (heat inactivated at 56 °C for 30 minutes), 1% PenStrep (50 U/ml penicillin, 100 µg/ml streptomycin), 2 mM L-glutamine and 0.5% fungizone. Mouse fibroblast cell lines were grown in DMEM medium with the same supplements. For splitting, cells were detached by incubation with 0.25% trypsin at 25-37 °C for 5-30 minutes and distributed to several dishes. Trypsin was inactivated by normal FBS concentrations. Splitting ratios were kept between 1:2 and 1:5. All cell lines were cultivated at 37 °C and a CO_2 concentration of 5%. Measurements were exclusively carried out between passages 5 and 30.

For plasmalogen precursor treatment studies, fibroblasts were supplemented with 20 µM hexadecylglycerol or batyl alcohol (each dissolved in ethanol; final ethanol concentration: 1%) for three subsequent days with medium changes every 24 hours. Thereafter, the cells were harvested and phospholipids determined as described below.

All studies involving human patient fibroblasts were approved without restrictions by the Ethical Review Board at the Medical University of Vienna (application number: 729/2010).

2.1.9 Mice

DAPAT knockout mice (outbred C57BL/6 x CD1) were originally received from the laboratory of Prof. Dr. Wilhelm Just (Heidelberg University Biochemistry Center), where these mice have been generated (Rodemer et al., 2003), and maintained at the local animal housing facility of the Medical University of Vienna. Issues concerning the regulations for the use of genetically modified animals were resolved and experiments involving these animals approved (BMWF-5.011/0003-II/10b/2009).
Mice were fed standard mouse chow with food and water ad libitum and were housed in a temperature- and humidity-controlled room with 12:12 hour light-dark cycle and a constant low level of acoustic background noise.

All animals received humane care in compliance with the Principles of Laboratory Animal Care (National Society for Medical Research) and the Guide for the Care and Use of Laboratory Animals, prepared by the National Academy of Sciences and published by the National Institutes of Health (NIH Publication No. 86-23, revised 1985).

2.2 Methods

2.2.1 Preparation of Cellular Membranes

The desired number of cells (5-20 dishes of 10 cm diameter) was grown to confluency, washed twice with sterile phosphate buffered saline (PBS) and scraped into homogenization buffer with 1x protease inhibitor. Cells were homogenized by 2 passages through a 23 G (gauge), and 3 passages each through a 25 G and a 27 G needle. Subsequently, nuclei and unbroken cells were pelleted by centrifugation at 5,700xg, 4 °C for 15 minutes and the postnuclear supernatant was transferred to an ultracentrifuge tube (Ultra-Clear Tube 14x95 mm). Ultracentrifugation was carried out at 100,000xg (23,800 rpm), 4 °C for 30 minutes in an SW 40 Ti rotor (Beckman). The resulting membrane pellet was resuspended in 10 μl/10^6 cells RIPA buffer with 1x protease inhibitor and stored at -20 °C or -80 °C.

Homogenization buffer: 250 mM sucrose, 3 mM imidazole, 1 mM EDTA; pH 7.4
25x protease inhibitor: 1 cOmplete Protease Inhibitor Cocktail Tablet in 2 ml dH$_2$O[6]
RIPA buffer: 50 mM Tris-Cl (pH 7.5), 150 mM NaCl, 1 mM EDTA, 1 mM EGTA, 1% NP-40 (vol/vol), 1% sodium deoxycholate (wt/vol), 0.1% sodium dodecyl sulfate (SDS) (wt/vol)

2.2.2 Preparation of Total Protein Extracts

The desired number of cells (~1 confluent 10 cm dish) was washed twice with sterile PBS and scraped into 1 ml/10^6 cells ice-cold RIPA buffer with 1x protease inhibitor. Cells were homogenized by 3 passages through a 27 G needle on ice and the homogenate was centrifuged at 16,100xg, 4 °C for 20 minutes in a tabletop centrifuge. The resulting supernatant was stored at -20 °C.

RIPA buffer: 50 mM Tris-Cl (pH 7.5), 150 mM NaCl, 1 mM EDTA, 1 mM EGTA, 1% NP-40 (vol/vol), 1% sodium deoxycholate (wt/vol), 0.1% SDS (wt/vol)
25x protease inhibitor: 1 cOmplete Protease Inhibitor Cocktail Tablet in 2 ml dH$_2$O

2.2.3 Isolation of Detergent-Resistant Membranes (DRMs)

Preparation of DRMs was basically performed as described by Lingwood & Simons (Lingwood and Simons, 2007). The whole isolation procedure was carried out on ice (harvesting of cells) or at 4 °C in a refrigerated room (residual steps).

The desired number of cells (~20 dishes of 10 cm diameter) was grown to confluency, washed once with sterile PBS and once with TNE and scraped into TNE buffer. Cells were pelleted by centrifugation at 400xg, 4 °C for 5 minutes and the pellet resuspended in 550 μl TNE supplemented with 1x protease inhibitor. Subsequently, the cells were homogenized by 25 passages through a 25 G needle. To 500 μl of the homogenate, 500 μl of TNE/protease inihibitor + 2% Triton X-100 (vol/vol) were

---

[6] dH$_2$O refers to deionized water.

added and the mixture was incubated on ice for 30 minutes. The sample was adjusted to 40% sucrose/TNE (wt/wt) by addition of 2 ml 56% sucrose/TNE (wt/wt), transferred to the bottom of an ultracentrifuge tube (Ultra-Clear Tube 14x95 mm) and overlaid with 8.5 ml 35% sucrose/TNE (wt/wt) and 0.5 ml 5% sucrose/TNE (wt/wt). Ultracentrifugation was carried out at 271,000xg (39,000 rpm), 4 °C for 18 hours in an SW 40 Ti rotor (Beckman). One ml-fractions were collected from the top and analyzed by western blotting for presence of raft markers or stored at -20 °C. A scheme of the procedure is presented in Figure 7.

TNE buffer: 150 mM NaCl, 2 mM EDTA, 50 mM Tris-Cl (pH 7.4)
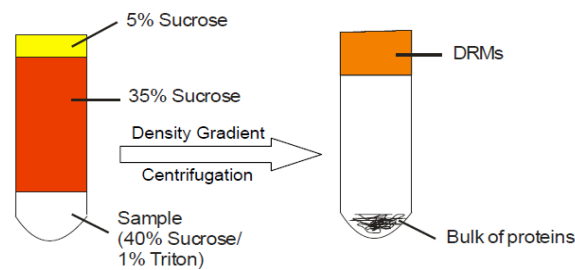25x protease inhibitor: 1 cOmplete Protease Inhibitor Cocktail Tablet in 2 ml dH$_2$O

Figure 7: Principle of DRM isolation. After Triton lysis, DRMs float to the lightest fractions of a sucrose gradient during centrifugation and can be separated from residual cellular material.

2.2.4 Determination of Protein Concentration

Protein samples were diluted to 100 µl with dH$_2$O and subsequently mixed with 1 ml pre-diluted Protein Assay reagent (final concentration 1:5). After 10 minutes incubation for dye color development, absorption at 595 nm was measured in a spectrophotometer. Standard curves were established by using BSA samples with protein concentrations ranging from 0 to 10 µg.

2.2.5 SDS Polyacrylamide Gel Electrophoresis (SDS-PAGE)

Protein samples were diluted to an appropriate volume with dH$_2$O and supplied with SDS sample buffer followed by heating at 85-99 °C (temperature according to protein of interest) for 10 minutes and centrifugation at 16,100xg, room temperature for 30 seconds to remove insoluble material. To enhance protein solubilization, urea was added to selected samples at a final concentration of 1 M prior to heating. Samples were applied to SDS gels of either 0.75 mm or 1.5 mm thickness. Separation was done at a constant current of 30 mA (0.75 mm gels) or 50 mA (1.5 mm gels), for 1-2 hours depending on sizes of the proteins to be detected (settings apply for two gels in one electrophoretic chamber of the Mini-PROTEAN® 3 system, Bio-Rad).

Acrylamide working solution: 30% acrylamide (wt/vol) , 0.8% bisacrylamide (wt/vol)
Polyacrylamide separation gel (12%; amount of acrylamide can be adapted): 12% acrylamide, 20% 1.5 M Tris-Cl (pH 8.8), 0.1% SDS, 0.15% TEMED, 0.5% APS; covered with a layer of isopropanol until polymerized
Polyacrylamide stacking gel: 4% acrylamide, 12.5% 1 M Tris-Cl (pH 6.8), 0.1% SDS, 0.15% TEMED, 0.5% APS

4x SDS sample buffer: 250 mM Tris-Cl (pH 6.8), 8% SDS (wt/vol), 40% glycerin (vol/vol), 20% β-mercaptoethanol (vol/vol), 0.008% bromophenol blue (wt/vol)
SDS running buffer: 2.5 mM Tris, 25 mM glycine, 0.1% SDS (wt/vol)

2.2.6   Western Blot

After SDS-PAGE, the gels were washed with water and equilibrated in blotting buffer. Sandwiches for semi-dry blotting were prepared as follows (all materials were pre-wet in blotting buffer): 3 sheets of Whatman paper (thickness: 3 mm; size: 8.5x5.5 cm) were put at the bottom of the Trans Blot Electrophoretic Transfer Cell followed by a nitrocellulose membrane (0.2 µm mesh) of the same size overlaid by the SDS gel. On top, 3 further sheets of Whatman paper were placed and residual buffer was removed. Settings for two blots (in one cell) were constant current of 260 mA with a maximum voltage of 25 V for 25-30 minutes (according to thickness of SDS gels and sizes of proteins to be detected).

Membranes were rinsed with water and incubated with Ponceau staining solution for 5 minutes followed by another wash step with water in order to visualize protein transfer efficiency. Blocking was carried out with 4% non-fat dry milk (wt/vol in TBST) for 2x30 minutes at room temperature. In some cases, additional blocking with 3% BSA/TBST (wt/vol) for 1 hour was done. After thorough washing with TBST, membranes were exposed to primary antibodies (diluted in TBST) overnight at 4 °C on a rocking platform. They were again washed with TBST and incubated with HRP-conjugated secondary antibodies (diluted in TBST) for 2 hours at room temperature, followed by washing in TBST. Signals were detected using the Immobilon Western HRP Substrate; Peroxide Solution and Luminol Reagent were mixed in a 1:1 ratio and the membrane incubated for 5 minutes under constant agitation. A photographic ECL film was applied for the desired time (according to strength of the signal) and then incubated in developing solution for 1 minute, followed by rinsing with H_2O and incubation in fixing solution for 5 minutes. If desired, the membrane was stripped for 3x5 minutes with stripping buffer, blocked as described and reprobed with additional antibodies.

Blotting buffer: 48 mM Tris, 39 mM glycine, 20% methanol (vol/vol), 0.0375% SDS (wt/vol)
TBST (Tris Buffered Saline/Tween): 25 mM Tris-Cl (pH 7.5), 150 mM NaCl, 0.05% Tween 20 (vol/vol)
Stripping buffer: 200 mM glycine, 500 mM NaCl; pH 2.5 (adjusted with HCl)
Ponceau working solution: 0.1% Ponceau S (wt/vol) in 5% (vol/vol) acetic acid
Developing working solution: 110 ml GBX developer/replenisher + 390 ml H_2O
Fixation working solution: 110 ml GBX fixer/replenisher + 390 ml H_2O

Concentrations of antibodies used: Mouse anti-actin, 1:50,000
Rabbit anti-CD55, 1:2,000
Rabbit anti-connexin 43, 1:32,000
Mouse anti-flotillin-1, 1:1,000
Rabbit anti-Thy-1, 1:5,000
Mouse anti-transferrin receptor, 1:2,000

Goat anti-rabbit IgG-HRP, 1:40,000
Goat anti-mouse Ig-HRP, 1:40,000

2.2.7 Immunofluorescence of Blood Samples

A drop of blood was taken from the tail tip of mice, streaked onto microscopy slides and air-dried. The slides were washed twice with PBS for 5 minutes, incubated in fixing solution at room temperature for 20 minutes, and again washed twice for 10 minutes. Samples were blocked with 10% BSA (wt/vol in PBS) at 37 °C for 30 minutes followed by primary antibody (diluted in PBS + 1% BSA) incubation at 37 °C for 30 minutes. The slides were washed twice with PBS and exposed to a fluorescent-dye labeled secondary antibody (diluted in PBS + 1% BSA) at 37 °C for 30 minutes in the dark. After two washing steps with PBS, the slides were rinsed with dH_2O and mounted with 5 µl geltol using a small cover slip.

Fixing solution: 3% paraformaldehyde (wt/vol), 1% picric acid (vol/vol) in PBS
PBS (Phosphate Buffered Saline): 137 mM NaCl, 2.7 mM KCl, 10 mM Na_2HPO_4, 2 mM KH_2PO_4; pH 7.4 (adjusted with NaOH)
Geltol: 6% glycerin (vol/vol), 2.4% Mowiol (wt/vol), 24 mM Tris-Cl (pH 8.5) (after addition of Tris-Cl, the solution was stirred at 50° C for 10 minutes followed by centrifugation at 5,000xg for 15 minutes)

Concentrations of antibodies used: Rat anti-Thy-1.2, 1:200

Goat anti-rat IgG-Cy3, 1:100

2.2.8 Immunofluorescence of Cultured Cells

Cells were grown on uncoated cover slips to the desired density. They were rinsed with sterile PBS, fixed with 3.7% formaldehyde (wt/vol in PBS) for 15 minutes and washed three times with PBS. The cover slips were blocked for 90 minutes at room temperature and washed with PBS. Primary antibodies diluted in PBS + 10% FBS (vol/vol) were applied for 2 hours in a humidity chamber at room temperature. After washing, secondary antibodies (in 10% FBS/PBS) were added for 1 hour at room temperature in the dark, the cells washed with PBS and mounted on a microscopy slide using 7 µl geltol.

Blocking solution: 1% BSA (wt/vol), 10% FBS (vol/vol) in PBS
PBS (Phosphate Buffered Saline): 137 mM NaCl, 2.7 mM KCl, 10 mM Na_2HPO_4, 2 mM KH_2PO_4; pH 7.4 (adjusted with NaOH)
Geltol: 6% glycerin (vol/vol), 2.4% Mowiol (wt/vol), 24 mM Tris-Cl (pH 8.5)

Concentrations of antibodies used: Rat anti-Thy-1.2, 1:250
                                     Rabbit anti-Thy-1, 1:250

                                     Donkey anti-rabbit IgG-Cy3, 1:400
                                     Goat anti-rat IgG-Cy3, 1:100

2.2.9 Preparation and Cultivation of Primary Myoblasts

Isolation of myoblasts and acetylcholine receptor cluster analyses were carried out in cooperation with the group of Dr. Ruth Herbst (Center for Brain Research, Medical University of Vienna). Experiments were performed together with Mag. Susan Luiskandl.

Newborn mice (postnatal day 0 to postnatal day 2) from DAPAT (+/-) x DAPAT (+/-) matings were sacrificed by cervical dislocation and the tail tip dissected for determination of genotype. After washing with ethanol, limbs were removed, freed of skin and subsequently stored at 37 °C in an atmosphere of 6% CO_2 overnight. After genotyping, for samples of interest, toes and large bones were removed and the residual tissue was placed in PBS/1% glucose. The tissue was broken into smaller pieces while getting rid of fat, bones, residual skin and tendons, and finally surgical scissors were used to generate pieces of ~1 mm^3. Muscle slurry was taken up in 1 ml PBS/1% glucose (wt/vol), then supplemented with 125 µl 2% trypsin and 125 µl 0.1% DNase II, and the mixture incubated at 37 °C/6% CO_2 for 30 minutes. After addition of 5 ml growth medium, residual pieces of muscle were broken up with the help of a pipet and cells collected by centrifugation at 400xg. The supernatant was removed, 2 ml growth medium were added and the mixture was triturated with a glass pipet until no more tissue pieces were visible. The volume was adjusted to 4-5 ml with growth medium and the solution passed through a cell strainer (70 µm mesh). The resulting suspension was plated onto an uncoated 60 mm-petri dish and incubated at 37 °C/6% CO_2 for 30 minutes to enable adherence of co-isolated fibroblasts. The petri dish was tilted and the supernatant containing myoblasts collected. Cells were counted and 5-8x10^5 cells each plated onto 35 mm-petri dishes coated with 0.2% gelatin followed by incubation at 37 °C/6% CO_2 with medium changes every 1-2 days.

Primary myoblast growth medium: DMEM + 10% FBS, 10% horse serum (HS), 1% PenStrep, 0.5% chicken embryo extract, 200 µl/100 ml interferon-gamma (100,000 units/µl)

2.2.10 Myotube Formation, Agrin Stimulation and Staining of Acetylcholine Receptor Clusters

Differentiation of confluent myoblasts was induced by a switch from growth to differentiation medium. During the differentiation process, medium was changed daily. Fluorodeoxyuridine (FUDR) was added to the medium 24 hours after differentiation was initiated in order to inhibit myoblast and fibroblast proliferation. Cells were generally used for agrin stimulation on day 2-3 after start of differentiation, depending on the formation of prominent myotubes.

Stimulation with recombinant agrin was done for 11 hours and the cells were subsequently stained with bungarotoxin-Alexa Fluor 594 at 37 °C/6% CO_2 for 1 hour. Myotubes were washed three times with PBS, fixed with 1% paraformaldehyde (wt/vol in PBS) for 10 minutes at room temperature, again washed three times and mounted under a cover slip with 8 µl Mowiol. The samples were kept in the dark at 4 °C until visualization by fluorescence microscopy.

Primary myoblast differentiation medium: DMEM + 10% FBS, 10% HS, 1% PenStrep
100x FUDR stock: 0.61 mM FUDR, 1.47 mM uridine in PBS
α-Bungarotoxin-Alexa Fluor 594: 1:5,000 in PBS

2.2.11 Isolation of DNA from Cultured Cells

DNA was isolated from cultured cells by using the DNeasy® Blood & Tissue Kit (Qiagen), according to the manufacturer's manual with an average cell number of ~5x10^6. DNA was generally eluted in a final volume of 200 µl elution buffer, of which 1 µl was included in subsequent PCR reactions.

2.2.12 Agarose Gel Electrophoresis

The desired amount of agarose (e.g. 1 g/100 ml buffer for a 1% gel) was taken up in TAE buffer and boiled for 3 minutes until agarose was fully dissolved. Ethidium bromide (final concentration 0.5 µg/ml) was added after a 10-minute cooling period, the gel poured into the corresponding trays and supplied with appropriate combs. After solidification, gel trays were placed in electrophoresis chambers filled with TAE buffer, samples applied and the gel was run at constant 90 V for about 1 hour. DNA was visualized using Gel Doc 2000 and the corresponding Gel Doc software (Bio-Rad).

TAE (Tris-Acetate-EDTA) buffer: 40 mM Tris-acetate, 1 mM EDTA; pH 8.0

2.2.13 Murine DAPAT Genotyping

DNA was obtained either from cultured cells using the DNeasy® Blood&Tissue Kit as described above or from mouse tails. Briefly, mouse tail tips (<5 mm) of 18-20 days-old-mice were resected and lysed in 150 µl Tail Lysis Reagent + 2 µl Proteinase K (final concentration: ~0.3 µg/µl) at 55 °C for 4 hours. The enzyme was inactivated by incubation at 85 °C for 45 minutes. Subsequently, the sample was centrifuged at 16,100xg, room temperature for 30 seconds and the supernatant stored at 4 °C until PCR analysis.

The PCR primers used were OLI 1626 (5′-CGATACCTACTTTGTCCCAATTAGC-3′), OLI 1627 (5′-GCTGGTCTCAAACAGCTACGTAGCTGA-3′) and OLI 1628 (5′-CGCATCGCCTTCTATCGCCTTCTTG-3′) with OLI 1626 and OLI 1627 amplifying exon 7 of the wild type DAPAT gene, and OLI 1628 and OLI 1627 amplifying the neomycin cassette-DAPAT junction of the DAPAT knockout allele (Rodemer et al., 2003).

PCR reactions consisted of 4 µl 10x GoTaq Buffer, 0.4 µl dNTPs (10 mM each), 1 µl of each oligonucleotide (10 pmol/µl), 11.5 µl dH$_2$O, 0.1 µl GoTaq Polymerase and 1 µl DNA (final volume: 20 µl).

After 4 minutes denaturation at 94 °C, PCR was performed for 30 cycles of 94 °C for 20 seconds followed by 60 °C for 20 seconds and 72 °C for 50 seconds. Final extension was done at 72 °C for 7 minutes, before cooling to 10 °C holding temperature.
The resulting fragments were ~650 bp in length for the wild type allele and ~860 bp for the knockout allele.

2.2.14 Murine Thy-1 Genotyping

DNA was obtained as described above. Primers used for Thy-1 genotyping experiments were OLI 1733 (5′-TGGGATTCTCGCCCGAGAGTC-3′), OLI 1734 (5′-TGGGATTCTCGCCCGAGAGTC-3′) and OLI 1735 (5′-GCCTGACAGCCTGCCTGGTGA-3′) with OLI 1733 and OLI 1735 amplifying the Thy-1.1 allele, and OLI 1734 and OLI 1735 amplifying the Thy-1.2 allele. For every sample, a separate reaction was set up for each primer combination. Reagent concentrations were as described for DAPAT genotyping.

PCR program: initial denaturation at 94 °C for 4 minutes followed by 30 cycles of 94 °C for 20 seconds, 57 °C for 20 seconds and 72 °C for 50 seconds. Final extension was done at 72 °C for 7 minutes, before cooling to 10 °C holding temperature.
The resulting PCR products were ~270 bp in length for both assays.

2.2.15 Measurement of Cellular Phospholipids

Determination of phospholipids in fibroblast lines was carried out in cooperation with the group of Prof. Dr. Felix Wieland (Heidelberg University Biochemistry Center); lipidomic analyses were performed by Dr. Alexander Brodde and Dr. Britta Brügger.

An appropriate number of cells (1-2 nearly confluent 10 cm dishes) was washed with sterile PBS and dH$_2$O and subsequently scraped into 1 ml of dH$_2$O. Extracts were obtained by homogenization using 23 G (2 passages), 25 G (2 passages) and 27 G (3 passages) needles. Cellular extracts were shock-frozen in liquid nitrogen and stored at -80 °C until mass spectrometry.

Mass spectrometric analyses were done on a triple quadrupole instrument equipped with a nano-electrospray ionization (ESI) source. The source temperature was set to 30 °C and a capillary voltage of ±600-900 V was applied, depending on the ion mode. Argon was used as collision gas at a nominal pressure of 2.5x10^{-3} mbar. Lipid standards dissolved in chloroform:methanol (1:2 vol/vol) were added to the extraction solvent prior to lipid extraction, which was performed according to the method of Bligh and Dyer (Bligh and Dyer, 1959). Dried lipids were dissolved in methanol containing 10 mM ammonium acetate. Quantification of phosphatidylcholine (PC) and sphingomyelin (SM) was performed as described (Brugger et al., 2004). Quantitation of phosphatidylethanolamine (PE) and phosphatidylserine (PS) was performed by neutral loss scanning, selecting for a neutral loss of 141 Da or 185 Da (positive ion mode), respectively, with a collision energy of 20 eV (Brodde, 2009; Zemski Berry and Murphy, 2004). Plasmenylethanolamine (PL-PE) quantitation was performed by precursor ion scanning for fragment ions 364 Da, 390 Da and 392 Da (positive ion mode, collision energy of 18-20 eV). Unsaturated PE and PS standards were synthesized and purified via HPLC (Koivusalo et al., 2001) and PL-PE standards were synthesized as described (Brodde, 2009; Paltauf and Hermetter, 1994). Quantitative analyses were performed as described (Brugger et al., 1997; Brugger et al., 2000). Phosphate determination was done according to Rouser (Rouser et al., 1970).

2.2.16 Behavioral Studies

All mice exposed to behavioral testing were males. With regard to mice being nocturnal animals, all trials were conducted after 6 p.m. under suitable dim light conditions.

Rotarod

Rotarod experiments were basically carried out as already described (Dumser et al., 2007). Briefly, 5 mice were placed on separate lanes on the rotating cylinder of an accelerating Rotarod apparatus. 30 to 60 seconds were allowed for familiarization. Subsequently, the accelerating mode was switched on. In a five minute period, the apparatus accelerated from 4 to 40 rpm and was left running at constant 40 rpm until a maximum time of 500 seconds from the start. Time from start to fall (in seconds) was automatically recorded. Two rotations of mice holding on to the cylinder were assessed as a fall.

A 3 day training/test scheme was applied: Mice were trained three times on two consecutive days followed by performance of the test in four consecutive trials on the third day. Suitable resting periods were allowed between the trials. Mean values of the best three trials on the test day were calculated for every mouse und used for statistical analysis.

Balance Beam

Mice were placed on the balance beam, a 60 cm long wooden bar located 23 cm above the ground. A horizontal midline was drawn on the beam to check for murine limb coordination deficits. Mice were allowed to explore their surroundings and were then relocated to one end of the bar. Movement across the beam was encouraged; a young healthy mouse typically runs swiftly across with all four paws at the top of the beam. Performances were evaluated according to a scoring system (see chapter 3.6.1) by two independent supervisors.

Three consecutive trials interrupted by suitable resting periods were carried out for each mouse. The best evaluation result (usually reached in the third trial) was chosen for statistical analysis.

CHAPTER 3
RESULTS

3.1 Phospholipid Profiles Reveal Compensatory Alterations in Ether Lipid-Deficient Human Cell Lines

The role of ether lipids in the living organism can be studied best in models, in which biosynthesis of these molecules is defect. In humans, ether lipid deficiency leading to RCDP is evoked by mutations in the peroxisomal enzymes DAPAT and AGPS as well as the PEX7 receptor responsible for the import of AGPS (see chapter 1.2.1). Therefore, primary fibroblast cell lines derived from skin biopsies of RCDP patients were obtained. All three types of the disease in their mild and severe forms were selected for this study. An overview of the mutations in the genes that are affected in each fibroblast line is given in Table 1.

Cell Line	Affected Gene	Mutations	Patient Phenotype
RCDP 1-1	PEX7	H285R/L292X	mild
RCDP 1-2	PEX7	H39P/W206X	severe
RCDP 1-3	PEX7	L292X/L292X	severe
RCDP 2-1	GNPAT[7]	c.c. 1937+5G>A	mild
RCDP 2-2	GNPAT	c. 1428delC/1428delC	severe
RCDP 3-1	AGPS	E471K/E471K	mild
RCDP 3-2	AGPS	T568M/T568M	severe

Table 1: Primary fibroblasts derived from RCDP patients and their corresponding mutations. Amino acid exchanges are indicated in the one-letter code. X designates the presence of a premature stop codon.

Prior to the examination of ether lipid-deficient cell lines, the phospholipid profile was studied in three human control fibroblast lines (derived from healthy patients). As depicted in Figure 8, phospholipids were divided into five different main classes, namely phosphatidylcholine (PC), phosphatidylethanolamine (PE), phosphatidylserine (PS), sphingomyelin (SM) and plasmenylethanolamine (PL-PE). PC was found to be the major phospholipid species accounting for about 40%[8] of the total phospholipid mass. The remaining phospholipid amount was distributed rather equally among the other four species, each making up approximately 10-15% of all phospholipids. Quantification of plasmenylethanolamines showed an average relative amount of about 12% in control cells.

---

[7] GNPAT encodes the DAPAT protein (see chapter 1.2).
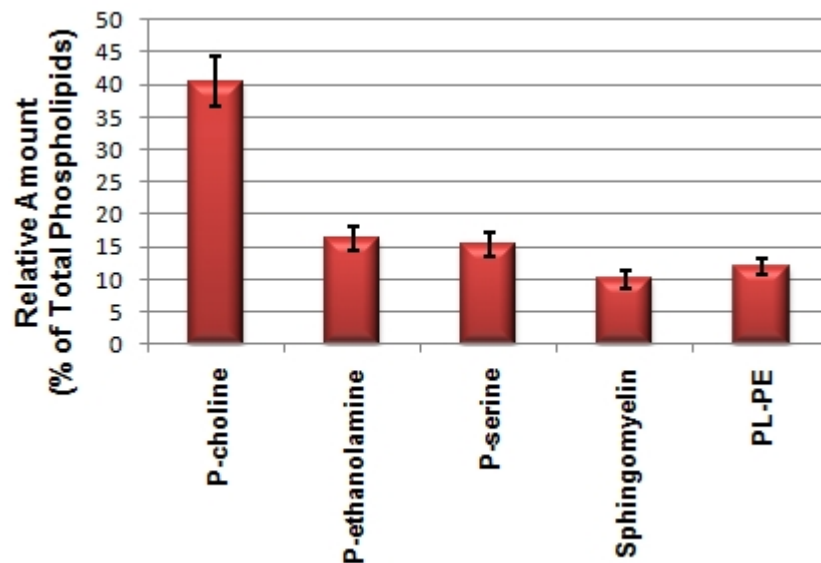[8] All percentages presented in chapter 3.1 and 3.2 are mole%.

Figure 8: Phospholipid profile of human control fibroblasts. Depicted values were calculated as means of three different cell lines each measured in biological triplicates. Error bars indicate standard deviations. P-, phosphatidyl-; PL-PE, plasmenylethanolamine

3.1.1 Plasmalogen Content of Human Cell Lines Only Partially Reflects Clinical Severity

In RCDP patients, the clinical phenotype has been observed to correlate with the amount of plasmalogens synthesized (Braverman et al., 2002). In order to determine, whether this holds true in cultured fibroblasts derived from patients, quantification of all ethanolamine plasmalogen species was performed by lipidomic analysis of cell lysates using nano-ESI mass spectrometry (in cooperation with Dr. Alexander Brodde and Dr. Britta Brügger). Three fibroblast lines originating from healthy individuals were chosen as control group.

In the latter, ethanolamine plasmalogens were found to account for 10-15% (see also Figure 8) of all measured phospholipids. Analysis of plasmalogen levels revealed a significant reduction of about 40% in fibroblasts of patients with a mild disease course when compared with control cells (Figure 9). In addition, plasmalogen amounts in cells derived from severely impaired patients were significantly lower than those in the "mild course" group and reached levels of about 15-40% of the control values. However, levels in fibroblasts from patients with severe phenotype turned out to be heterogeneous with some cells behaving rather like cells from the "mild course" (RCDP 1-3, RCDP 3-2) group and others exhibiting very low plasmalogen amounts (RCDP 1-2, RCDP 2-2). Morphologically, there was no difference between the different cell lines of the "severe course" group with the exception of a slower growth rate of RCDP 1-3 and RCDP 3-2 compared with all other patient and control cell lines. Thus, owing to the observed heterogeneity, only fibroblast lines RCDP 1-2 and RCDP 2-2 should be considered as severely affected by ether lipid deficiency.

Taken together, though, these results confirm the observation of a direct correlation between the residual levels of plasmalogen and disease severity in RCDP patients.
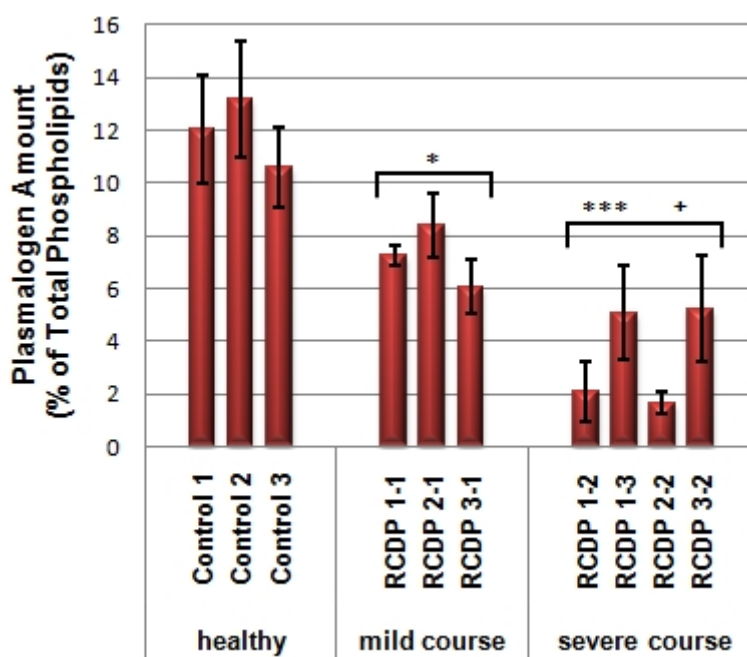
Figure 9: Ethanolamine plasmalogen levels in control and RCDP patient fibroblasts. Significant reductions can be observed in cells of patients with mild and severe disease courses, respectively, as compared to control cells. Error bars indicate standard deviations (n=3 for each individual cell line[9]). *** $P<0.001$ compared with "healthy" group; * $P<0.05$ compared with "healthy" group; + $P<0.05$ compared with "mild course" group. Statistical analysis was carried out using one-way ANOVA followed by Bonferroni's multiple comparison test.

3.1.2 The Distribution of Fatty Alcohols at the sn-1 Position of Plasmalogens Is Altered in Fibroblast Cultures Deficient in Ether Lipid Synthesis

In plasmalogens, the sn-1 position is occupied by a saturated or monounsaturated (only in case of C18) alkyl chain with a length of 16 or 18 carbon atoms. To judge, which of these species are dominant in human fibroblasts and whether the alkyl chain distribution is changed upon reduction of plasmalogens, the proportion of each species was determined by mass spectrometry.

In control fibroblasts, C16:0 was the most frequent species at the sn-1 position accounting for more than 40% of all ethanolamine plasmalogens (see Figure 10). Concerning C18 chains, the saturated form seemed to be more abundant than the monounsaturated form. However, it is of notice that this distribution was quite heterogeneous within the three different control lines, e.g. with C18:0 accounting for ~40% of PL-PEs in one control line as opposed to less than 30% in another. The distribution in fibroblasts mildly affected by ether lipid deficiency mainly reflected that of the control group, although a slight tendency to replace C16:0 with C18:0 could be observed. In cells derived from patients suffering from severe RCDP, changes in the fatty alcohol profile of the sn-1 position were discovered: The amounts of C18:0 were lowered in all respective cell lines, whereas in turn the levels of the other two species were slightly increased. Interestingly, these differences between fibroblasts of severely affected patients and controls were even more pronounced, when only the more slowly growing cell lines (RCDP 1-3 and RCDP 3-2) were considered. Yet, these observations

---

[9] Each value of a given cell line represents an independent, separate culture, from which phospholipids were extracted for analysis.

have to be treated with caution due to the heterogeneity at the sn-1 position in the control group. Figure 10B shows an overview of the alkyl chain composition at sn-1 in the three different groups.
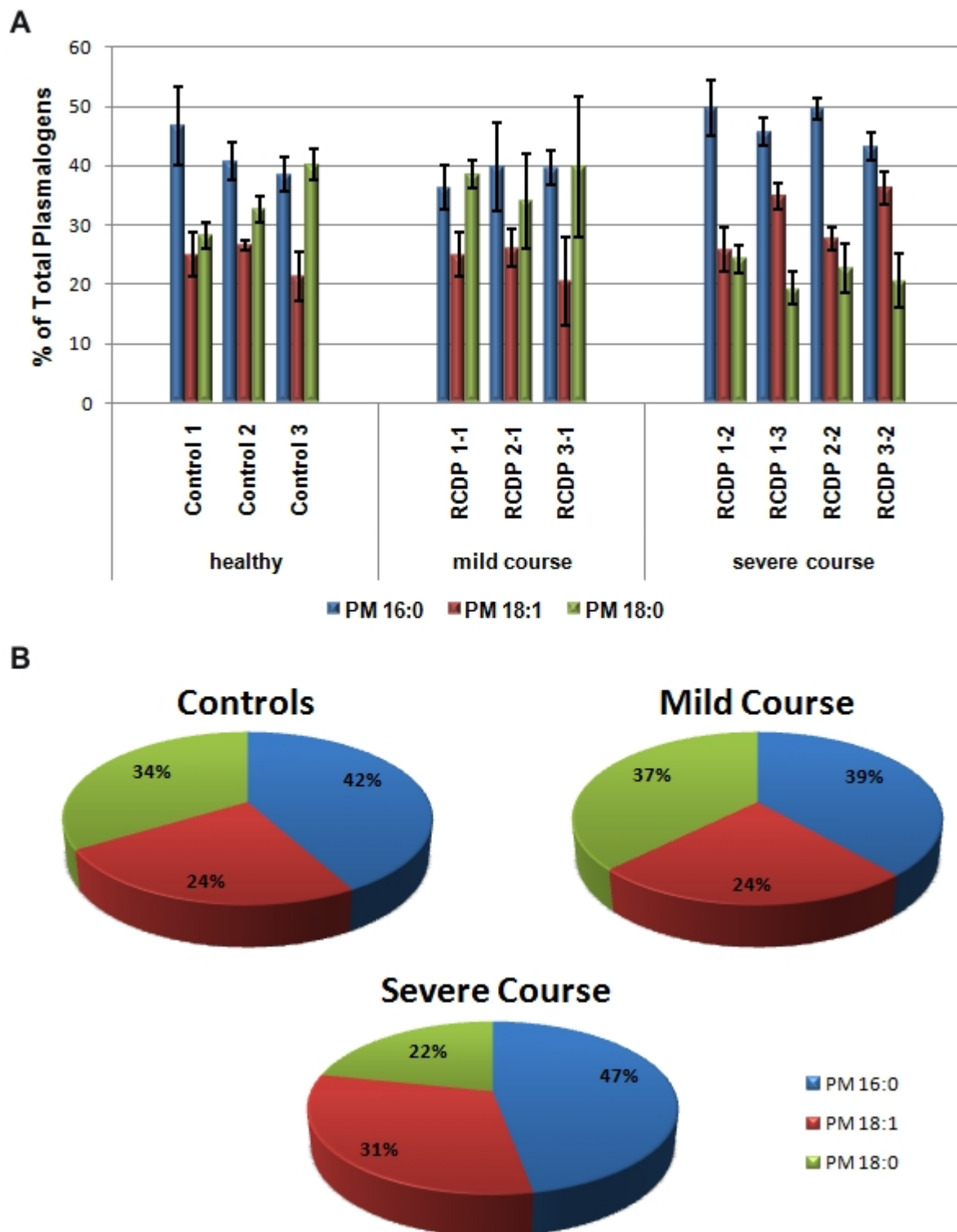

Figure 10: Fatty alcohol distribution at the sn-1 position of ethanolamine plasmalogens. (A) Sn-1 alkyl chain profile in the individual cell lines of control and RCDP patients. C18:0 is reduced in all severely affected fibroblast lines, but not in the mildly affected ones. Error bars indicate standard deviations (n=3 for each individual cell line). (B) Overview of fatty alcohol composition in the different patient groups. Values represent means of all cell lines of the respective group. PM, plasmalogen

3.1.3 Plasmalogen Loss Is Mainly Compensated by a Rise in Phosphatidylethanolamine Levels

Fibroblasts derived from severely affected RCDP patients have considerably lower amounts of plasmalogens than control cells. This observation led to the question, whether a loss of one major phospholipid class would provoke compensatory changes in the phospholipid profile of patient cells. Therefore, the main phospholipid classes were studied in RCDP 1-2 and RCDP 2-2, the fibroblast lines most severely affected by ether lipid deficiency, and compared with control lines (Figure 11). Levels of phosphatidylcholine and –serine did not differ from control cell values in patient cells. However, in case of phosphatidylethanolamine, a remarkable increase could be observed. The relative PE amount almost doubled from about 14-18% in control cells to 26-27% in plasmalogen-deficient cell lines. In contrast, sphingomyelin levels rather seemed to be decreased in cells lacking ether lipid synthesis. Thus, PE appears to be the only molecule replacing missing plasmalogens with the other main phospholipid classes remaining mostly unchanged.
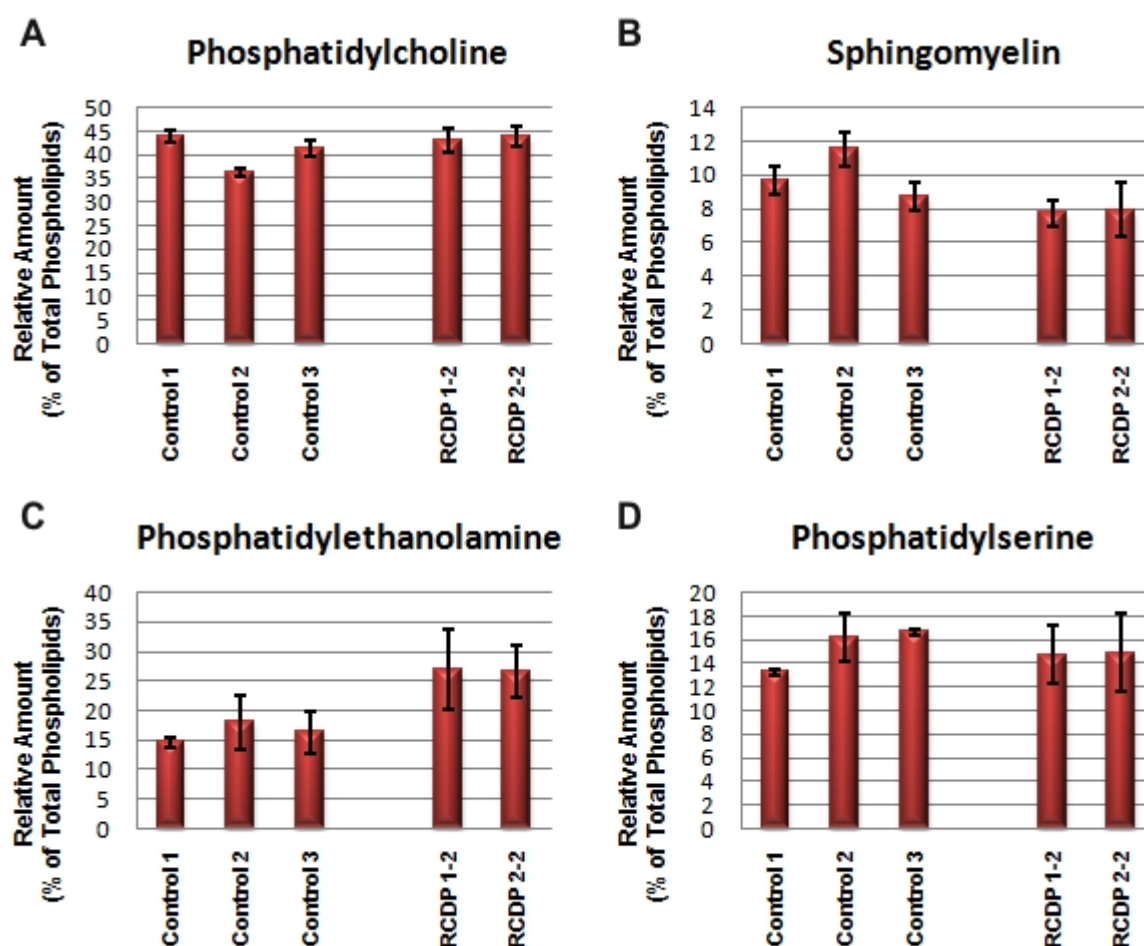

Figure 11: Compensatory mechanisms in ether lipid-deficient cell lines. Relative levels of phosphatidylcholine (A), sphingomyelin (B), phosphatidylethanolamine (C) and phosphatidylserine (D) in three control lines and two RCDP fibroblast lines severely affected by ether lipid deficiency. Lack of ether lipids is counterbalanced by a pronounced rise in phosphatidylethanolamine. Error bars indicate standard deviations (n=3 for each cell line).

Results

Thus, it seemed likely that the total amount of ethanolamine phospholipids is kept at a constant level in cultured fibroblasts. In order to test this hypothesis, plasmenyl- and phosphatidylethanolamines were added up and the resulting values of control and patient cells compared to each other (see Figure 12). The results demonstrated that indeed the total amount of ethanolamine phospholipids was similar in patient fibroblasts and control cells. In all examined lines, ethanolamine phospholipids reached about 26-32% of the total phospholipid mass analyzed. However, the species accounting for these numbers were different between controls and patient cell lines; whereas in controls the ether-containing ethanolamines (PL-PE) made up more than 40% of total ethanolamine phospholipids, this proportion was drastically reduced to about 5% in patient fibroblasts (Figure 12B).
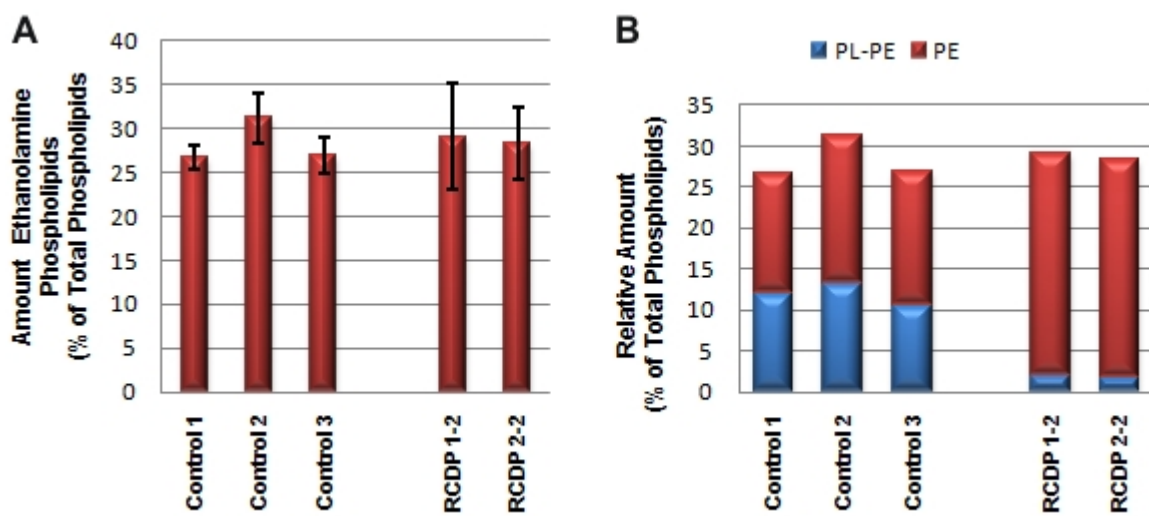

Figure 12: Compensation of plasmalogen deficiency by phosphatidylethanolamine. (A) The relative amount of total ethanolamine phospholipids is unchanged in cell lines lacking plasmalogens when compared with control cells (n=3 for each cell line). Error bars indicate standard deviations. (B) Distribution of ethanolamine phospholipids among plasmalogen and non-plasmalogen forms in control cells and ether lipid-deficient cells. PL-PE, plasmenylethanolamine; PE, phosphatidylethanolamine

3.2 Batyl Alcohol and Hexadecylglycerol Are Highly Potent in Restoring Plasmalogen Levels in Culture

Peroxisomal plasmalogen synthesis can be bypassed by the application of a substance containing a glycerol backbone and a pre-formed ether linkage at the sn-1 position. Several publications report a rise in plasmalogen levels resulting from supplementation of cultured cells with batyl alcohol (BA, 1-O-octadecyl-rac-glycerol) (Schrakamp et al., 1988) or 1-O-hexadecylglycerol (HDG) (Honsho et al., 2010; Styger et al., 2002; Zoeller et al., 2002). Both of these compounds have a glycerol backbone, which is linked to a saturated C18 or C16 chain, respectively, via an ether bond at the sn-1 position. Therefore, supplementation with BA and HDG provides the cell with a utilizable ether lipid and enables the circumvention of the peroxisomal steps of ether lipid biosynthesis. To further elucidate the effects and the mechanism of action of these plasmalogen precursors, the phospholipid profile of treated fibroblasts was examined in more detail.

3.2.1 The sn-1 Alkyl Chain of Restored Plasmalogens Is Determined by the Structure of Their Precursors

A control fibroblast line and a patient line severely deficient in plasmalogen biosynthesis were treated with 20 μM HDG or BA for three consecutive days with medium changes every 24 hours. The respective cells under normal culture conditions and after treatment with ethanol, the solvent for BA and HDG, served as controls. In addition, the phosphate form of HDG (1-O-hexadecyl-2-hydroxy-sn-glycero-3-phosphate; HDG-P) was evaluated concerning its ability to permeate cultured cells and restore plasmalogen levels.

Results confirmed that all three tested compounds drastically increase the amounts of ethanolamine plasmalogens in cultured fibroblasts (see Figure 13A). Already in treated control cells, the levels were strongly elevated to about 150% (with BA and HDG-P) or even 200% (with HDG) compared with untreated cells.

In the ether lipid-deficient cell line, supplementation with the solvent ethanol alone did not show any beneficial effect. In contrast, treatment with all precursors raised plasmalogen amounts to values higher than those in untreated control cells. As in controls, HDG displayed a stronger potency to restore plasmalogens than BA. Supplementation with HDG led to levels of about 185% of control values, whereas BA treated fibroblasts reached about 130% of controls. A remarkably strong increase in ethanolamine plasmalogen amount was also observed in patient fibroblasts treated with HDG-P, indicating that also this substance is highly efficacious in restoring plasmalogen levels in culture.

In order to judge whether all fatty alcohol species are reconstituted in a similar way by precursor treatment, a closer look was taken at the alkyl chain distribution at the sn-1 position in treated cell lines. As already described in chapter 3.1.2, the sn-1 position of plasmalogens is occupied by either a 16:0, an 18:0 or an 18:1 fatty alcohol, with the 16:0 species usually being the most prominent type. However, in fibroblast cultures supplemented with precursor lipids, the situation turned out to be different (see Figure 13B). Precursor treatment in every case recovered only one species, namely the one representing the chain length of the respective precursor; e.g. treatment with HDG resulted in an increase in only the 16:0 species. Plasmalogens containing other fatty alcohol species did not show elevated levels. This consequence of precursor treatment could be observed in control as well as in plasmalogen-deficient cells, with the effects being more pronounced in patient cells due to their very low basal plasmalogen amounts.

Therefore, these results demonstrate that the sn-1 position of plasmalogen precursors is not remodeled upon their metabolism to plasmalogens.
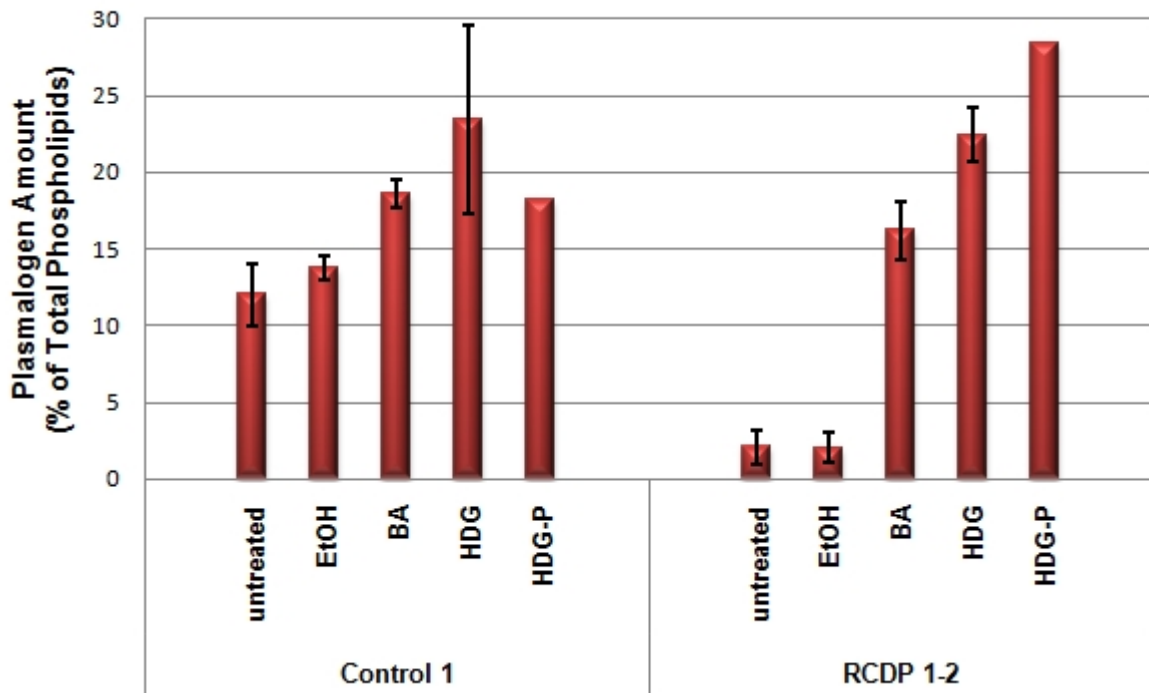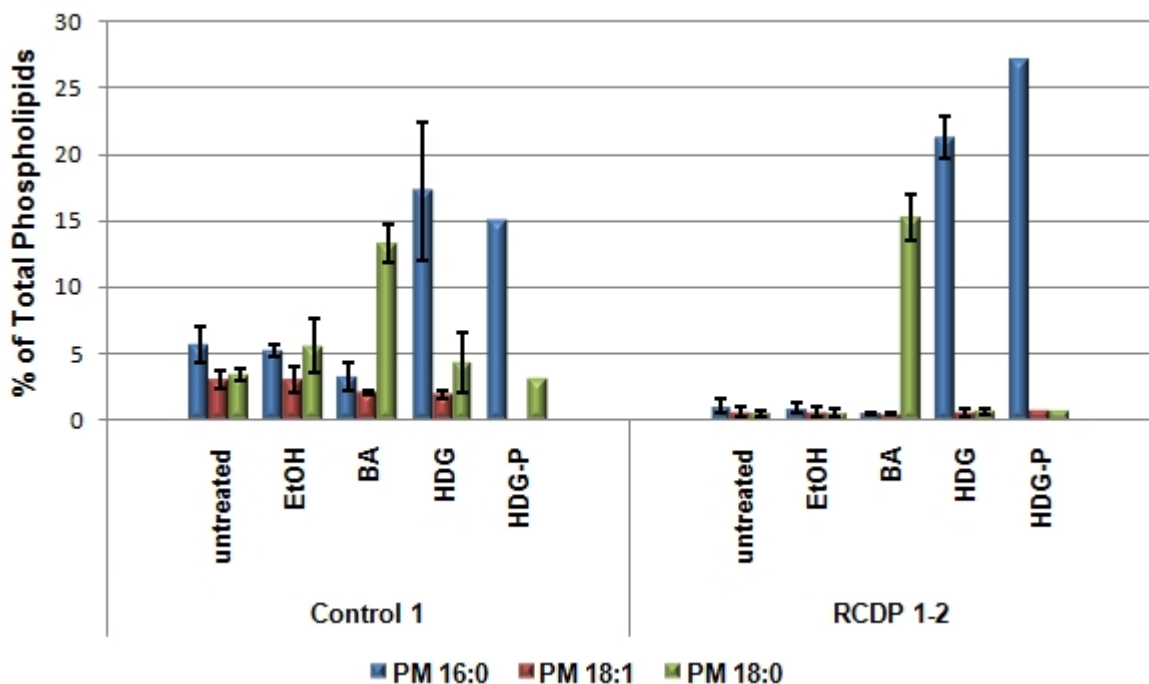

Figure 13: Reconstitution of plasmalogen levels by ether lipid precursors. (A) Treatment of control and plasmalogen-deficient patient fibroblasts increases ethanolamine plasmalogen amounts to values higher than those of untreated control cells. (B) Overview of alkyl chain distribution at sn-1 position of ethanolamine plasmalogens after treatment with precursor lipids. Restored plasmalogens exhibit exclusively chain lengths that represent those of the precursor molecule used for treatment. All error bars indicate standard deviations (n=3 for each cell line and treatment with exception of HDG-P treatments, where n=1). EtOH, ethanol; BA, batyl alcohol; HDG, hexadecylglycerol; HDG-P, hexadecylglycero-phosphate; PM, plasmalogen

3.2.2 Cellular Ethanolamine Phospholipid Levels Are Kept Constant upon Treatment with Plasmalogen Precursors

Plasmalogen precursor treatment of ether lipid-deficient fibroblasts restores plasmalogens to higher than control levels. In order to determine if this drastic change also results in alterations in other phospholipid classes, the main phospholipids were exposed to further analysis.

As was the case upon loss of plasmalogens, compensatory mechanisms following precursor treatment were mainly mediated by phosphatidylethanolamines (see Figure 14). In control as well as in patient cells, a profound reduction in the amount of PE could be observed after supplementation with BA or HDG. PE levels dropped from 15% and 27% of total phospholipids in untreated control and patient fibroblasts, respectively, to values of about 5% as a consequence of precursor administration. Contrary to PE, the levels of the other major phospholipid classes (phosphatidylcholine, sphingomyelin and phosphatidylserine) remained largely unchanged. Only in case of PC, a slight decrease was discovered after HDG supplementation, which however was of minor significance compared with the dramatic changes in PE levels. Control treatment with ethanol alone did not provoke any phospholipid changes, confirming that the observed differences were indeed a consequence of precursor application.
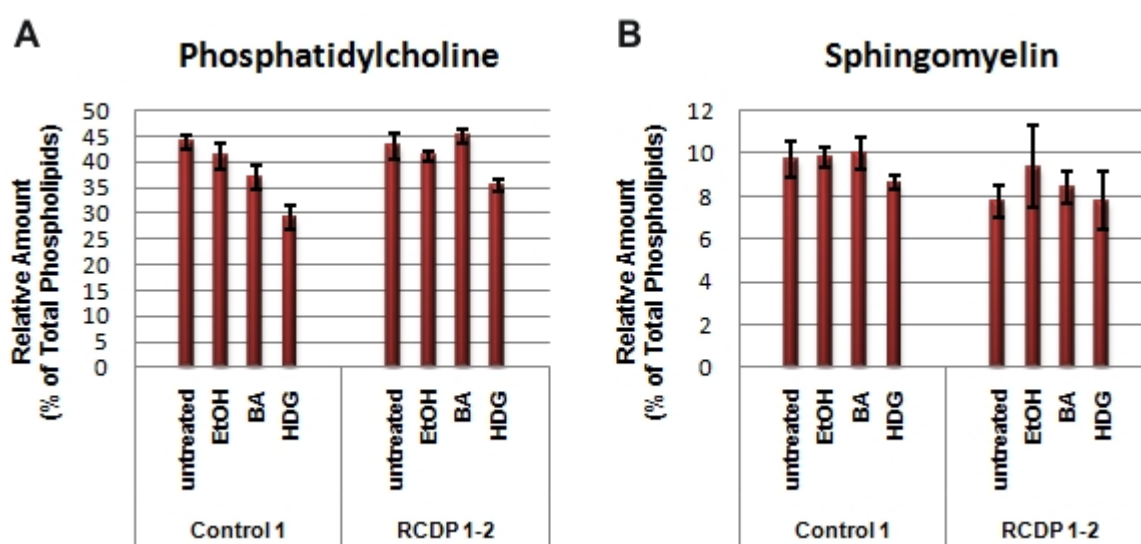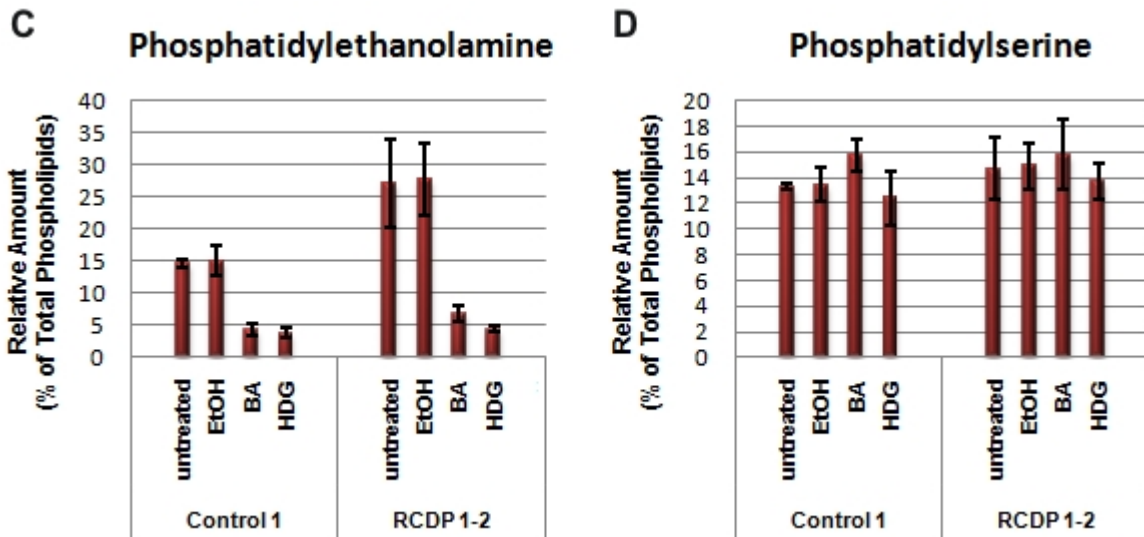
Figure 14: General phospholipid profiles after treatment of fibroblast cultures with plasmalogen precursors. Relative levels of phosphatidylcholine (A), sphingomyelin (B), phosphatidylethanolamine (C) and phosphatidylserine (D) in treated and untreated control and plasmalogen-deficient cells. The increase in ethanolamine plasmalogens provoked by precursor treatment is counterbalanced by a reduction of phosphatidylethanolamine levels. Error bars indicate standard deviations (n=3 for each cell line and treatment). EtOH, ethanol; BA, batyl alcohol; HDG, hexadecylglycerol

As a similar compensation by PE had already been observed in cells deficient in ether lipid biosynthesis (see chapter 3.1.3), these results suggest a regulatory mechanism that maintains a constant level of ethanolamine phospholipids in the cell. To verify this assumption, plasmenyl- and phosphatidylethanolamines were summed up as described above and the total ethanolamine phospholipid amounts compared in precursor-treated and untreated fibroblasts (Figure 15). The resulting values were similar in all examined samples. In untreated or mock-treated fibroblasts, the major part of ethanolamines was made up by non-ether phospholipids. However, in cells supplied with ether lipid precursors, a high level of plasmalogen ethanolamines was found at the expense of the non-ether lipid form (see Figure 15B). Remarkably, total amounts of ethanolamine phospholipids were slightly lower in BA-treated fibroblasts (controls as well as patient cells) than in all others.

Together with the compensatory mechanisms revealed in chapter 3.1.3, these results point to the fact that total ethanolamine phospholipids are kept constant under different circumstances – a rise in phosphatidylethanolamines accounts for a loss of plasmenylethanolamines and vice versa.
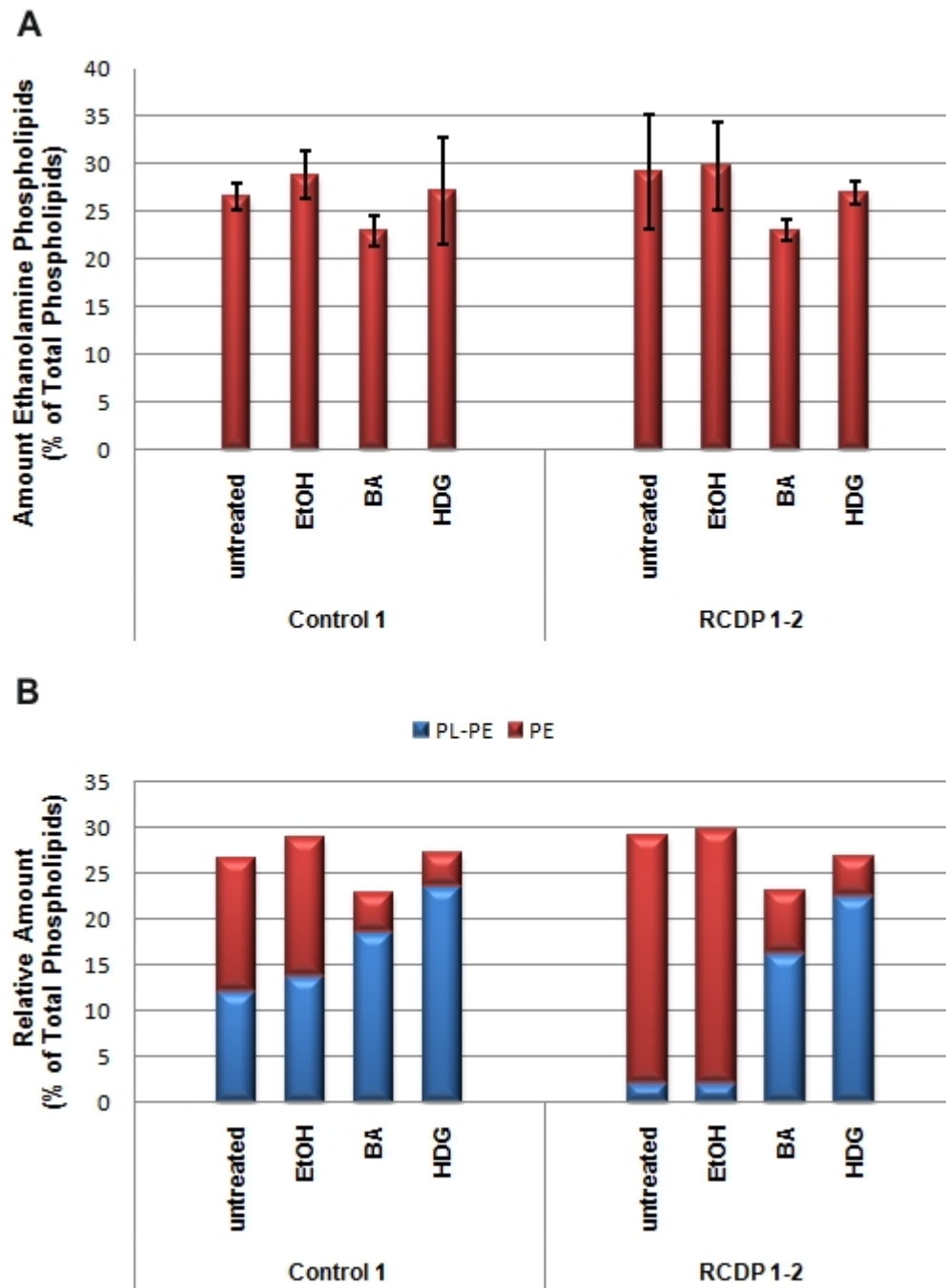
Figure 15: Compensation of a surplus of plasmalogens by phosphatidylethanolamine. (A) Overview of total ethanolamine phospholipid levels in treated and untreated control and RCDP fibroblasts. Reduction of PE counterbalances the rise in PL-PE following ether lipid precursor treatment, leading to rather similar total ethanolamine values in all treated and untreated cell lines. Error bars indicate standard deviations (n=3 for each cell line and treatment). (B) Distribution of ethanolamine phospholipids among plasmalogen and non-plasmalogen forms in treated and untreated control and ether lipid-deficient cells. EtOH, ethanol; BA, batyl alcohol; HDG, hexadecylglycerol; PL-PE, plasmenylethanolamine; PE, phosphatidylethanolamine

3.3 Peroxisomal Ether Lipid Synthesis Is Not Required for Surface Expression of the GPI-Anchored Protein Thy-1 in Mammals

As alkylacylglycerol-containing GPI anchors cannot be formed under conditions of ether lipid deficiency, the question was addressed whether or not the surface localization of GPI-anchored proteins is affected by the loss of ether lipids. Two different model organisms were employed for this approach: On the one hand, cells obtained from an ether lipid-deficient mouse, the DAPAT knockout (ko) mouse (Rodemer et al., 2003), were analyzed. On the other hand, surface expression of a GPI-anchored protein was studied in primary fibroblast cultures derived from patients suffering from RCDP (see chapter 3.1).

3.3.1 Surface Localization of Murine Thy-1

Analysis of Murine Genotypes

Because DAPAT (-/-) mice are infertile, heterozygous animals were mated to produce homozygous mutant offspring. Thus, in order to study cells of ether lipid-deficient mice, as a prerequisite, their genotype had to be determined. This was done routinely by a PCR approach using DNA obtained from mouse tails or cultured cells: In DAPAT ko mice, exons 5-7 of the DAPAT gene are replaced by a DAPAT/neomycin cassette (Rodemer et al., 2003), which can be easily detected and discriminated from the wild type (wt) allele with the help of the corresponding PCR primers. Subsequently to PCR reactions, the samples were applied to a 1.5% agarose gel containing ethidium bromide. Band sizes visible upon UV exposition indicated the genotypes of the corresponding samples. Figure 16 shows a representative example of a standard DAPAT genotyping assay, identifying the genotypes of two ko mice (M1, M6), one wt mouse (M2) and three heterozygotes (M3, M4, M5).
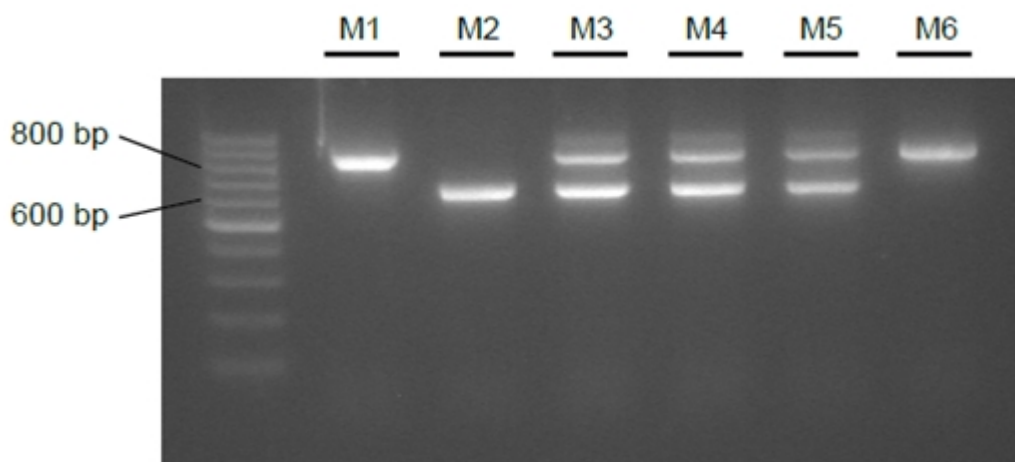
Figure 16: Representative example of PCR determination of DAPAT genotypes. Larger bands (~860 bp) indicate the presence of a ko allele, whereas smaller fragments (~650 bp) result from amplification of the wt allele. M, mouse

In addition to the DAPAT genotype, also the Thy-1 genotype of the mice studied needed to be identified. In mice, two alleles of Thy-1 exist, which code for the Thy-1.1 and the Thy-1.2 glycoprotein, respectively. These two differ only in a single amino acid at position 89, arginine in Thy-1.1 and glutamine in Thy-1.2 (Williams and Gagnon, 1982), due to a single nucleotide polymorphism (SNP) in the murine Thy-1 gene. Only very few mouse strains, for example AKR/J, A or Thy-1.1,

express the Thy-1.1 allele. However, most strains, including the abundant ones C57BL/6 or Swiss, possess the Thy-1.2 epitope. In contrast, rat Thy-1, which is highly homologous to the murine protein, is solely of the Thy-1.1 type.

The mice employed in Thy-1 surface localization experiments were of mixed background meaning that their genotype concerning Thy-1 was uncertain. Due to the fact that a Thy-1.2-specific antibody was used for immunofluorescence studies, the presence of this epitope had to be demonstrated prior to staining experiments. In order to distinguish between Thy-1.1 and Thy-1.2, an allele-specific PCR assay was established with downstream primers that selectively address the difference between the two variants (see Figure 17A). In addition, the primers were designed in a way that rat DNA could serve as a positive control for Thy-1.1 (see Figure 17B). Genotyping samples were routinely checked on 1.8% agarose gels (see Figure 17C for an example). As illustrated, mice expressing the Thy-1.1 (M1, M3) variant were as well identified as mice harboring the Thy-1.2 antigen (M2, M4). The detection of Thy-1.1 only in rat DNA (RT1, RT2) revealed the successful establishment of the assay.
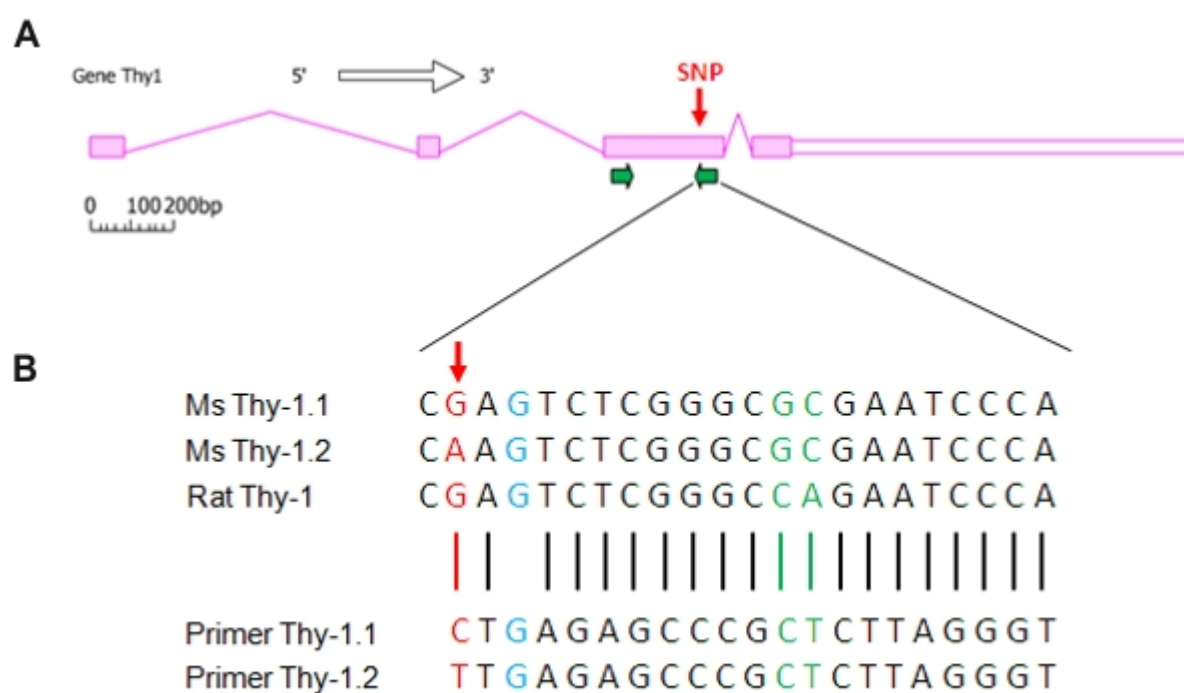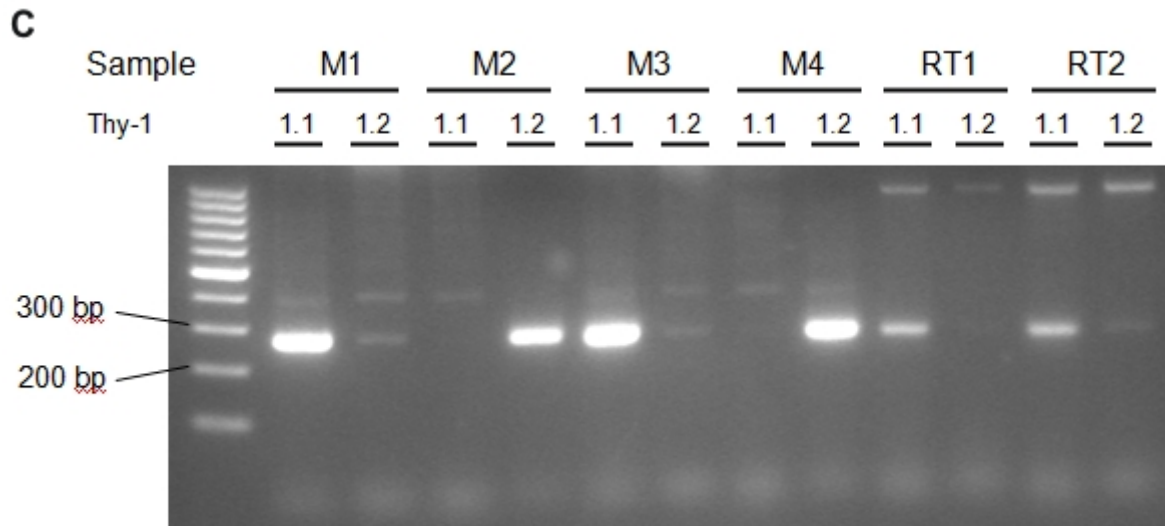
Figure 17: Thy-1 genotyping. (A) Murine Thy-1 gene structure (source: http://www.ncbi.nlm.nih.gov/IEB/Research/Acembly). Primers employed for genotyping are indicated as green arrows. SNP, single nucleotide polymorphism; (B) Strategy for reverse primer design. Allele-specific primers were constructed in a fashion complementary to the coding strand. The Thy-1.1/1.2 SNP is indicated by a red arrow; a one-base-pair mismatch (depicted in blue) was introduced to increase selectivity of the primer for the corresponding allele. Mismatches displayed in green were deliberately accepted to enable the recognition of both rat and mouse DNA. Ms, mouse; (C) Representative example of Thy-1 genotype determination. Fragments of ~270 bp indicate the presence of the respective allele (Thy-1.1 or Thy-1.2); M, mouse; RT, rat

Immunofluorescent Staining of Thy-1

Murine wt and DAPAT ko embryonic fibroblast lines (MEFs) carrying the allele coding for Thy-1.2 were employed for fluorescent staining of Thy-1. Immunofluorescence was performed as described (see chapter 2.2) and the cells visualized using fluorescence microscopy. Based on the fact that the protocol used does not involve any permeabilization step, which would permit antibody entry into the cytoplasm, the observed staining resulted exclusively from binding of antibodies to molecules on the outer membrane surface.

Immunofluorescent detection of Thy-1.2 revealed an intense punctate staining of wt as well as ko fibroblasts (see Figure 18). This indicates that, in spite of the failure to synthesize alkylacylglycerol, the GPI-anchored Thy-1 is successfully delivered to the plasma membrane under ether lipid-deficient conditions.
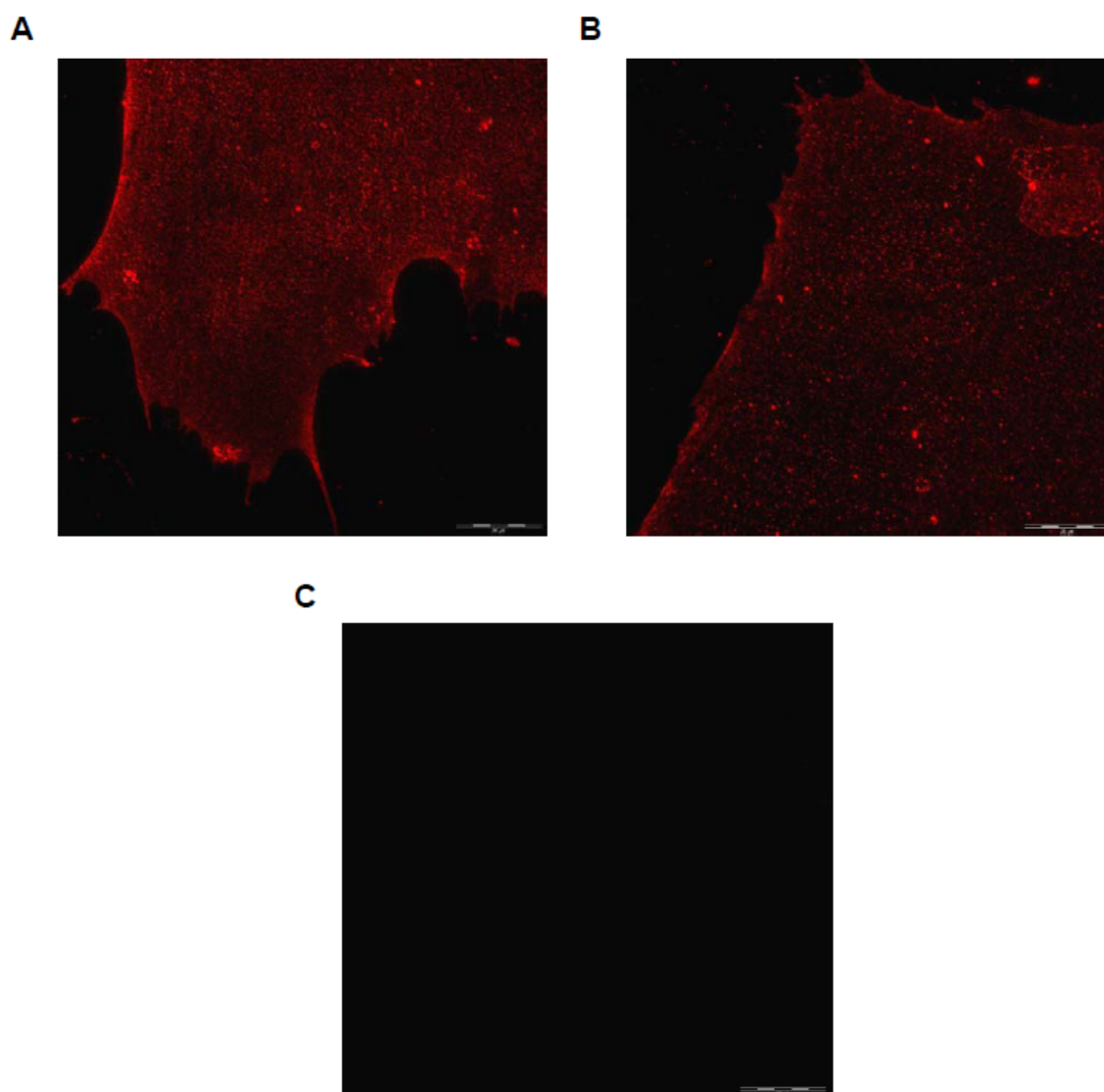
Figure 18: Surface expression of Thy-1 in murine embryonic fibroblasts. Thy-1 is clearly visible on the surface of both wt (A) and DAPAT ko (B) fibroblasts. An antibody control (secondary antibody only) is shown in (C). Original magnification: 60x; scale bars: 20 µm

The punctate distribution of Thy-1 on the surface is highly likely to indicate the distribution of Thy-1-containing membrane rafts. Based on this, it is of notice that in ko fibroblasts the space between individual dots seems to be larger than in wt cells, probably pointing to the fact that ko fibroblasts have fewer Thy-1-positive rafts. In addition, the average size of single Thy-1 spots appears slightly larger in ko MEFs, which could suggest larger rafts resulting from fusion of smaller domains.

In addition to fibroblasts, Thy-1 surface expression was also analyzed in murine T cells. For this purpose, a drop of blood was drawn from the tail tip of 18-20 days old mice after biopsy for genotyping and streaked onto microscopic glass slides. Staining was carried out as described in the "Methods" section (cf. chapter 2.2). Again, only proteins on the outer cell surface were detected. Immunofluorescence microscopy showed a nice surface staining of T cells in blood of wt and ko mice without any visible differences between the different genotypes (Figure 19). Erythrocytes, by far the most abundant cells in the blood, surrounding stained T cells did not express Thy-1 and were therefore not labeled in this experiment. Out of 38 ko mice examined, all exhibited Thy-1 surface

positive T cells confirming that mice deficient in ether lipid biosynthesis are generally able to transport GPI-anchored proteins efficiently to the external face of the plasma membrane.
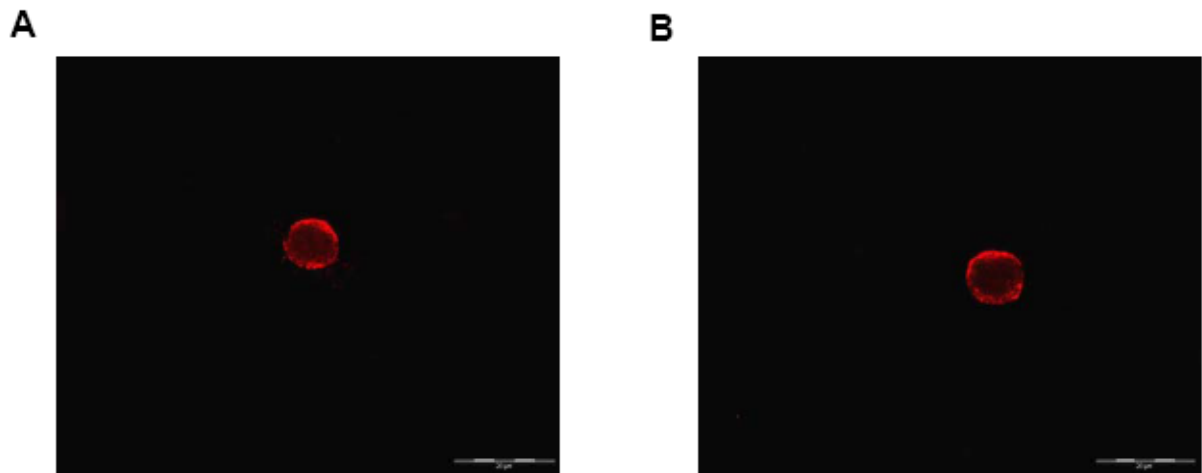

Figure 19: Surface expression of Thy-1 in blood streaks derived from control (A) and DAPAT ko (B) mice. Thy-1 is highly abundant on the surface of both wt and ko T cells. In contrast, surrounding erythrocytes do not express Thy-1 and are therefore not stained. Original magnification: 60x; scale bars: 20 μm

3.3.2   Surface Localization of Human Thy-1

In order to evaluate, if also in humans affected by ether lipid deficiency GPI anchors are properly directed to the plasma membrane, the respective patient fibroblasts were stained for Thy-1 in a similar fashion as described for murine cells. The RCDP patient cell line 2-2 was chosen as most suitable model for this experiment due to the very low plasmalogen content of these cells in culture (see chapter 3.1.1) and the severe phenotype of the respective patient.

Again, staining was performed without any permeabilization to examine surface exposition of the Thy-1 antigen. Similar to what had been observed in mouse fibroblasts, Thy-1 was found to be expressed and transported to the surface by fibroblasts deficient in ether lipid synthesis. Staining for the GPI-anchored protein in RCDP patient cells revealed a pattern that closely resembled that in control fibroblasts (see Figure 20). In patient fibroblasts, as in murine DAPAT ko fibroblasts, the average size of the individual, differentiated dots, probably indicating raft structures, appeared a little larger than in controls. However, from the results of these studies, it can be concluded that ether lipid synthesis is not necessary for the expression and surface localization of GPI-anchored proteins in murine or human cells.
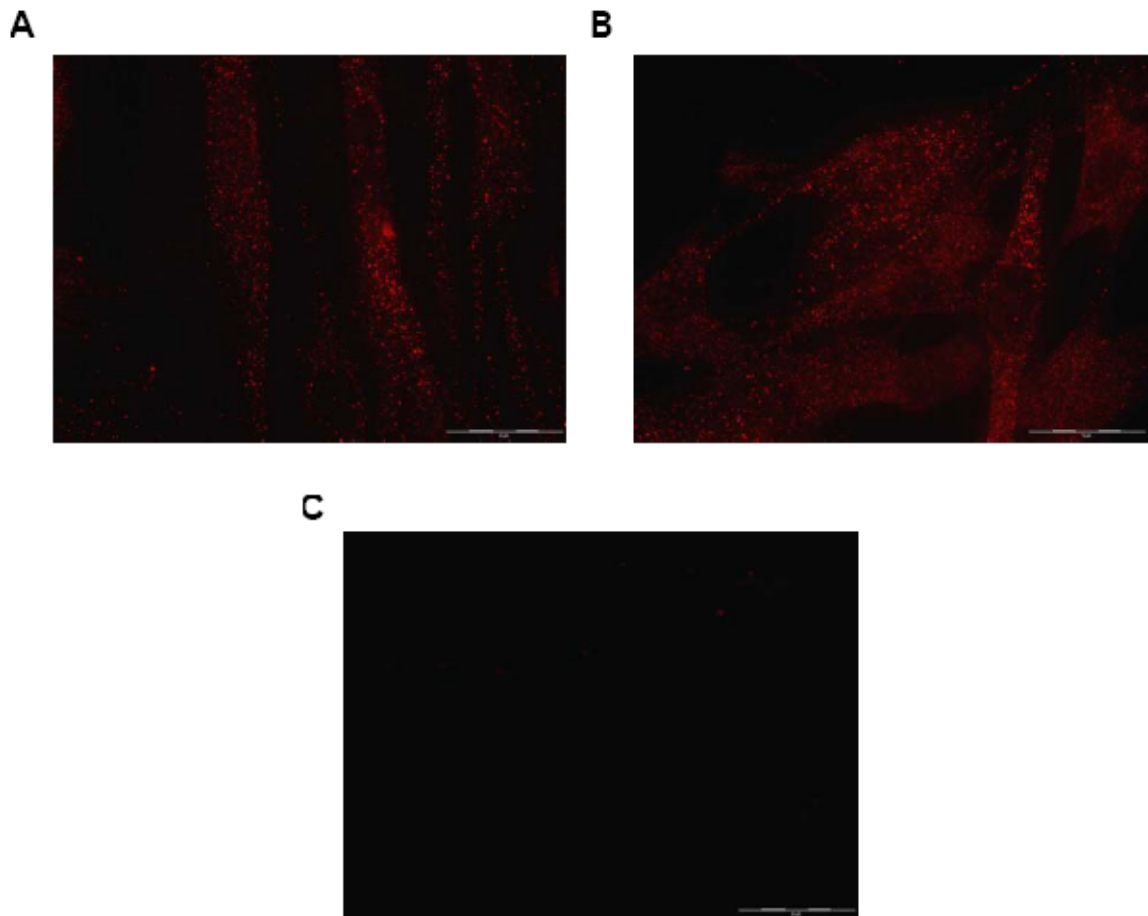
Figure 20: Surface expression of Thy-1 in human fibroblasts. Thy-1 is expressed on the surface of both control cells (A) and fibroblasts deficient in ether lipid biosynthesis (B). An antibody control is depicted in (C). Original magnification: 40x; scale bars: 50 µm

3.4 Relative Amounts of Some Membrane Raft Proteins Are Dysregulated in Ether Lipid-Deficient Human Fibroblasts

Plasmalogens are essential constituents of cellular membranes, especially of membrane rafts. Therefore, it can be assumed that, upon deficiency of ether lipids, membranes undergo some rearrangement in order to compensate for the loss of these molecules. To determine, if any of these changes affect the levels of raft- and non-raft-associated membrane proteins in human patients, RCDP fibroblast cell lines were subjected to western blot analysis.

For this purpose, total proteins were prepared from three normal human fibroblast lines and two lines each derived from patients suffering from the mild (cell lines RCDP 2-1 and RCDP 3-1; cf. Table 1) and severe form (cell lines RCDP 2-2 and RCDP 1-2) of RCDP, respectively. Protein contents were determined by the Bradford assay, equal amounts of protein loaded onto SDS gels and protein levels examined by western blot analysis (Figure 21).

Figure 21: Western blot analysis of membrane protein amounts in total extracts of human fibroblasts. The relative amounts of a membrane-associated raft protein (flotillin-1) (A), a membrane-spanning raft protein (connexin 43) (B), GPI-anchored proteins (Thy-1, CD55) (C) and a non-raft transmembrane protein (transferrin receptor) (D) were determined. C1-C3 indicate control lines; 2-1 and 3-1 belong to the "mild disease course" group; 2-2 and 1-2 are fibroblasts derived from patients with most severe plasmalogen deficiency. Separating gel concentrations varied from 9% to 12% acrylamide, applied protein amounts were between 7 and 25 µg (according to the protein to be detected). After detection of membrane proteins, the same blots were reprobed for β-actin as a loading control. β-Act, β-actin

In order to obtain a rather complete picture, the examined proteins included:

- A membrane-associated raft protein, flotillin-1, whose connection with the plasma membrane is dependent on its palmitoylation (Morrow et al., 2002);
- a membrane-spanning raft protein, connexin 43 (Cx43), containing four transmembrane domains (Goodenough et al., 1996);
- GPI-anchored proteins, Thy-1 and CD55; and
- a transmembrane protein known not to be associated with membrane rafts (transferrin receptor).

Although the relative levels of several proteins appeared to be rather heterogeneous already in the three control lines, some remarkable irregularities could be observed, especially in severely affected patient fibroblasts (see Figure 21). Flotillin-1 seemed to be enriched in two of the cell lines defective in DAPAT (RCDP 2-1 and 2-2), but not in any other fibroblast line deficient in ether lipid synthesis. Surprisingly, a similar pattern was observed for the non-raft marker transferrin receptor – probably these two cell lines generally contain a higher amount of membrane proteins in relation to cytosolic ones. Striking abnormalities were found in case of the transmembrane protein connexin 43: Compared to controls, the protein was almost absent in cell line RCDP 2-2. Additionally, reductions were also determined in the second line derived from a severely impaired patient (RCDP 1-2) and a mildly affected line (RCDP 3-1). In mammals, Cx43 occurs in three different phosphorylation states (Musil et al., 1990) leading to three slightly distinct bands (partly visible in Figure 21 and Figure 22). All three variants were affected equally by the loss of Cx43 and there was no observable difference in phosphorylation state between control and plasmalogen-deficient cell lines.

Both of the examined GPI-anchored proteins were rather hard to detect in total cell extracts (partly because of the background produced by the antibodies used). Nevertheless, abnormalities in their relative amounts were again discovered in cell lines derived from severely impaired patients. Thy-1 showed rather equal intensities in all cell lines except RCDP 2-2, in which it was almost absent. In contrast, CD55 seemed to be reduced in both severely affected lines. However, the levels in three different control lines exhibited a remarkable variability as well. Taken together, dysbalances in membrane protein amounts were observed in plasmalogen-deficient cell lines and were particularly pronounced in a cell line defective in the DAPAT protein (RCDP 2-2).

In order to exclude the possibility of different cell sizes leading to varying amounts of membrane proteins and to avoid the high background level produced by some antibodies in total extracts, crude membrane preparations of the same cell lines were performed to confirm the obtained results. Equal protein amounts were again applied to SDS gels and analyzed by immunoblotting (see Figure 22). The non-raft protein transferrin receptor served as loading control in spite of the fact that its levels seemed to be slightly variable in total extracts.
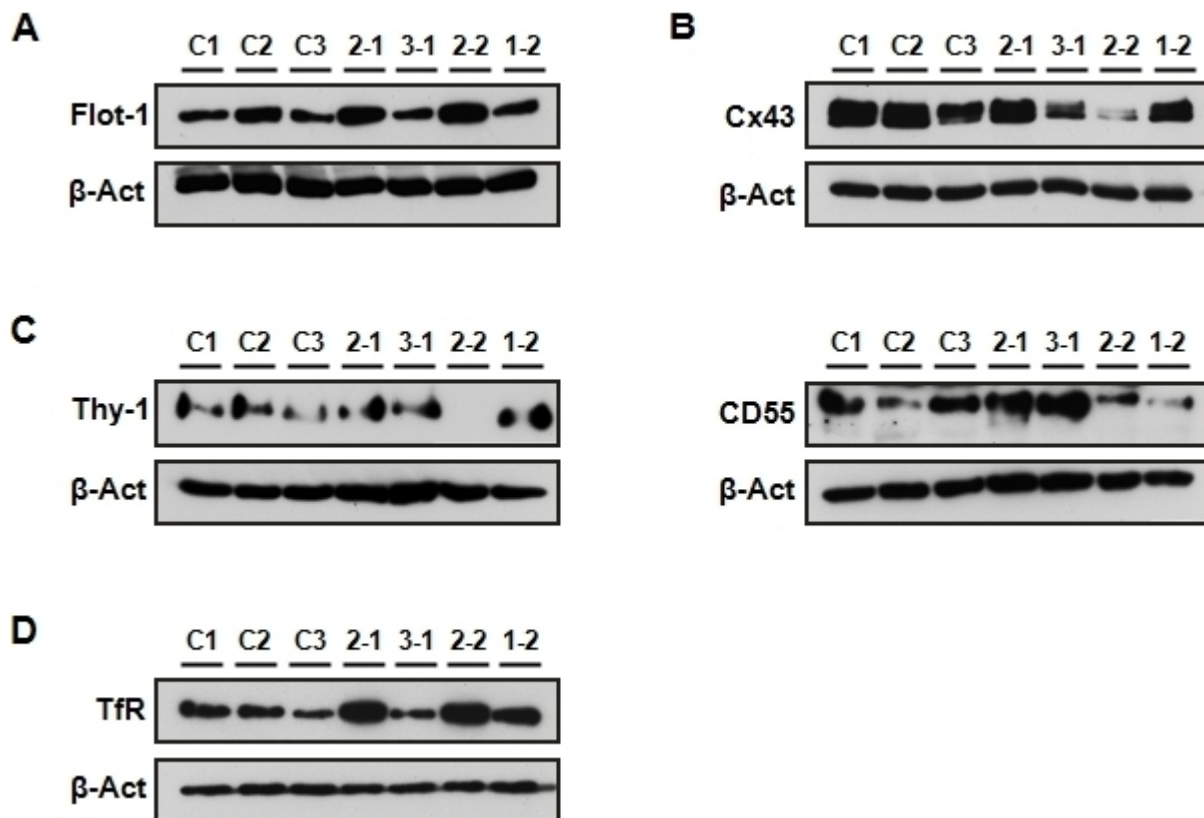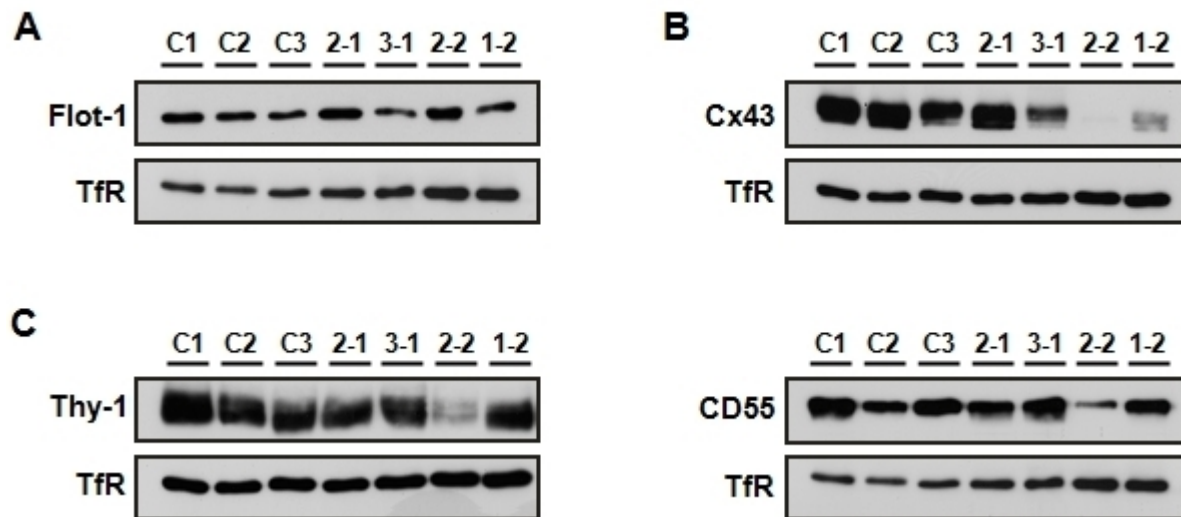
Figure 22: Western blot analysis of membrane protein amounts in crude membrane preparations of human fibroblasts. The relative amounts of a membrane-associated raft protein (flotillin-1) (A), a membrane-spanning raft protein (connexin 43) (B) and GPI-anchored proteins (Thy-1, CD55) (C) were determined. C1-C3 indicate control lines; 2-1 and 3-1 belong to the "mild disease course" group, and 2-2 and 1-2 are fibroblasts derived from patients with most severe plasmalogen deficiency. Separating gel concentrations varied from 9% to 12% acrylamide, applied protein amounts were between 5 and 8 µg (according to the protein to be detected). After detection of raft proteins, the same blots were reprobed for TfR as a loading control. The displayed results are representative of two independent preparations. TfR, transferrin receptor

The results illustrated in Figure 22 were in good agreement with the findings of western blot analysis in total extracts. Flotillin-1 levels in membrane preparations appeared rather similar in all cell lines with slightly stronger bands visible in the two DAPAT-deficient fibroblast lines RCDP 2-1 and RCDP 2-2. Concerning the amounts of Cx43, obvious differences were visible as already observed in the total extract. Cell line RCDP 2-2 exhibited very low Cx43 levels in the membrane-enriched fraction compared with all other lines. In addition, the amounts were clearly decreased in lines RCDP 3-1 and RCDP 1-2.

Both examined GPI-anchored proteins (Thy-1 and CD55) were severely reduced in RCDP 2-2. However, the second cell line derived from a patient with severe disease course, RCDP 1-2, did not show any noticeable differences in comparison with control and mildly affected cell lines. The latter behaved like control cells in all cases with exception of Cx43 levels in line RCDP 3-1.

3.5 Thy-1 Associates with Membrane Rafts, But Floats to Slightly Higher Density in Ether Lipid-Deficient Human Fibroblasts

When being integrated into the plasma membrane, GPI-anchored proteins are thought to be selectively targeted to membrane raft domains (see chapter 1.4). In ether lipid-deficient cell lines, the lipid portion of the GPI anchor does not contain the ether form alkylacylglycerol. The consequences of this defect for the membrane distribution of these proteins are still unclear. In chapter 3.3.2, it was shown that association with the plasma membrane is still possible in human RCDP fibroblasts that are severely defective in ether lipid synthesis. However, the correct localization of GPI-anchored proteins to membrane rafts cannot be determined, but only hypothesized from immunofluorescence methods. Instead, biochemical approaches are required to get an insight into the raft association of the GPI anchor under conditions of ether lipid deficiency.

Therefore, the concept of detergent-resistant membranes (DRMs) was applied to RCDP and control fibroblasts. Three control cell lines and two lines each derived from mildly affected RCDP patients and RCDP patients with a severe phenotype, respectively, were tested concerning the DRM association of a GPI-anchored protein. Fibroblasts were lysed in 1% Triton X-100 and, subsequently, DRMs were isolated by density gradient centrifugation as described (see chapter 2.2.3). DRMs are characterized by their flotation abilities, meaning that – after lysis – during centrifugation they float to the light fractions at the top of a sucrose gradient (see Figure 7). However, in every DRM experiment, the presence of raft-like structures in the top fraction has to be proven by a marker protein, which is typical of these membrane subdomains. Here, flotillin-1, a widely used raft marker (Morrow and Parton, 2005), was used for this purpose. In contrast, the transferrin receptor (TfR) was engaged as marker of the non-raft membrane fraction. A constant number of confluent cell culture dishes was utilized for density gradient experiments; the protein amount loaded onto SDS gels for analysis was normalized by determining the total protein content of all gradient fractions. Equal volumes of the fractions originating from the same gradient were applied and the exposure times for development of western blots kept in similar ranges throughout the whole experiment. In all gradients, protein content proved to be very low and hardly detectable by a classical Ponceau staining in the top (=DRM) fractions. In contrast, high amounts of protein were detected in the detergent-soluble fractions. This is in line with literature about DRM isolation, which states that – compared to the total amount of protein in a cell – a very minor part of proteins is DRM-associated.

Figure 23A shows the distribution of the raft marker (flotillin-1), a GPI-anchored protein (Thy-1), which – at least under normal conditions – is supposed to localize to membrane rafts as well, and the non-raft marker (TfR) in control fibroblast cell lines. Flotillin as well as Thy-1 are almost exclusively found in the topmost fractions of the gradient, whereas transferrin receptor is located in the lowermost fractions, where all detergent-soluble proteins, including cytosolic and non-raft membrane proteins, are expected. A third control cell line showed identical results with regard to the distribution of all three examined proteins (data not shown). However, in all controls also some flotillin was detected in detergent-soluble fractions.

A

B

C
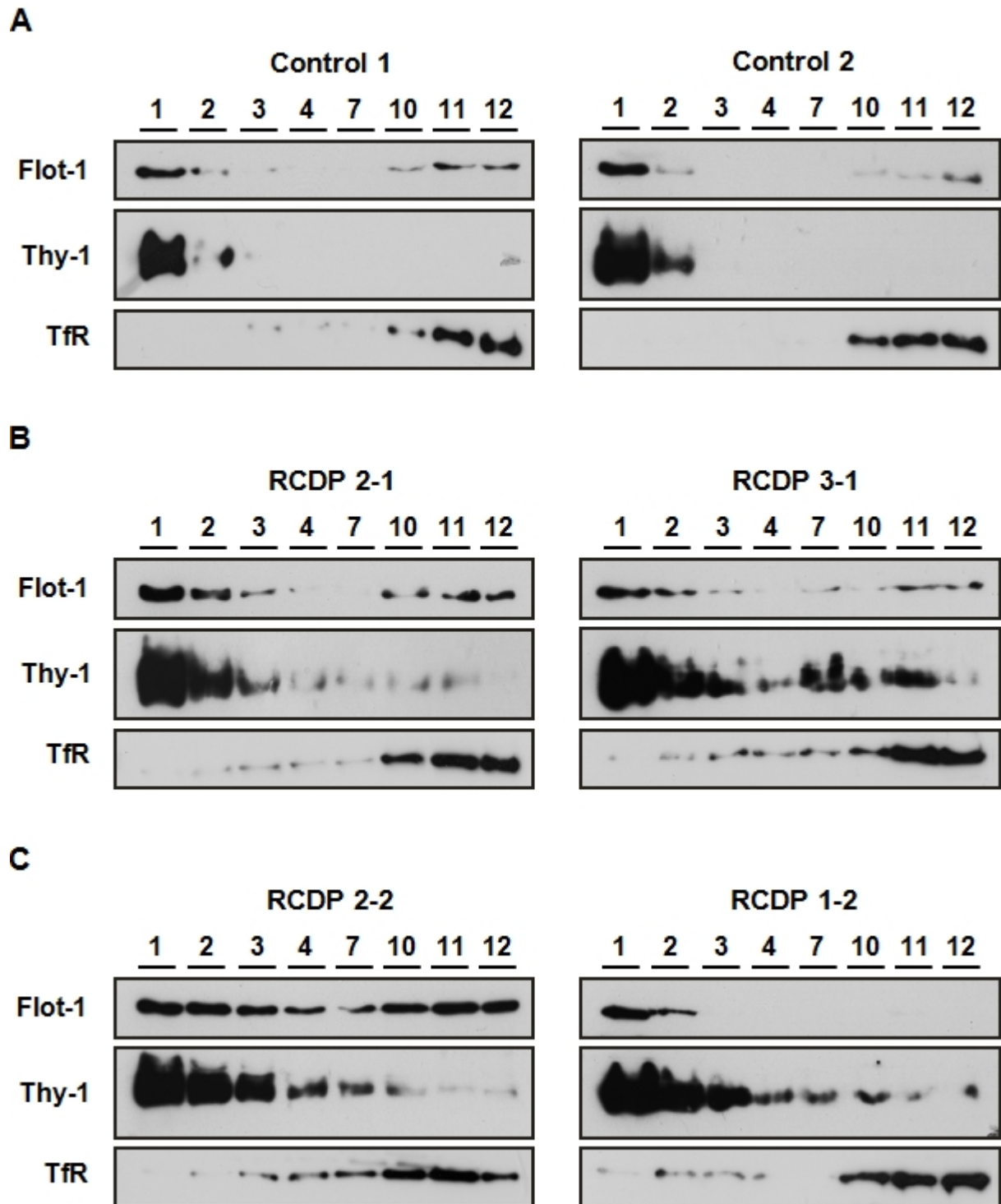
Figure 23: Western blot analysis of DRMs isolated from control (A) and RCDP fibroblast cell lines representing the mild (B) and the severe (C) form of the disease. Twelve fractions were collected from each sucrose gradient from the top; "1" indicates the lightest fraction. For illustration, only the top four fractions (1-4; detergent-resistant material), one medium density fraction (7) and the three lowest fractions (10-12; detergent-soluble material) are shown. Thy-1 is heavily glycosylated and appears therefore as a smear rather than a distinct band. Concentration of separation gel: 12% acrylamide. All three examined proteins were detected on the same blots by stripping and reprobing with the corresponding antibodies. Total protein amounts were equal in all SDS gels; equal volumes of the fractions originating from the same gradient were applied. Flot-1, flotillin-1; TfR, transferrin receptor

Fibroblasts representing the mild and severe form of RCDP (Figure 23B and C, respectively) exhibited a somewhat different distribution of marker and GPI-anchored proteins. Although TfR was present in the lowermost fractions and largely excluded from the DRM fractions as was the case in control lines, RCDP cell lines differed from control lines with respect to the localization of raft proteins. Flotillin distribution was rather similar to control cell lines with exception of line RCDP 2-2 (carrying mutations in the GNPAT gene), in which the amount in detergent-soluble fractions was approximately equal to that in the detergent-resistant portion. Thy-1, however, showed an increased tendency to shift to fractions of higher density, which could be observed in cells derived from mildly as well as severely affected patients. Whereas in control cells Thy-1 was only detectable in the lightest two fractions, it was distributed over more, if not all fractions in RCDP cell lines, even though the highest amounts were still present in the top fractions. In all four patient fibroblast lines, signals were clearly visible in fraction 3 (where no Thy-1 was detected in controls) and traces even in fractions 10-12.

Taken together, these results suggest differences in the DRM-association of the representative GPI-anchored protein Thy-1, which, however, demand further confirmation by additional DRM experiments.

3.6 Formation of the Neuromuscular Junction Is Modified in the DAPAT Ko Mouse

Continuous observation of their behavior in the cage shows profound deficiencies of the motor system in DAPAT (-/-) mice. Teigler and collaborators indicated weak performance of these mice in several behavioral tests that also involve motor function, but no data are provided (Teigler et al., 2009). Thus, in the following approach, motor deficiencies were first confirmed and scored using motor-behavioral tests. In order to study the mechanisms underlying the motor deficits, a closer look was then taken at the neuromuscular junction (NMJ), a structure, where the synapses between motor nerves and muscle fibers are formed. NMJ formation was studied in vitro by using myotubes derived from DAPAT ko mice.

3.6.1 DAPAT Ko Mice Show Abnormalities in Motor Ability

Two different age cohorts (3-4 months, 7 months) of male mice were subjected to testing on an accelerating Rotarod treadmill and on a balance beam.

Rotarod

The latency to fall off an accelerating Rotarod apparatus was measured in order to evaluate motor coordination abilities. Experiments revealed apparent differences in motor skills between DAPAT ko and age-matched wt mice (see Figure 24) that, however, were not statistically significant according to a Mann-Whitney rank sum test (P=0.189 for 3-4 months old mice; P= 0.140 for 7 months old mice). Observations suggested that ko mice – probably due to their impaired visual abilities and overall physical handicaps – stayed much more focused on their task, while wt mice spent more time exploring their surroundings (especially at the beginning of the test) and therefore suffered early falls in some cases.

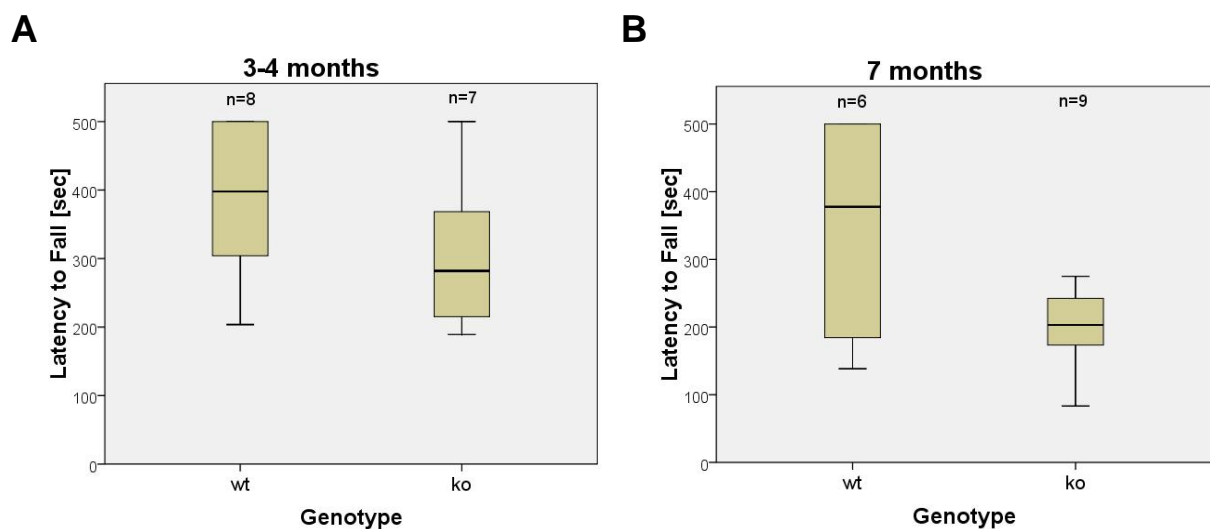Figure 24: Motor behavior of 3-4 months old (A) and 7 months old (B) DAPAT ko and wt mice on an accelerating (4-40 rpm) Rotarod treadmill. Box plot graphics show the median values; 1st and 3rd quartiles (50% of values) are boxed, whiskers indicate highest and lowest values within 1.5 times the interquartile range. For statistical analysis, Mann-Whitney rank sum test was used (3-4 months: P=0.189; 7 months: P=0.140).

Overall, the mean value of performance in wt mice stayed relatively similar – though more variable – in older animals compared with younger ones, whereas motor behavior of older ko mice was slightly poorer than that of younger ones, which, however, exhibited considerable variation.

Balance Beam

The performance in the trials of age-matched wt and ko mice on the balance beam, a wooden rod of about 2 cm diameter, that they had to cross three times, was judged according to a scoring system as indicated in Table 2.

Score	Description
1	Performs task without problem, stepping with all four paws on top quarter of the rod
2	Performs task, slipping with hind paws below top quarter of the rod
3	Performs task, slipping with hind paws below midline of the rod
4	Performs task poorly, dragging hind limbs below midline or slipping with front and hind limbs below midline
5	Cannot perform task; falls off the beam

Table 2: Scoring system for evaluation of performance on the balance beam; grading steps of 0.5 were employed for more exact evaluation (e.g. 2.5 for occasional slipping below the midline)

Differences between wt and ko animals (age cohorts as described above) were clearly visible on the balance beam and also proved to be highly significant ($P<0.001$ for age 3-4 months; $P=0.003$ for age 7 months). Although wt mice appeared to be timid as well, when first confronted with the balance beam task, which is likely to be due to their sparse movement associated with caging, they were mostly able to cross the bar without any problems and with their feet mainly above the drawn midline (see Figure 25). In contrast, DAPAT ko mice displayed marked deficits in motor ability during the balance beam test. Most of them could not cross the bar in a proper fashion, many refused to cross the rod at the beginning of the training sessions. Additionally, ko mice were not able to keep their hind limbs on the top of the beam (above the midline). Instead, their hind feet slid down repeatedly, leading to forward movement in a crawling manner while straddling the rod. Some ko animals completely failed to execute the task, as they quickly fell off the bar even after several training efforts.

Regarding both ko and wt mice, motor performance decreased with higher age, while the relative differences between the two groups (wt; ko) stayed comparably similar.

A

B

C
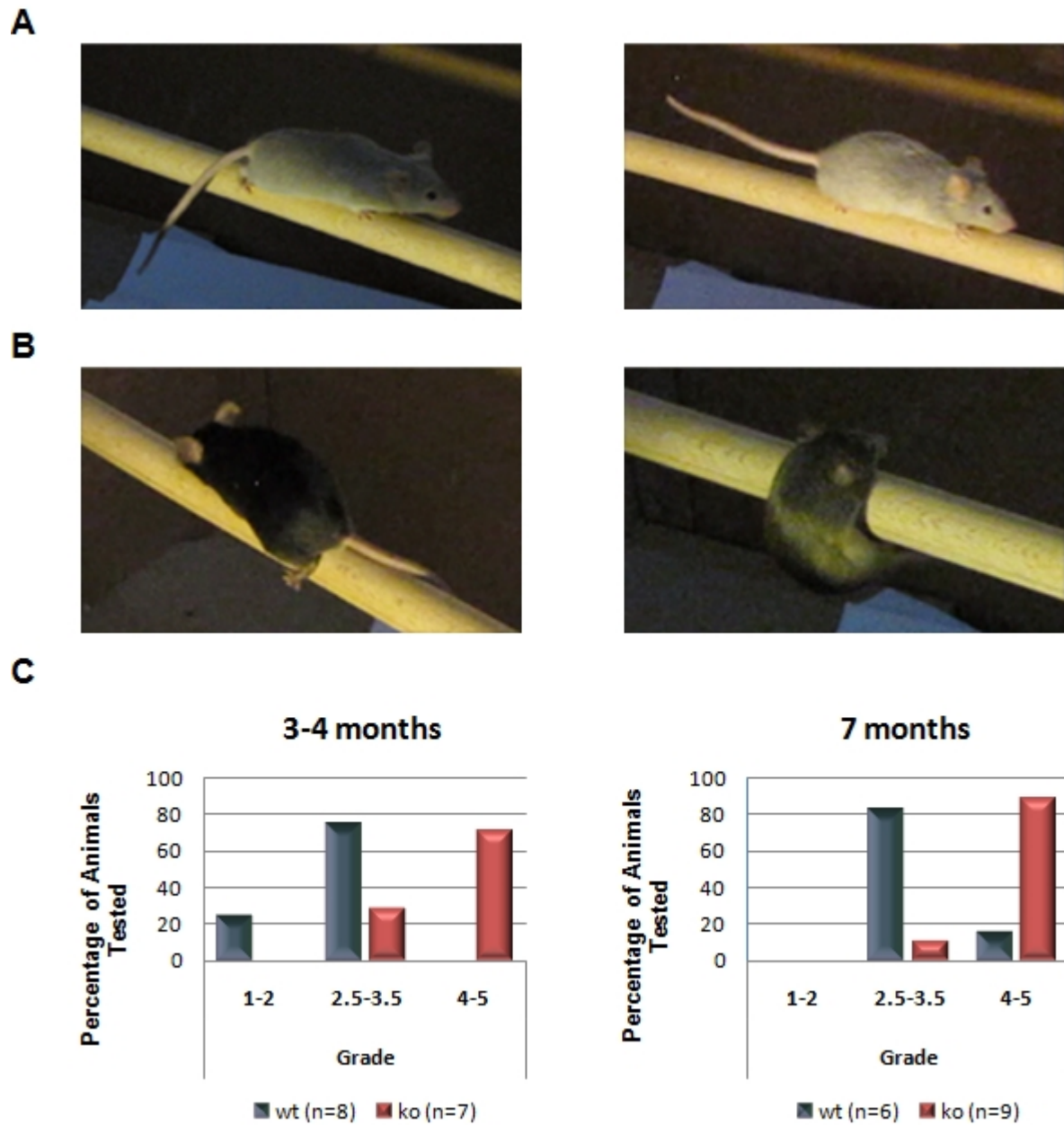
Figure 25: Motor skills of wt and DAPAT ko mice on the balance beam. (A) Performance of wt mice (7 months) on the beam: Mice cross the rod quickly after learning, with their hind limbs usually above the midline. (B) Performance of ko mice (7 months) on the beam: Hind limbs are usually below the midline and the mice rather crawl than run across the rod. (C) Overall balance beam performance of 3-4 months old (left) and 7 months old (right) wt and DAPAT ko mice; statistical differences were highly significant ($P<0.001$ for age 3-4 months, $P=0.003$ for age 7 months) upon analysis using Mann-Whitney rank sum test.

3.6.2 Smaller Acetylcholine Receptor Clusters Are Formed in DAPAT Ko Myotubes

To evaluate the proper in vitro formation of agrin-elicited acetylcholine receptor (AChR) clusters, which mimics the development of a neuromuscular junction, primary myoblasts were isolated from newborn DAPAT ko and control mice. Myoblasts were, as far as possible, separated from fibroblasts and kept in culture for a few days until they reached confluency, meaning that the cellular processes were in close proximity to each other. Fusion of myoblasts, similar to the formation of muscle fibers in vivo, was induced by a switch to differentiation medium. Progress in the formation of myotubes as a result of myoblast fusion was observed by light microscopy. After two to three days of differentiation, clustering of AChRs, which, in the living organism, are crucial for the regulation of electrical activity and the contractile state of the muscle, was induced by addition of recombinant agrin to the medium. Agrin is a 200 kDa protein, which is deposited by nerve cells and has been shown to cause clustering of pre-existing AChRs on the surface of cultured myotubes (Godfrey et al., 1984; McMahan, 1990), an effect that is mediated by the receptor tyrosine kinase MuSK (muscle specific kinase) (Glass et al., 1996). After overnight stimulation with agrin, AChR clusters were stained with fluorescent-dye-coupled α-bungarotoxin, which binds irreversibly to muscular AChR, and visualized by fluorescence microscopy.

During culturing, myoblasts derived from ko animals seemed to exhibit slower growth than those derived from wt mice. Total numbers of isolated myoblasts were lower as well, which, however, could also be a consequence of incidental differences in the isolation procedure. In addition, overall size of myotubes appeared smaller in ko cultures, which could be assigned to differences in myoblast numbers. However, although these differences were noticed in several isolations, they were not quantified and can therefore only serve as preliminary observations.

Staining of AChRs revealed that agrin-induced clusters can be as efficiently formed in myotubes derived from ko animals as in wt myotubes (see Figure 26A and B for a representative example). Quantification of cluster size (in terms of length) and number in the different cultures was executed by fluorescence microscopic tools. The summary of one representative experiment is indicated in Figure 26C and D: Although cluster length values showed a relatively great variation, slight differences could be discovered between wt and ko cultures. However, these did not reach statistical significance in this experiment (P=0.093). In contrast, the number of clusters (in relation to the length of myotubes) was not changed between the two groups. The observed small difference in the mean value in this case is highly likely to be due to random sampling variability (P=0.861).
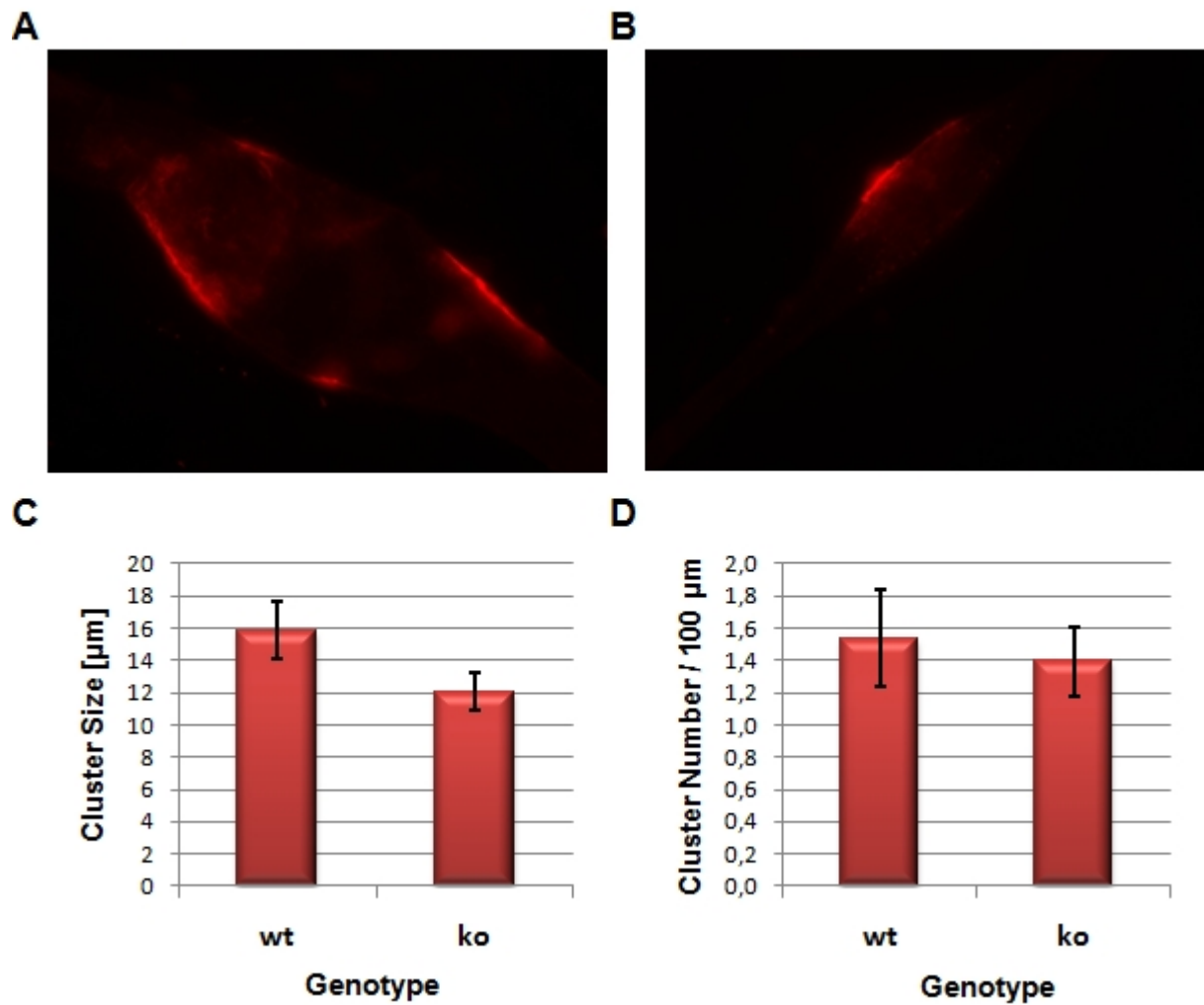
Figure 26: Formation of acetylcholine receptor clusters in cultured murine myotubes. Fluorescence microscopic analysis of AChR clusters stained with α-bungarotoxin in wt (A) and DAPAT ko (B) myotubes. There are no apparently visible differences in cluster formation and shape between knockout and control cultures. Original magnification of microscopic images: 63x. (C) Quantification of AChR cluster size (length) in cultured myotubes. Total numbers of evaluated clusters were 39 in case of the wt and 33 in case of the ko culture. Mean values are depicted with error bars representing S.E.M. values. Statistical analysis was carried out using a two-tailed Student's t-test (P=0.093). (D) Cluster number in relation to myotube length. Numbers of evaluated myotubes were 19 in each case. Mean values are depicted with error bars representing S.E.M. values. Statistical analysis was carried out using Mann-Whitney rank sum test (P=0.861).

CHAPTER 4
DISCUSSION

The present thesis is intended to contribute to the clarification of the role of ether lipids in physiological and pathological processes. Notably, the material used is derived directly from either human patients suffering from ether lipid deficiency or a corresponding mouse model and is therefore in close relation to the respective disease, RCDP. Ultimately, this and further studies should bring us closer to the understanding and – as a consequence – the cure or at least a relief of this severe disease.

In the course of this work, the general phospholipid profiles of control fibroblasts and fibroblasts deficient in ether lipid biosynthesis were examined. In controls, PC was identified as the major phospholipid species with the remaining phospholipid mass quite equally shared among PE, PS, SM and PL-PE. The values obtained are mainly in line with recent publications reporting phospholipid composition in fibroblasts (Murphy et al., 2006; Murphy et al., 2000b; Styger et al., 2002). Only the percentage of PS described in literature tends to be a bit lower than that in the present work.

A main focus of this diploma thesis was on the examination of plasmalogens in fibroblasts derived from RCDP patients. Nowadays, RCDP is reported as a disease with rather heterogeneous appearance especially concerning its severity. Many affected children do not survive their first years of life, whereas others display only some of the typical RCDP symptoms and reach a more advanced age. For the present study, three different skin fibroblast lines derived from patients who suffered from such a mild form of the disease were available. Line RCDP 1-1 harbors one allele with a non-functional copy of PEX7 (L292X mutation; see below); the second allele carries a different mutation (H285R), which is supposed to enable normal folding of the protein, but leads to decreased affinity for binding partners (Braverman et al., 2002). In cell line RCDP 2-1, a homozygous mutation in one of the splice donor sites of the GNPAT gene induces impaired splicing of the mRNA, resulting in a milder form of RCDP due to residual DAPAT activity. Finally, in cell line RCDP 3-2, which carries a homozygous AGPS mutation, AGPS appears largely degraded but displays residual activity, as has been concluded from the rate of plasmalogen biosynthesis (Itzkovitz et al., 2009). Lipidomic analysis in this work revealed a significant reduction of plasmenylethanolamines in all three mutant cell lines when compared with controls. The obtained values were between 50 and 70% of the control mean. This is in good agreement with the observation that the degree of plasmalogen deficiency determines disease severity (Braverman et al., 2002). Plasmalogens in mildly affected fibroblasts are markedly reduced, but still a considerable amount of these lipids is present to fulfill its functions. However, compared with the present analysis, other publications describe slightly lower plasmalogen levels in patients with mild RCDP, e.g. Braverman and collaborators report plasmalogen levels of ~30% in red blood cells (RBC) of these individuals (Braverman et al., 2002). Besides, a mouse model representing the mild variant of RCDP exhibits 30-50% RBC plasmalogen levels as compared to controls (Braverman et al., 2010). In addition to fibroblasts of mildly affected patients, four fibroblast

Discussion

lines derived from patients suffering from severe RCDP were analyzed: Cell lines RCDP 1-2 and 1-3 each express two non-functional copies of PEX7. In cell line RCDP 2-2, a homozygous single base pair deletion in exon 10 of the GNPAT gene was identified and shown to be the consequence of paternal isodisomy of chromosome 10 (Nimmo et al., 2010). The fourth severely affected fibroblast line (RCDP 3-2) carries a homozygous AGPS mutation rendering the AGPS protein non-functional (Itzkovitz et al., 2009). Interestingly, all of these cultures exhibited severely reduced, but still substantial amounts of plasmenylethanolamines. Furthermore, two of the cell lines (RCDP 1-3 and RCDP 3-2) rather behaved like cells of the "mild course" group, as they displayed plasmalogen levels of about 40% of the control mean, whereas the other two severely affected lines (RCDP 1-2 and RCDP 2-2) reached only ~15%.

In principle, complete deficiency in plasmalogen biosynthesis was expected in all fibroblast lines derived from RCDP patients of the "severe course" group, as all of them carry mutations that fully inhibit the peroxisomal steps of ether lipid formation. The high value measured for cell line RCDP 1-3 is especially surprising, as these fibroblasts carry the L292X mutation in both PEX7 alleles. This mutation is found at extraordinarily high frequency in RCDP type I patients (Braverman et al., 1997; Brites et al., 1998), which has been shown to be the result of a founder effect in a Caucasian population (Braverman et al., 2000). Although near normal mRNA levels are produced, the resulting protein has been proven to be non-functional (Braverman et al., 2002; Motley et al., 2002). The high plasmalogen levels obtained are also surprising with regard to the results of Braverman et al. and Nimmo et al., who found nearly non-detectable rates of RBC plasmalogens and plasmalogen biosynthesis in fibroblasts of patients homozygous for the deleterious L292X mutation and the RCDP type II patient carrying the homozygous deletion in the GNPAT gene (cell line RCDP 2-2) (Braverman et al., 2002; Nimmo et al., 2010). However, in cultured cells deficient in ether lipid biosynthesis, residual amounts of plasmalogens have been observed by other groups as well: CHO cells defective in DAPAT or AGPS exhibit plasmenylethanolamine levels of about 10% of the wild type level (Mankidy et al., 2010; Nagan et al., 1997). Moreover, almost 50% of the control PL-PE value was demonstrated in fibroblasts of Zellweger patients, which due to their inability to assemble peroxisomes should also be highly deficient in synthesizing ether lipids (Styger et al., 2002). From these observations, the question of the origin of these residual plasmalogens under conditions of deficient ether lipid synthesis arises. Possibly, an alternative, non-peroxisomal pathway of ether lipid synthesis exists e.g. involving a non-peroxisomal DAPAT activity, like the one described by Schlossman and Bell (Schlossman and Bell, 1976, 1977). Alternatively, in case of PEX7 mutations, some AGPS could be transported to the peroxisome in a complex with DAPAT in a PEX5-dependent fashion. Such a "piggy-back" mechanism would be PEX7-independent and would occur also in the absence of the functional PTS2 receptor. However, both of the mentioned possibilities seem rather unlikely, as they do not account for the low plasmalogen levels found in RBCs of patients and the low plasmalogen biosynthesis rate in fibroblasts. Instead, it appears highly probable that cultured cells can take up plasmalogens or ether lipid precursors, which are utilizable for plasmalogen biosynthesis, from the culture medium containing FBS. This explanation is also in line with the observation that cell lines RCDP 1-3 and RCDP 3-2 exhibited slower growth in culture: more slowly dividing cells could incorporate higher amounts of plasmalogens from the medium, before they have to "share" the lipids with their daughter cells. To prove this assumption, the use of plasmalogen-free culture medium (e.g. synthetic FBS substitution products) would be required and is intended for future experiments involving ether lipid-deficient fibroblasts. Nevertheless, the findings made in this study reveal significant differences in ethanolamine plasmalogen levels between healthy controls, patients suffering from the mild form of RCDP and patients affected by the severe form of the disease.

Concerning the fatty alcohol distribution at the sn-1 position of ethanolamine plasmalogens, mass spectrometric analysis identified C16:0 as the predominant species followed by C18:0 and C18:1. This is basically in accordance with the values reported in a similar experiment with wild type CHO cells (Mankidy et al., 2010). However, the pattern of the different alkyl chains was rather diverse in three different control lines, pointing to a rather random incorporation at the sn-1 position. The sn-1 chain in plasmalogens is determined by a fatty alcohol introduced by AGPS. This alcohol is predominantly produced by the fatty acyl-CoA reductase, Far1 (Honsho et al., 2010), which preferably uses saturated and monounsaturated fatty acyl-CoAs with chain lengths of 16 or 18 carbon atoms as substrates (Cheng and Russell, 2004), at the outer peroxisomal membrane surface. The alkyl chain distribution at the sn-1 position in the examined control lines therefore rather reflects the incidental availability of fatty acyl-CoAs used by Far1 than a predetermined pattern of fatty alcohol incorporation. However, in all fibroblast lines of severe RCDP patients, there was a consistently lower percentage of C18:0 at the sn-1 position. In case the residual plasmalogen levels of these cell lines were derived from remaining cellular biosynthesis mediated by a "piggy-back" mechanism or an alternative pathway, the offered sn-1 profile points towards either a different availability of fatty acids under conditions of defective peroxisomal ether lipid biosynthesis or – in case of an alternative pathway – a different substrate specificity of one of the involved enzymes. On the other hand, if RCDP fibroblasts utilize precursors or plasmalogens provided by the culture medium, the observed pattern at the sn-1 position might just represent the structure of the provided molecule, as the sn-1 chain is not remodeled after uptake of an ether lipid precursor (see below).

As expected on the basis of other papers, plasmalogen deficiency in cultured fibroblasts could be successfully overcome by supplementation with hexadecylglycerol and batyl alcohol. Remarkably, also HDG attached to a phosphate at the sn-3 position, was able to permeate the fibroblasts and proved at least as efficient for recovery of plasmalogen levels as the other two compounds. Astonishingly, three-day-treatment did not only restore plasmalogens to the amounts reached in controls but, moreover, exceeded the control values by far. HDG-treated fibroblasts, for example, exhibited as much as 22% plasmenylethanolamines out of all detected phosholipids compared with ~12% measured in control cells. In contrast, 72-hour-treatment of DAPAT-deficient CHO cells with 20 µM HDG – an equal concentration as used in the present study – was reported to result in PL-PE levels slightly above the wild type value (Nagan et al., 1998). Another publication describes the restoration of plasmenylethanolamines to only about 65% of the control level after 24-hour-supplementation of Zellweger fibroblasts with 20 µg/ml (~63 µM) HDG (Styger et al., 2002) – a higher concentration, but shorter time than applied here. The results obtained for RCDP patient cells indicate that uptake and utilization of plasmalogen precursors in human fibroblasts occur extremely efficiently, if the respective substances are added in micromolar concentrations for a sufficient time. Notably, the cells take up and most probably utilize more ether lipid precursors than they synthesize themselves in the absence of any culture medium supplement. This may indicate that plasmalogens are highly favorable lipids for fibroblasts, as the cells apparently engulf as much of these compounds as is available.

Lipidomic analysis of the sn-1 chain after treatment showed clearly that the composition of the precursor molecule determines the sn-1 composition of the final plasmalogen. Treatment with HDG (a C16 glycerol ether) only restored plasmenylethanolamines with a C16:0 chain, whereas supplementation with BA led to a strong increase in C18:0 plasmalogens. This result is in line with the observations of Mankidy and collaborators, who describe a similar determination effect at sn-1 in a DAPAT-deficient CHO cell line after application of several precursor substances (Mankidy et al.,

2010). Evidently, the sn-1 moiety does not undergo any rearrangement after uptake of the precursor as opposed to the sn-2 chain, which has been shown to be deacylated and, subsequently, reacylated with other fatty acid residues (Mankidy et al., 2010). Surprisingly, in a mouse model of mild RCDP (see chapter 1.2.2), treatment with batyl alcohol increased the blood levels of all plasmalogen species (C16:0, C18:0 and C18:1). Possibly, a multicellular organism enables a more complex and versatile utilization of a supplemented precursor molecule. Alternatively, the precursor might, e.g. by some feedback mechanism, stimulate further synthesis of ether lipids, which to a low extent is possible in this Pex7 hypomorphic mouse. In the latter case, one would hypothesize that in a complete knockout the full spectrum at the sn-1 position cannot be recovered.

So far, it is not known, whether the composition of the sn-1 moiety has any effect on the function of plasmalogens. Therefore, there might be no physiological difference between supplementing cells with HDG or with BA in order to regain plasmalogens. However, if a regeneration of the full spectrum of different plasmenylethanolamines is intended, at least in culture, a mixture of precursors each containing either C16:0, C18:0 or C18:1 has to be applied. Although BA and HDG provide highly valuable tools for cell culture work, it remains questionable, whether these substances are potentially capable of curing RCDP. BA treatment of the Pex7 hypomorphic mouse and of RCDP patients resulted in elevated RBC plasmalogen levels[10] (Braverman et al., 2010; Das et al., 1992). However, an appreciable relief of the symptoms has neither been achieved in mice nor in human patients. On the one hand, the reason for this could be the inability of the used precursors to cross the blood-brain barrier. For this to change, the sn-2 and sn-3 positions would have to be modified in order to increase the permeability of the applied molecules. On the other hand, a dietary alkylglycerol supplement could be subject to degradation in the liver, before it reaches peripheral tissues and restores plasmalogen levels there. The enzyme alkylglycerol monooxygenase (AGMO), which is most abundant in the liver and the small intestine (Watschinger et al., 2010), cleaves the O-alkyl-ether bond preferably in alkylglycerols with C16, C15 and C18 chains, rendering BA and HDG perfect substrates for this enzyme. In order to allow for effective long-term benefits of dietary ether lipid supplementations, it may, therefore, be necessary to bypass the activity of AGMO. This could be accomplished, for example, by the introduction of a 1′-double bond (as it is present in plasmalogens), which abolishes the activity of the monooxygenase (Taguchi and Armarego, 1998). The examination of the capability of such or a similar substance to restore plasmalogen levels and – in consequence – the application in vivo are desirable future aims.

Upon mass spectrometric phospholipid analyses of untreated and precursor (BA, HDG)-treated control and RCDP patient cells, it became apparent that the cells employ compensatory mechanisms in response to the loss and gain of ether lipids. In patient fibroblasts with hardly any plasmenylethanolamines, the level of phosphatidylethanolamine was greatly increased. In contrast, after the regeneration of plasmalogens by precursors, the amount of PE declined significantly so that the total portion of ethanolamine phospholipids was kept constant at about 25-30% of total phospholipids in every case. A similar compensatory mechanism involving PE has also been observed in CHO cells deficient in ether lipid biosynthesis (Honsho et al., 2008; Nagan et al., 1997; Nagan et al., 1998). Additionally, increased PE – together with a slight rise in sphingomyelin amount, which was not detected in RCDP fibroblasts in the course of my thesis work – accounts for a loss of PL-PEs in synaptosomes and synaptosome membrane rafts in the DAPAT knockout mouse model (Brodde,

---

[10] These results were also confirmed by a recent clinical study involving mild and severe RCDP patients (International Standard Randomized Controlled Trial Number 44820021: Alcohol supplementation in rhizomelic chondrodysplasia punctata in the Netherlands).

2009; Rodemer et al., 2003). Thus, cells apparently require a certain, predetermined proportion of ethanolamine phospholipids, which is maintained under every condition.

GPI-anchored proteins are highly important molecules for mammals, as they perform a multitude of fundamental tasks in virtually all kinds of tissues. However, in spite of extensive scientific studies, the biological function of a 1-alkyl chain in the lipid moiety of the GPI anchor, which is present in a large subset of GPI-anchored proteins, is not clear yet. Since this ether bond-containing lipid has been shown to be dependent on the peroxisomal pathway of ether lipid synthesis, now a variety of useful tools – namely model systems that are deficient in this kind of pathway – is available to study the significance of the alkyl chain. Based on the chemical nature of the GPI anchor, the assumption is obvious that the ether-containing chain might play a role in membrane anchoring of the respective proteins. Yet, the present study offers – by immunofluorescent staining methods – the first proof that in human and murine ether lipid biosynthesis-deficient cells an endogenous GPI-anchored protein can be efficiently transported to the outer surface of the plasma membrane, similar as in the respective control cells. Singh and collaborators additionally showed that, after transfection with a plasmid expressing GPI-anchored alkaline phosphatase, this protein could be detected at the surface of CHO-K1 cells, a CHO cell line deficient in peroxisomes, and in DAPAT-defective murine macrophages (Singh et al., 1994). Given that Thy-1 has been shown to at least in part contain an alkyl chain in its GPI anchor in mice and in rats (Homans et al., 1988; Jayachandran, 2007), all these results suggest that correct targeting of GPI-anchored proteins can take place even in the absence of ether lipids and that a 1-alkyl chain in the lipid moiety of the anchor is not essential for the membrane localization of these proteins. Apparently, the utilization of diacylglycerol can – at least in case of Thy-1 – fully compensate for the inability to synthesize alkylacylglycerol in terms of membrane anchorage.

Apart from membrane trafficking and anchoring, there are several other possibilities, how deficient ether lipid biosynthesis may affect GPI-anchored proteins. A further question that was addressed in my thesis was, whether the deficiency in ether lipid synthesis has any influence on the general level of GPI-anchored proteins in fibroblasts of human RCDP patients. Rodemer and collaborators reported the reduction of a GPI-anchored protein, but also of other membrane-raft-associated proteins in DAPAT-deficient mice (Rodemer et al., 2003). Therefore, there are two conceivable ways, how a defect in ether lipid synthesis might change the amounts of GPI-anchored proteins. First, the inability to integrate an alkyl chain could interfere with normal GPI-protein expression e.g. by some feedback mechanism. More likely, however, as plasmalogens have been demonstrated to be essential components of raft domains (Pike et al., 2002), these might be structurally changed upon loss of plasmalogens and – as a consequence – the stability and half life of raft proteins could be dysregulated resulting in altered total amounts of these proteins. Surprisingly, in human RCDP fibroblasts, no consistent alterations in the relative amounts of raft proteins compared with non-raft proteins were observed. Instead, individual proteins showed several changes in certain cell lines. Contrary to what had been described for the DAPAT ko mouse, in human patient fibroblasts, no decrease in the amount of flotillin-1 could be seen. Some cell lines even exhibited increased levels, as judged from western blot analysis of total cellular extracts. However, since also the amount of the non-raft protein transferrin receptor, which previously had been shown to be grossly normal in DAPAT- and AGPS-deficient human fibroblasts (Thai et al., 2001), appeared elevated, this is likely to be due to an increased membrane surface compared with other cell lines.

Discussion

The latter assumption is also supported by the fact that in membrane-enriched fractions all cell lines showed rather equal levels of flotillin-1 and transferrin receptor.

Concerning the amounts of GPI-anchored proteins, both studied proteins, Thy-1 and CD55, displayed a similar pattern; protein levels were normal, as compared to control cell lines, in mild RCDP fibroblasts. However, a severe decrease was detected in one (RCDP 2-2), but not the other (RCDP 1-2) severely deficient cell line. As this reduction does not seem to generally affect raft proteins (mind the unaltered levels of flotillin-1), this result rather suggests that the inability to synthesize alkylacylglycerol for the lipid moiety of the anchor is responsible for the dysregulated levels of GPI-anchored proteins in this specific cell line. Nevertheless, the question remains, why these changes can only be observed in one out of two cell lines derived from severe RCDP patients, especially because these two lines showed very similar levels of residual plasmalogens in mass spectrometric analyses. Seemingly, ether lipid deficiency alone is not sufficient to induce such differences, but another factor, e.g. a certain genetic modifier, is required.

In addition to GPI-anchored proteins, also the gap-junctional transmembrane protein connexin 43, which is targeted to membrane rafts as well (Schubert et al., 2002), was found to be reduced in the severely affected cell line RCDP 2-2. In contrast to the two GPI-anchored proteins, a decrease in Cx43 levels was, even if less drastical, also noticed in a second severe RCDP cell line. Interestingly, a similar depletion of Cx43 was also observed in embryonic fibroblasts derived from DAPAT knockout mice (Rodemer et al., 2003). Connexin 43 is known to play important roles in a variety of tissues, e.g. it has recently been shown to be crucial for the development of the lung (Nagata et al., 2009). However, the protein exerts its main functions in the mammalian heart, where it is the predominant connexin subtype. Cx43 is essential for normal ventricular function and the development of the heart outflow tract and is present in mammalian cardiomyocytes already in early stages of fetal development (Van Kempen et al., 1996). As a consequence, mice lacking Cx43 show a broad range of severe cardiac deficiencies and die soon after birth (Reaume et al., 1995; Ya et al., 1998). In humans, disturbances in Cx43 expression have been suggested to account for arrhythmia, a life-threatening condition of abnormal electrical activity in the heart (Poelzing and Rosenbaum, 2004). Remarkably, the patient, who cell line RCDP 2-2, showing the most severe reduction in Cx43 levels, originated from, suffered from a lethal congenital heart defect called tetralogy of Fallot (TOF) (Nimmo et al., 2010), a condition, in which Cx43 levels and distribution have been reported to be altered (Kolcz et al., 2005). Another possible connection between plasmalogen deficiency and Cx43 dysregulation is presented by Styger and collaborators: In their studies on fibroblasts derived from Zellweger patients, they observed a significant increase in number and signaling activity of β-adrenoceptors, which proved to be dependent on impaired ether lipid biosynthesis (Styger et al., 2002). Stimulation of β-adrenoceptors is known to upregulate the level of Cx43 expression (Salameh et al., 2009; Xia et al., 2009). The increase in adrenoceptor number and activity in ether lipid-deficient cells might therefore reflect an effort to compensate for the reduction of Cx43 in such cells.

Currently, it cannot be judged unambiguously, whether the reduction of Cx43 that was determined in RCDP 2-2 fibroblasts is a secondary effect of the heart defect observed in this patient, or whether plasmalogen depletion causes Cx43 deficiency, finally resulting in heart malformations. However, the fact that decreased Cx43 was also observed in DAPAT ko mouse fibroblasts and does not seem to be restricted to heart tissue, strengthens the latter hypothesis. Even if heart defects are not a fully penetrant symptom assigned to RCDP, there is a striking accumulation of RCDP patients suffering from heart disease, indicating an association between the two. In addition to Nimmo and collaborators, several other groups report RCDP cases with TOF (Akgun et al., 2010; Kazemian et al., 2009), arrhythmia (Dilli et al., 2008) and other kinds of heart lesions (Fourie, 1995; Pascolat et al.,

2003). Still, substantial knowledge about the contribution of the lack of ether lipids to these cardiac deficiencies is missing. Also, it remains unclear, why some RCDP patients develop heart defects and others do not. However, connexin 43 and associated signaling pathways may constitute a good starting point to study the role of ether lipids in heart development or functioning.

As discussed above, GPI-anchored proteins are efficiently incorporated into the membrane in spite of a deficiency in ether lipid synthesis. However, immunofluorescence studies cannot shed light on the correct localization to raft subdomains. Therefore, DRM isolation experiments were employed to examine the raft association of GPI-anchored proteins in RCDP fibroblasts and led to interesting results. Although Thy-1 mostly co-migrated with the raft marker flotillin-1 in sucrose density gradient centrifugation, it appeared to a larger extent also in fractions of slightly higher density in cells derived from both mild and severe RCDP patients. This implies that GPI-anchored proteins are still targeted to detergent-resistant membrane domains even under conditions of ether lipid deficiency, but the membrane surroundings seem somehow changed as compared to cells of healthy control patients. However, in part, this behavior was also observed for flotillin-1. Generally, the obtained results are in line with those of other groups, who did not discover any changes in DRM association of endogenous and transfected GPI-anchored proteins in ether lipid synthesis-deficient CHO cells (Honsho et al., 2008; Kanzawa et al., 2009). Both of these studies, though, conducted plain detergent extraction instead of a density gradient and thus only offer two fractions – one DRM-associated and one non-DRM fraction – in their figures. Therefore, slight changes as observed in the present experiment, are not revealed. Membrane rafts constitute highly fragile structures that can easily be disturbed by several influences like cellular aging (Inomata et al., 2006), cholesterol sequestration (Persaud-Sawin et al., 2009; Sheets et al., 1999) and others. In that respect, it is not surprising that a depletion of plasmalogens and alkylacyl-GPI anchors induces changes in these subdomains, especially in view of the fact that plasmalogens are strongly enriched in membrane rafts (Pike et al., 2002).
Similar to what was discussed above, it remains unresolved, whether the detected differences should be assigned to the changed GPI anchor lipid moiety or to the lack of plasmalogens. Targeting the first possibility, a change from alkylacylglycerol to diacylglycerol might influence the association of GPI-anchored proteins with rafts or a certain class of rafts. Apparently, the lack of alkylacylglycerol does not generally abolish the connection of GPI-anchored proteins with raft microdomains, as happens in case of shortened fatty acid chains in the lipid moiety (Benting et al., 1999). However, there are several subtypes of these domains and different raft markers are known to be targeted to one, but not the other kind of raft (Schnitzer et al., 1995; Wilson et al., 2004). The slight modification of the lipid moiety could change the affinity of a GPI-anchored protein for one or the other subtype, e.g. in this case the preference of the protein would be shifted towards a subdomain of somewhat higher density. On the other hand, the depletion of plasmalogens is very likely to cause changes in the composition and maybe also the assembly of membrane rafts, as is also hypothesized by Rodemer and collaborators based on their observations in tissues derived from the DAPAT ko mouse (Rodemer et al., 2003). Studies on plasmalogen-deficient cell and model membranes report alterations in membrane fluidity and gel-to-liquid transition (Hermetter et al., 1989; Paltauf, 1994). Similarly, in the plasmalogen-deficient fibroblasts used in this diploma thesis, a changed density of membrane rafts due to the forced modification of phospholipid composition is conceivable. A slight general change of raft microdomains would also account for the fact that not only GPI-anchored proteins, but in some cases also the raft marker flotillin-1 exhibited the shift to higher density fractions. Additionally to these considerations, several publications also record impairments in cholesterol transport and distribution in ether lipid-deficient mammalian cells (Munn et al., 2003; Rodemer et al., 2003; Thai et

Discussion

al., 2001). Whether this is a consequence of raft alterations or rather causes them, is not known. However, these observations substantiate the assumption of changes in lipid rafts due to the lack of ether lipids.

Finally, it is to notice that also a minor reduction of plasmalogen levels seems to be sufficient to cause the raft modifications observed in this study. This can be concluded from the similar floating behavior, especially of the GPI-anchored protein Thy-1, in cells affected by mild and severe ether lipid deficiency. Due to the enrichment of plasmalogens in membrane rafts, these subdomains might be more vulnerable than other parts of the membrane in case of a reduction of plasmalogens. Taken together and in view of the current literature, all obtained results point towards an important role of plasmalogens in membrane rafts. Nevertheless, further experiments are needed to confirm the proposed correlations and to elucidate the exact effect of ether lipid deficiency on these membrane domains.

In order to quantify motor deficits, which are apparent upon long-term observations in the DAPAT ko mouse, two different behavioral test paradigms, both of which are routinely used for the assessment of motor behavior, were applied. Although the results of Rotarod tests were not statistically significant, a clear trend of DAPAT ko mice to fall off the treadmill earlier than wild type controls was visible. The lack of significance can on the one hand be attributed to relatively low n-numbers (for this type of test) and high variability in the performance especially of wild type mice. On the other hand, not only motor skills, but also other factors like motivation, anxiety or general sensory abilities (smell, vision, etc.) are supposed to contribute to the performance on the Rotarod apparatus even after several training sessions. However, in combination with the balance beam experiments, which proved highly significant impairments in DAPAT ko mice, these results indicate a clear motor deficiency of ether lipid-deficient mice in comparison with wild type littermates. This is in agreement with the observations of Teigler and collaborators, who rudimentarily reported deficits of DAPAT ko mice in Rotarod and vertical pole tests. In the latter publication, though, these impairments were assigned to cerebellar abnormalities (Teigler et al., 2009). Nevertheless, there might also be other reasons accounting for a motor impairment in these mice. Several recent publications associate poor performances on either the balance beam or the Rotarod with neuromuscular dysfunction (Gomez et al., 1997; Pelkonen and Yavich, 2011; Shi et al., 2010). Thus, some defect in the formation of the neuromuscular junction (NMJ) in ether lipid-deficient mice is conceivable. In the present study, NMJ formation was examined in a cell culture model of differentiated myotubes stimulated with agrin. The number of resulting acetylcholine receptor clusters proved unchanged in myotubes derived from DAPAT ko animals as compared to wt myotubes; in contrast, size of the clusters appeared smaller in the mutants. As the results presented here, so far, refer to only one quantified experiment, it is not surprising that statistical significance was not reached. However, further experiments and optimization of myoblast cultivation will be carried out to confirm the detected changes.

Generally, the formation of the neuromuscular synapse is a highly complicated process, whose molecular basis has not been fully elucidated yet. MuSK is known to be a key player in this process, as it is able to induce or at least stabilize clustering of acetylcholine receptors, the main prerequisite for NMJ formation (Glass et al., 1996; Hoch, 2003). Mice lacking MuSK do not form neuromuscular junctions and die immediately after birth (DeChiara et al., 1996). Interestingly, two groups showed independently that, after agrin stimulation, MuSK is partitioned into membrane rafts (Stetzkowski-Marden et al., 2006; Zhu et al., 2006). Furthermore, other main components of the process, e.g. the scaffolding protein rapsyn, were identified as raft proteins and even acetylcholine receptor clustering

itself takes place in these specialized membrane domains (Pato et al., 2008; Zhu et al., 2006). Zhu and collaborators actually demonstrated that, upon disruption of rafts by the cholesterol extracting agent methyl-β-cyclodextrin or the chemical agent PDMP[11], MuSK signaling and the phosphorylation of acetylcholine receptors, which initiates cluster formation (Borges and Ferns, 2001; Wallace, 1995), are almost fully abolished (Zhu et al., 2006). Therefore, a disturbance of membrane rafts evoked by the lack of plasmalogens or altered distribution of GPI-anchored proteins might easily account for an impaired formation of the neuromuscular junction and could be the cause of the observed reduction in size of agrin-elicited acetylcholine receptor clusters in DAPAT-deficient myotubes. However, additional experiments are required to reveal the role of ether lipids in the multifactorial process of NMJ formation. In a further step, the situation in vivo, e.g. in an ether lipid-deficient mouse model, should be studied. In contrast to the myoblast culture experiments, where only the postsynaptic part of the synapse is targeted, this would also involve the presynaptic, i.e. the neuronal, side of the neuromuscular junction. To date, it is not known, how ether lipid deficiency influences innervation of the muscle. Many proteins mediating contact or signaling between nerve and muscle are associated with membrane rafts or GPI anchors – as an example, the GPI-anchored ephrin A-2 has been localized to the neuromuscular synapse (Lai and Ip, 2003). The effect of the lack of ether lipids on all these factors can only be speculated on at the moment. Finally, as an ultimate goal, possible disturbances need to be correlated with the phenotype in the respective mouse model and in human patients to identify the molecular origin of the many severe symptoms observed in RCDP.

Considering all aspects covered in the present diploma thesis, it seems very likely that an inability to synthesize ether lipids has serious consequences for membrane rafts contributing to the severe phenotype in mammals lacking these lipids. Although some of the data can be considered as preliminary, the entirety of the presented results demonstrates a key role of ether lipids in these membrane domains. However, the exact underlying mechanisms are still unclear rendering rafts under conditions of ether lipid deficiency a topic of major interest for further scientific work. Future experiments should address the questions, how raft formation, stability and functionality are affected by the lack of ether lipids. Also, the influence on individual raft proteins – with special attention to GPI-anchored proteins – has to be further clarified to ultimately elucidate the relation between membrane raft alterations and the symptoms in ether lipid-deficient individuals.

---

[11] D-threo-1-phenyl-2-decanoylamino-3-morpholino-1-propanol

CHAPTER 5

REFERENCES

Agne, B., Meindl, N.M., Niederhoff, K., Einwachter, H., Rehling, P., Sickmann, A., Meyer, H.E., Girzalsky, W., and Kunau, W.H. (2003). Pex8p: an intraperoxisomal organizer of the peroxisomal import machinery. Mol Cell 11, 635-646.

Akgun, C., Akbayram, S., Tuncer, O., Taskin, G., and Ceylan, A. (2010). Chondrodysplasia punctata associated with tetralogy of Fallot in a newborn infant. Genet Couns 21, 253-256.

Baes, M., Gressens, P., Baumgart, E., Carmeliet, P., Casteels, M., Fransen, M., Evrard, P., Fahimi, D., Declercq, P.E., Collen, D., et al. (1997). A mouse model for Zellweger syndrome. Nat Genet 17, 49-57.

Benting, J., Rietveld, A., Ansorge, I., and Simons, K. (1999). Acyl and alkyl chain length of GPI-anchors is critical for raft association in vitro. FEBS Lett 462, 47-50.

Bligh, E.G., and Dyer, W.J. (1959). A rapid method of total lipid extraction and purification. Can J Biochem Physiol 37, 911-917.

Borges, L.S., and Ferns, M. (2001). Agrin-induced phosphorylation of the acetylcholine receptor regulates cytoskeletal anchoring and clustering. J Cell Biol 153, 1-12.

Braverman, N., Chen, L., Lin, P., Obie, C., Steel, G., Douglas, P., Chakraborty, P.K., Clarke, J.T., Boneh, A., Moser, A., et al. (2002). Mutation analysis of PEX7 in 60 probands with rhizomelic chondrodysplasia punctata and functional correlations of genotype with phenotype. Hum Mutat 20, 284-297.

Braverman, N., Dodt, G., Gould, S.J., and Valle, D. (1998). An isoform of pex5p, the human PTS1 receptor, is required for the import of PTS2 proteins into peroxisomes. Hum Mol Genet 7, 1195-1205.

Braverman, N., Steel, G., Lin, P., Moser, A., Moser, H., and Valle, D. (2000). PEX7 gene structure, alternative transcripts, and evidence for a founder haplotype for the frequent RCDP allele, L292ter. Genomics 63, 181-192.

Braverman, N., Steel, G., Obie, C., Moser, A., Moser, H., Gould, S.J., and Valle, D. (1997). Human PEX7 encodes the peroxisomal PTS2 receptor and is responsible for rhizomelic chondrodysplasia punctata. Nat Genet 15, 369-376.

Braverman, N., Zhang, R., Chen, L., Nimmo, G., Scheper, S., Tran, T., Chaudhury, R., Moser, A., and Steinberg, S. (2010). A Pex7 hypomorphic mouse model for plasmalogen deficiency affecting the lens and skeleton. Mol Genet Metab 99, 408-416.

Brites, P., Motley, A., Hogenhout, E., Hettema, E., Wijburg, F., Heijmans, H.S., Tabak, H.F., Distel, B., and Wanders, R.J. (1998). Molecular basis of rhizomelic chondrodysplasia punctata type I: high frequency of the Leu-292 stop mutation in 38 patients. J Inherit Metab Dis 21, 306-308.

Brites, P., Motley, A.M., Gressens, P., Mooyer, P.A., Ploegaert, I., Everts, V., Evrard, P., Carmeliet, P., Dewerchin, M., Schoonjans, L., et al. (2003). Impaired neuronal migration and endochondral

References

ossification in Pex7 knockout mice: a model for rhizomelic chondrodysplasia punctata. Hum Mol Genet 12, 2255-2267.

Brites, P., Waterham, H.R., and Wanders, R.J. (2004). Functions and biosynthesis of plasmalogens in health and disease. Biochim Biophys Acta 1636, 219-231.

Brocard, C., and Hartig, A. (2006). Peroxisome targeting signal 1: is it really a simple tripeptide? Biochim Biophys Acta 1763, 1565-1573.

Brocard, C., Kragler, F., Simon, M.M., Schuster, T., and Hartig, A. (1994). The tetratricopeptide repeat-domain of the PAS10 protein of Saccharomyces cerevisiae is essential for binding the peroxisomal targeting signal-SKL. Biochem Biophys Res Commun 204, 1016-1022.

Brodde, A. (2009). Funktion von Etherlipiden: Die Rolle von Plasmalogenen bei der präsynaptischen Neurotransmission (Doctoral Thesis) (Heidelberg, Ruprecht-Karls-Universität).

Brown, A.J., and Snyder, F. (1982). Alkyldihydroxyacetone-P synthase. Solubilization, partial purification, new assay method, and evidence for a ping-pong mechanism. J Biol Chem 257, 8835-8839.

Brown, D.A., and London, E. (1998). Functions of lipid rafts in biological membranes. Annu Rev Cell Dev Biol 14, 111-136.

Brown, D.A., and Rose, J.K. (1992). Sorting of GPI-anchored proteins to glycolipid-enriched membrane subdomains during transport to the apical cell surface. Cell 68, 533-544.

Brugger, B., Erben, G., Sandhoff, R., Wieland, F.T., and Lehmann, W.D. (1997). Quantitative analysis of biological membrane lipids at the low picomole level by nano-electrospray ionization tandem mass spectrometry. Proc Natl Acad Sci U S A 94, 2339-2344.

Brugger, B., Graham, C., Leibrecht, I., Mombelli, E., Jen, A., Wieland, F., and Morris, R. (2004). The membrane domains occupied by glycosylphosphatidylinositol-anchored prion protein and Thy-1 differ in lipid composition. J Biol Chem 279, 7530-7536.

Brugger, B., Sandhoff, R., Wegehingel, S., Gorgas, K., Malsam, J., Helms, J.B., Lehmann, W.D., Nickel, W., and Wieland, F.T. (2000). Evidence for segregation of sphingomyelin and cholesterol during formation of COPI-coated vesicles. J Cell Biol 151, 507-518.

Burdett, K., Larkins, L.K., Das, A.K., and Hajra, A.K. (1991). Peroxisomal localization of acyl-coenzyme A reductase (long chain alcohol forming) in guinea pig intestine mucosal cells. J Biol Chem 266, 12201-12206.

Caras, I.W., Weddell, G.N., Davitz, M.A., Nussenzweig, V., and Martin, D.W., Jr. (1987). Signal for attachment of a phospholipid membrane anchor in decay accelerating factor. Science 238, 1280-1283.

Chazal, N., and Gerlier, D. (2003). Virus entry, assembly, budding, and membrane rafts. Microbiol Mol Biol Rev 67, 226-237.

Cheng, J.B., and Russell, D.W. (2004). Mammalian wax biosynthesis. I. Identification of two fatty acyl-Coenzyme A reductases with different substrate specificities and tissue distributions. J Biol Chem 279, 37789-37797.

Das, A.K., Holmes, R.D., Wilson, G.N., and Hajra, A.K. (1992). Dietary ether lipid incorporation into tissue plasmalogens of humans and rodents. Lipids 27, 401-405.

Datta, S.C., Ghosh, M.K., and Hajra, A.K. (1990). Purification and properties of acyl/alkyl dihydroxyacetone-phosphate reductase from guinea pig liver peroxisomes. J Biol Chem 265, 8268-8274.

de Vet, E.C., Ijlst, L., Oostheim, W., Dekker, C., Moser, H.W., van Den Bosch, H., and Wanders, R.J. (1999). Ether lipid biosynthesis: alkyl-dihydroxyacetonephosphate synthase protein deficiency leads to reduced dihydroxyacetonephosphate acyltransferase activities. J Lipid Res 40, 1998-2003.

de Vet, E.C., van den Broek, B.T., and van den Bosch, H. (1997). Nucleotide sequence of human alkyl-dihydroxyacetonephosphate synthase cDNA reveals the presence of a peroxisomal targeting signal 2. Biochim Biophys Acta 1346, 25-29.

DeChiara, T.M., Bowen, D.C., Valenzuela, D.M., Simmons, M.V., Poueymirou, W.T., Thomas, S., Kinetz, E., Compton, D.L., Rojas, E., Park, J.S., et al. (1996). The receptor tyrosine kinase MuSK is required for neuromuscular junction formation in vivo. Cell 85, 501-512.

Deeg, M.A., Humphrey, D.R., Yang, S.H., Ferguson, T.R., Reinhold, V.N., and Rosenberry, T.L. (1992). Glycan components in the glycoinositol phospholipid anchor of human erythrocyte acetylcholinesterase. Novel fragments produced by trifluoroacetic acid. J Biol Chem 267, 18573-18580.

Di Marzo, V. (1995). Arachidonic acid and eicosanoids as targets and effectors in second messenger interactions. Prostaglandins Leukot Essent Fatty Acids 53, 239-254.

Dilli, D., Yasar, H., Baydar, Z., Dilmen, U., Ceylaner, S., Altug, N., and Karadeniz, S. (2008). A Case of Rhizomelic Chondrodysplasia Punctata Complicated with Fetal Arrhythmia Erciyes Medical Journal 30 (4), 278-283.

Distel, B., Erdmann, R., Gould, S.J., Blobel, G., Crane, D.I., Cregg, J.M., Dodt, G., Fujiki, Y., Goodman, J.M., Just, W.W., et al. (1996). A unified nomenclature for peroxisome biogenesis factors. J Cell Biol 135, 1-3.

Dixit, E., Boulant, S., Zhang, Y., Lee, A.S., Odendall, C., Shum, B., Hacohen, N., Chen, Z.J., Whelan, S.P., Fransen, M., et al. (2010). Peroxisomes are signaling platforms for antiviral innate immunity. Cell 141, 668-681.

Dumser, M., Bauer, J., Lassmann, H., Berger, J., and Forss-Petter, S. (2007). Lack of adrenoleukodystrophy protein enhances oligodendrocyte disturbance and microglia activation in mice with combined Abcd1/Mag deficiency. Acta Neuropathol 114, 573-586.

Faust, P.L., and Hatten, M.E. (1997). Targeted deletion of the PEX2 peroxisome assembly gene in mice provides a model for Zellweger syndrome, a human neuronal migration disorder. J Cell Biol 139, 1293-1305.

Felde, R., and Spiteller, G. (1995). Plasmalogen oxidation in human serum lipoproteins. Chem Phys Lipids 76, 259-267.

Ford, D.A., and Gross, R.W. (1989). Plasmenylethanolamine is the major storage depot for arachidonic acid in rabbit vascular smooth muscle and is rapidly hydrolyzed after angiotensin II stimulation. Proc Natl Acad Sci U S A 86, 3479-3483.

References

Ford, D.A., Hazen, S.L., Saffitz, J.E., and Gross, R.W. (1991). The rapid and reversible activation of a calcium-independent plasmalogen-selective phospholipase A2 during myocardial ischemia. J Clin Invest 88, 331-335.

Fourie, D.T. (1995). Chondrodysplasia punctata: case report and literature review of patients with heart lesions. Pediatr Cardiol 16, 247-250.

Fujita, M., and Kinoshita, T. (2010). Structural remodeling of GPI anchors during biosynthesis and after attachment to proteins. FEBS Lett 584, 1670-1677.

Gaposchkin, D.P., and Zoeller, R.A. (1999). Plasmalogen status influences docosahexaenoic acid levels in a macrophage cell line. Insights using ether lipid-deficient variants. J Lipid Res 40, 495-503.

Glaser, P.E., and Gross, R.W. (1994). Plasmenylethanolamine facilitates rapid membrane fusion: a stopped-flow kinetic investigation correlating the propensity of a major plasma membrane constituent to adopt an HII phase with its ability to promote membrane fusion. Biochemistry 33, 5805-5812.

Glass, D.J., Bowen, D.C., Stitt, T.N., Radziejewski, C., Bruno, J., Ryan, T.E., Gies, D.R., Shah, S., Mattsson, K., Burden, S.J., et al. (1996). Agrin acts via a MuSK receptor complex. Cell 85, 513-523.

Godfrey, E.W., Nitkin, R.M., Wallace, B.G., Rubin, L.L., and McMahan, U.J. (1984). Components of Torpedo electric organ and muscle that cause aggregation of acetylcholine receptors on cultured muscle cells. J Cell Biol 99, 615-627.

Goldfine, H. (2010). The appearance, disappearance and reappearance of plasmalogens in evolution. Prog Lipid Res 49, 493-498.

Gomez, C.M., Maselli, R., Gundeck, J.E., Chao, M., Day, J.W., Tamamizu, S., Lasalde, J.A., McNamee, M., and Wollmann, R.L. (1997). Slow-channel transgenic mice: a model of postsynaptic organellar degeneration at the neuromuscular junction. J Neurosci 17, 4170-4179.

Goodenough, D.A., Goliger, J.A., and Paul, D.L. (1996). Connexins, connexons, and intercellular communication. Annu Rev Biochem 65, 475-502.

Gorgas, K., Teigler, A., Komljenovic, D., and Just, W.W. (2006). The ether lipid-deficient mouse: tracking down plasmalogen functions. Biochim Biophys Acta 1763, 1511-1526.

Gould, S.J., Keller, G.A., Hosken, N., Wilkinson, J., and Subramani, S. (1989). A conserved tripeptide sorts proteins to peroxisomes. J Cell Biol 108, 1657-1664.

Haeryfar, S.M., and Hoskin, D.W. (2004). Thy-1: more than a mouse pan-T cell marker. J Immunol 173, 3581-3588.

Hajra, A.K., Horie, S., and Webber, K.O. (1988). The role of peroxisomes in glycerol ether lipid metabolism. Prog Clin Biol Res 282, 99-116.

Han, X. (2005). Lipid alterations in the earliest clinically recognizable stage of Alzheimer's disease: implication of the role of lipids in the pathogenesis of Alzheimer's disease. Curr Alzheimer Res 2, 65-77.

Han, X., Holtzman, D.M., and McKeel, D.W., Jr. (2001). Plasmalogen deficiency in early Alzheimer's disease subjects and in animal models: molecular characterization using electrospray ionization mass spectrometry. J Neurochem 77, 1168-1180.

Hazen, S.L., Stuppy, R.J., and Gross, R.W. (1990). Purification and characterization of canine myocardial cytosolic phospholipase A2. A calcium-independent phospholipase with absolute f1-2 regiospecificity for diradyl glycerophospholipids. J Biol Chem 265, 10622-10630.

Hermetter, A., Rainer, B., Ivessa, E., Kalb, E., Loidl, J., Roscher, A., and Paltauf, F. (1989). Influence of plasmalogen deficiency on membrane fluidity of human skin fibroblasts: a fluorescence anisotropy study. Biochim Biophys Acta 978, 151-157.

Hoch, W. (2003). Molecular dissection of neuromuscular junction formation. Trends Neurosci 26, 335-337.

Hoefler, G., Hoefler, S., Watkins, P.A., Chen, W.W., Moser, A., Baldwin, V., McGillivary, B., Charrow, J., Friedman, J.M., Rutledge, L., et al. (1988). Biochemical abnormalities in rhizomelic chondrodysplasia punctata. J Pediatr 112, 726-733.

Homans, S.W., Ferguson, M.A., Dwek, R.A., Rademacher, T.W., Anand, R., and Williams, A.F. (1988). Complete structure of the glycosyl phosphatidylinositol membrane anchor of rat brain Thy-1 glycoprotein. Nature 333, 269-272.

Honke, K., Zhang, Y., Cheng, X., Kotani, N., and Taniguchi, N. (2004). Biological roles of sulfoglycolipids and pathophysiology of their deficiency. Glycoconj J 21, 59-62.

Honsho, M., Asaoku, S., and Fujiki, Y. (2010). Posttranslational regulation of fatty acyl-CoA reductase 1, Far1, controls ether glycerophospholipid synthesis. J Biol Chem 285, 8537-8542.

Honsho, M., Yagita, Y., Kinoshita, N., and Fujiki, Y. (2008). Isolation and characterization of mutant animal cell line defective in alkyl-dihydroxyacetonephosphate synthase: localization and transport of plasmalogens to post-Golgi compartments. Biochim Biophys Acta 1783, 1857-1865.

Houjou, T., Hayakawa, J., Watanabe, R., Tashima, Y., Maeda, Y., Kinoshita, T., and Taguchi, R. (2007). Changes in molecular species profiles of glycosylphosphatidylinositol anchor precursors in early stages of biosynthesis. J Lipid Res 48, 1599-1606.

Ikezawa, H. (2002). Glycosylphosphatidylinositol (GPI)-anchored proteins. Biol Pharm Bull 25, 409-417.

Inomata, M., Shimada, Y., Hayashi, M., Kondo, H., and Ohno-Iwashita, Y. (2006). Detachment-associated changes in lipid rafts of senescent human fibroblasts. Biochem Biophys Res Commun 343, 489-495.

Itzkovitz, B.J., Jiralerspong, S., Potti, M., Steinberg, S., and Braverman, N. (2009). Molecular Analysis of AGPS in two probands with RCDP type 3 reveals two novel alleles. In 59th Annual Meeting of the American Society of Human Genetics (Honolulu, Hawaii).

Jacobson, K., Mouritsen, O.G., and Anderson, R.G. (2007). Lipid rafts: at a crossroad between cell biology and physics. Nat Cell Biol 9, 7-14.

Jayachandran, U. (2007). Alkyl-Acyl GPI Anchor Synthesis Depends on the Peroxisomal Pathway of Ether Lipid Biosynthesis (Doctoral Thesis) (Heidelberg, Ruprecht-Karls-Universität).

Jones, C.L., and Hajra, A.K. (1977). The subcellular distribution of acyl CoA: dihydroxyacetone phosphate acyl transferase in guinea pig liver. Biochem Biophys Res Commun 76, 1138-1143.

References

Kanzawa, N., Maeda, Y., Ogiso, H., Murakami, Y., Taguchi, R., and Kinoshita, T. (2009). Peroxisome dependency of alkyl-containing GPI-anchor biosynthesis in the endoplasmic reticulum. Proc Natl Acad Sci U S A 106, 17711-17716.

Kawagoe, K., Kitamura, D., Okabe, M., Taniuchi, I., Ikawa, M., Watanabe, T., Kinoshita, T., and Takeda, J. (1996). Glycosylphosphatidylinositol-anchor-deficient mice: implications for clonal dominance of mutant cells in paroxysmal nocturnal hemoglobinuria. Blood 87, 3600-3606.

Kazemian, M., Fakhraee, S.H., Borjian, L., and Hassas Yeganeh, M. (2009). A Case of Rhizomelic Chondrodysplasia Panctata with Congenital Heart Disease. Journal of Babol University of Medical Sciences 11 (1).

Kinoshita, T., Fujita, M., and Maeda, Y. (2008). Biosynthesis, remodelling and functions of mammalian GPI-anchored proteins: recent progress. J Biochem 144, 287-294.

Koivusalo, M., Haimi, P., Heikinheimo, L., Kostiainen, R., and Somerharju, P. (2001). Quantitative determination of phospholipid compositions by ESI-MS: effects of acyl chain length, unsaturation, and lipid concentration on instrument response. J Lipid Res 42, 663-672.

Kolcz, J., Drukala, J., Bzowska, M., Rajwa, B., Korohoda, W., and Malec, E. (2005). The expression of connexin 43 in children with Tetralogy of Fallot. Cell Mol Biol Lett 10, 287-303.

Komljenovic, D., Sandhoff, R., Teigler, A., Heid, H., Just, W.W., and Gorgas, K. (2009). Disruption of blood-testis barrier dynamics in ether-lipid-deficient mice. Cell Tissue Res 337, 281-299.

Lai, K.O., and Ip, N.Y. (2003). Central synapse and neuromuscular junction: same players, different roles. Trends Genet 19, 395-402.

Lanyon-Hogg, T., Warriner, S.L., and Baker, A. (2010). Getting a camel through the eye of a needle: the import of folded proteins by peroxisomes. Biol Cell 102, 245-263.

Lazarow, P.B., and Fujiki, Y. (1985). Biogenesis of peroxisomes. Annu Rev Cell Biol 1, 489-530.

Lee, T.C., Qian, C.G., and Snyder, F. (1991). Biosynthesis of choline plasmalogens in neonatal rat myocytes. Arch Biochem Biophys 286, 498-503.

Leidich, S.D., Drapp, D.A., and Orlean, P. (1994). A conditionally lethal yeast mutant blocked at the first step in glycosyl phosphatidylinositol anchor synthesis. J Biol Chem 269, 10193-10196.

Lessig, J., and Fuchs, B. (2009). Plasmalogens in biological systems: their role in oxidative processes in biological membranes, their contribution to pathological processes and aging and plasmalogen analysis. Curr Med Chem 16, 2021-2041.

Levental, I., Grzybek, M., and Simons, K. (2010). Greasing their way: lipid modifications determine protein association with membrane rafts. Biochemistry 49, 6305-6316.

Lingwood, D., and Simons, K. (2007). Detergent resistance as a tool in membrane research. Nat Protoc 2, 2159-2165.

Lingwood, D., and Simons, K. (2010). Lipid rafts as a membrane-organizing principle. Science 327, 46-50.

Ma, C., and Subramani, S. (2009). Peroxisome matrix and membrane protein biogenesis. IUBMB Life 61, 713-722.

Mankidy, R., Ahiahonu, P.W., Ma, H., Jayasinghe, D., Ritchie, S.A., Khan, M.A., Su-Myat, K.K., Wood, P.L., and Goodenowe, D.B. (2010). Membrane plasmalogen composition and cellular cholesterol regulation: a structure activity study. Lipids Health Dis 9, 62.

Martinez, M. (1992). Abnormal profiles of polyunsaturated fatty acids in the brain, liver, kidney and retina of patients with peroxisomal disorders. Brain Res 583, 171-182.

Marzioch, M., Erdmann, R., Veenhuis, M., and Kunau, W.H. (1994). PAS7 encodes a novel yeast member of the WD-40 protein family essential for import of 3-oxoacyl-CoA thiolase, a PTS2-containing protein, into peroxisomes. EMBO J 13, 4908-4918.

Maxwell, M., Bjorkman, J., Nguyen, T., Sharp, P., Finnie, J., Paterson, C., Tonks, I., Paton, B.C., Kay, G.F., and Crane, D.I. (2003). Pex13 inactivation in the mouse disrupts peroxisome biogenesis and leads to a Zellweger syndrome phenotype. Mol Cell Biol 23, 5947-5957.

Mayor, S., and Rao, M. (2004). Rafts: scale-dependent, active lipid organization at the cell surface. Traffic 5, 231-240.

Mayor, S., and Riezman, H. (2004). Sorting GPI-anchored proteins. Nat Rev Mol Cell Biol 5, 110-120.

McMahan, U.J. (1990). The agrin hypothesis. Cold Spring Harb Symp Quant Biol 55, 407-418.

Morrow, I.C., and Parton, R.G. (2005). Flotillins and the PHB domain protein family: rafts, worms and anaesthetics. Traffic 6, 725-740.

Morrow, I.C., Rea, S., Martin, S., Prior, I.A., Prohaska, R., Hancock, J.F., James, D.E., and Parton, R.G. (2002). Flotillin-1/reggie-2 traffics to surface raft domains via a novel golgi-independent pathway. Identification of a novel membrane targeting domain and a role for palmitoylation. J Biol Chem 277, 48834-48841.

Moser, A., Moser, H., Kreiter, N., and Raymond, G.V. (1996). Life expectancy in rhizomelic chondrodysplasia punctata. Am J Hum Genet 59, A99.

Motley, A.M., Brites, P., Gerez, L., Hogenhout, E., Haasjes, J., Benne, R., Tabak, H.F., Wanders, R.J., and Waterham, H.R. (2002). Mutational spectrum in the PEX7 gene and functional analysis of mutant alleles in 78 patients with rhizomelic chondrodysplasia punctata type 1. Am J Hum Genet 70, 612-624.

Motley, A.M., Hettema, E.H., Hogenhout, E.M., Brites, P., ten Asbroek, A.L., Wijburg, F.A., Baas, F., Heijmans, H.S., Tabak, H.F., Wanders, R.J., et al. (1997). Rhizomelic chondrodysplasia punctata is a peroxisomal protein targeting disease caused by a non-functional PTS2 receptor. Nat Genet 15, 377-380.

Munn, N.J., Arnio, E., Liu, D., Zoeller, R.A., and Liscum, L. (2003). Deficiency in ethanolamine plasmalogen leads to altered cholesterol transport. J Lipid Res 44, 182-192.

Munro, S. (2003). Lipid rafts: elusive or illusive? Cell 115, 377-388.

Murphy, E.J., Huang, H.M., Cowburn, R.F., Lannfelt, L., and Gibson, G.E. (2006). Phospholipid mass is increased in fibroblasts bearing the Swedish amyloid precursor mutation. Brain Res Bull 69, 79-85.

Murphy, E.J., Schapiro, M.B., Rapoport, S.I., and Shetty, H.U. (2000a). Phospholipid composition and levels are altered in Down syndrome brain. Brain Res 867, 9-18.

References

Murphy, E.J., Zhang, H., Sorbi, S., Rapoport, S.I., and Gibson, G.E. (2000b). Phospholipid composition and levels are not altered in fibroblasts bearing presenilin-1 mutations. Brain Res Bull 52, 207-212.

Musil, L.S., Cunningham, B.A., Edelman, G.M., and Goodenough, D.A. (1990). Differential phosphorylation of the gap junction protein connexin43 in junctional communication-competent and -deficient cell lines. J Cell Biol 111, 2077-2088.

Nagan, N., Hajra, A.K., Das, A.K., Moser, H.W., Moser, A., Lazarow, P., Purdue, P.E., and Zoeller, R.A. (1997). A fibroblast cell line defective in alkyl-dihydroxyacetone phosphate synthase: a novel defect in plasmalogen biosynthesis. Proc Natl Acad Sci U S A 94, 4475-4480.

Nagan, N., Hajra, A.K., Larkins, L.K., Lazarow, P., Purdue, P.E., Rizzo, W.B., and Zoeller, R.A. (1998). Isolation of a Chinese hamster fibroblast variant defective in dihydroxyacetonephosphate acyltransferase activity and plasmalogen biosynthesis: use of a novel two-step selection protocol. Biochem J 332 (Pt 1), 273-279.

Nagan, N., and Zoeller, R.A. (2001). Plasmalogens: biosynthesis and functions. Prog Lipid Res 40, 199-229.

Nagata, K., Masumoto, K., Esumi, G., Teshiba, R., Yoshizaki, K., Fukumoto, S., Nonaka, K., and Taguchi, T. (2009). Connexin43 plays an important role in lung development. J Pediatr Surg 44, 2296-2301.

Nimmo, G., Monsonego, S., Descartes, M., Franklin, J., Steinberg, S., and Braverman, N. (2010). Rhizomelic chrondrodysplasia punctata type 2 resulting from paternal isodisomy of chromosome 1. Am J Med Genet A 152A, 1812-1817.

Nuoffer, J.M., Pfammatter, J.P., Spahr, A., Toplak, H., Wanders, R.J., Schutgens, R.B., and Wiesmann, U.N. (1994). Chondrodysplasia punctata with a mild clinical course. J Inherit Metab Dis 17, 60-66.

Orlean, P., and Menon, A.K. (2007). Thematic review series: lipid posttranslational modifications. GPI anchoring of protein in yeast and mammalian cells, or: how we learned to stop worrying and love glycophospholipids. J Lipid Res 48, 993-1011.

Paltauf, F. (1994). Ether lipids in biomembranes. Chem Phys Lipids 74, 101-139.

Paltauf, F., and Hermetter, A. (1994). Strategies for the synthesis of glycerophospholipids. Prog Lipid Res 33, 239-328.

Pascolat, G., Zindeluk, J.L., Abrao, K.C., Rodrigues, F.M., and Guedes, C.I. (2003). [Rhizomelic chondrodysplasia punctata - case report]. J Pediatr (Rio J) 79, 189-192.

Pato, C., Stetzkowski-Marden, F., Gaus, K., Recouvreur, M., Cartaud, A., and Cartaud, J. (2008). Role of lipid rafts in agrin-elicited acetylcholine receptor clustering. Chem Biol Interact 175, 64-67.

Paulick, M.G., and Bertozzi, C.R. (2008). The glycosylphosphatidylinositol anchor: a complex membrane-anchoring structure for proteins. Biochemistry 47, 6991-7000.

Pelkonen, A., and Yavich, L. (2011). Neuromuscular pathology in mice lacking alpha-synuclein. Neurosci Lett 487, 350-353.

Persaud-Sawin, D.A., Banach, L., and Harry, G.J. (2009). Raft aggregation with specific receptor recruitment is required for microglial phagocytosis of Abeta42. Glia 57, 320-335.

Pike, L.J. (2006). Rafts defined: a report on the Keystone Symposium on Lipid Rafts and Cell Function. J Lipid Res 47, 1597-1598.

Pike, L.J., Han, X., Chung, K.N., and Gross, R.W. (2002). Lipid rafts are enriched in arachidonic acid and plasmenylethanolamine and their composition is independent of caveolin-1 expression: a quantitative electrospray ionization/mass spectrometric analysis. Biochemistry 41, 2075-2088.

Platta, H.W., Girzalsky, W., and Erdmann, R. (2004). Ubiquitination of the peroxisomal import receptor Pex5p. Biochem J 384, 37-45.

Poelzing, S., and Rosenbaum, D.S. (2004). Altered connexin43 expression produces arrhythmia substrate in heart failure. Am J Physiol Heart Circ Physiol 287, H1762-1770.

Pont, S. (1987). Thy-1: a lymphoid cell subset marker capable of delivering an activation signal to mouse T lymphocytes. Biochimie 69, 315-320.

Prescott, S.M., Zimmerman, G.A., Stafforini, D.M., and McIntyre, T.M. (2000). Platelet-activating factor and related lipid mediators. Annu Rev Biochem 69, 419-445.

Purdue, P.E., Skoneczny, M., Yang, X., Zhang, J.W., and Lazarow, P.B. (1999). Rhizomelic chondrodysplasia punctata, a peroxisomal biogenesis disorder caused by defects in Pex7p, a peroxisomal protein import receptor: a minireview. Neurochem Res 24, 581-586.

Purdue, P.E., Zhang, J.W., Skoneczny, M., and Lazarow, P.B. (1997). Rhizomelic chondrodysplasia punctata is caused by deficiency of human PEX7, a homologue of the yeast PTS2 receptor. Nat Genet 15, 381-384.

Quinn, P.J. (2010). A lipid matrix model of membrane raft structure. Prog Lipid Res 49, 390-406.

Rayapuram, N., and Subramani, S. (2006). The importomer--a peroxisomal membrane complex involved in protein translocation into the peroxisome matrix. Biochim Biophys Acta 1763, 1613-1619.

Reaume, A.G., de Sousa, P.A., Kulkarni, S., Langille, B.L., Zhu, D., Davies, T.C., Juneja, S.C., Kidder, G.M., and Rossant, J. (1995). Cardiac malformation in neonatal mice lacking connexin43. Science 267, 1831-1834.

Redman, C.A., Thomas-Oates, J.E., Ogata, S., Ikehara, Y., and Ferguson, M.A. (1994). Structure of the glycosylphosphatidylinositol membrane anchor of human placental alkaline phosphatase. Biochem J 302 (Pt 3), 861-865.

Rege, T.A., and Hagood, J.S. (2006). Thy-1 as a regulator of cell-cell and cell-matrix interactions in axon regeneration, apoptosis, adhesion, migration, cancer, and fibrosis. FASEB J 20, 1045-1054.

Reiss, D., Beyer, K., and Engelmann, B. (1997). Delayed oxidative degradation of polyunsaturated diacyl phospholipids in the presence of plasmalogen phospholipids in vitro. Biochem J 323 (Pt 3), 807-814.

Rhodin, J. (1958). Electron microscopy of the kidney. Am J Med 24, 661-675.

Roberts, W.L., Myher, J.J., Kuksis, A., and Rosenberry, T.L. (1988). Alkylacylglycerol molecular species in the glycosylinositol phospholipid membrane anchor of bovine erythrocyte acetylcholinesterase. Biochem Biophys Res Commun 150, 271-277.

References

Rodemer, C., Thai, T.P., Brugger, B., Kaercher, T., Werner, H., Nave, K.A., Wieland, F., Gorgas, K., and Just, W.W. (2003). Inactivation of ether lipid biosynthesis causes male infertility, defects in eye development and optic nerve hypoplasia in mice. Hum Mol Genet 12, 1881-1895.

Rouser, G., Fkeischer, S., and Yamamoto, A. (1970). Two dimensional then layer chromatographic separation of polar lipids and determination of phospholipids by phosphorus analysis of spots. Lipids 5, 494-496.

Rudd, P.M., Morgan, B.P., Wormald, M.R., Harvey, D.J., van den Berg, C.W., Davis, S.J., Ferguson, M.A., and Dwek, R.A. (1997). The glycosylation of the complement regulatory protein, human erythrocyte CD59. J Biol Chem 272, 7229-7244.

Salameh, A., Krautblatter, S., Karl, S., Blanke, K., Gomez, D.R., Dhein, S., Pfeiffer, D., and Janousek, J. (2009). The signal transduction cascade regulating the expression of the gap junction protein connexin43 by beta-adrenoceptors. Br J Pharmacol 158, 198-208.

Schedin, S., Sindelar, P.J., Pentchev, P., Brunk, U., and Dallner, G. (1997). Peroxisomal impairment in Niemann-Pick type C disease. J Biol Chem 272, 6245-6251.

Schlossman, D.M., and Bell, R.M. (1976). Triacylglycerol synthesis in isolated fat cells. Evidence that the sn-glycerol-3-phosphate and dihydroxyacetone phosphate acyltransferase activities are dual catalytic functions of a single microsomal enzyme. J Biol Chem 251, 5738-5744.

Schlossman, D.M., and Bell, R.M. (1977). Microsomal sn-glycerol 3-phosphate and dihydroxyacetone phosphate acyltransferase activities from liver and other tissues. Evidence for a single enzyme catalizing both reactions. Arch Biochem Biophys 182, 732-742.

Schnitzer, J.E., McIntosh, D.P., Dvorak, A.M., Liu, J., and Oh, P. (1995). Separation of caveolae from associated microdomains of GPI-anchored proteins. Science 269, 1435-1439.

Schrakamp, G., Schalkwijk, C.G., Schutgens, R.B., Wanders, R.J., Tager, J.M., and van den Bosch, H. (1988). Plasmalogen biosynthesis in peroxisomal disorders: fatty alcohol versus alkylglycerol precursors. J Lipid Res 29, 325-334.

Schroeder, R., London, E., and Brown, D. (1994). Interactions between saturated acyl chains confer detergent resistance on lipids and glycosylphosphatidylinositol (GPI)-anchored proteins: GPI-anchored proteins in liposomes and cells show similar behavior. Proc Natl Acad Sci U S A 91, 12130-12134.

Schubert, A.L., Schubert, W., Spray, D.C., and Lisanti, M.P. (2002). Connexin family members target to lipid raft domains and interact with caveolin-1. Biochemistry 41, 5754-5764.

Schuck, S., Honsho, M., Ekroos, K., Shevchenko, A., and Simons, K. (2003). Resistance of cell membranes to different detergents. Proc Natl Acad Sci U S A 100, 5795-5800.

Schutgens, R.B., Bouman, I.W., Nijenhuis, A.A., Wanders, R.J., and Frumau, M.E. (1993). Profiles of very-long-chain fatty acids in plasma, fibroblasts, and blood cells in Zellweger syndrome, X-linked adrenoleukodystrophy, and rhizomelic chondrodysplasia punctata. Clin Chem 39, 1632-1637.

Shah, M.B., and Sehgal, P.B. (2007). Nondetergent isolation of rafts. Methods Mol Biol 398, 21-28.

Sheets, E.D., Holowka, D., and Baird, B. (1999). Critical role for cholesterol in Lyn-mediated tyrosine phosphorylation of FcepsilonRI and their association with detergent-resistant membranes. J Cell Biol 145, 877-887.

Shi, L., Butt, B., Ip, F.C., Dai, Y., Jiang, L., Yung, W.H., Greenberg, M.E., Fu, A.K., and Ip, N.Y. (2010). Ephexin1 is required for structural maturation and neurotransmission at the neuromuscular junction. Neuron 65, 204-216.

Simons, K., and Ikonen, E. (1997). Functional rafts in cell membranes. Nature 387, 569-572.

Sindelar, P.J., Guan, Z., Dallner, G., and Ernster, L. (1999). The protective role of plasmalogens in iron-induced lipid peroxidation. Free Radic Biol Med 26, 318-324.

Singer, S.J., and Nicolson, G.L. (1972). The fluid mosaic model of the structure of cell membranes. Science 175, 720-731.

Singh, H., Beckman, K., and Poulos, A. (1993). Exclusive localization in peroxisomes of dihydroxyacetone phosphate acyltransferase and alkyl-dihydroxyacetone phosphate synthase in rat liver. J Lipid Res 34, 467-477.

Singh, N., Zoeller, R.A., Tykocinski, M.L., Lazarow, P.B., and Tartakoff, A.M. (1994). Addition of lipid substituents of mammalian protein glycosylphosphoinositol anchors. Mol Cell Biol 14, 21-31.

Smart, E.J., Ying, Y.S., Mineo, C., and Anderson, R.G. (1995). A detergent-free method for purifying caveolae membrane from tissue culture cells. Proc Natl Acad Sci U S A 92, 10104-10108.

Stafforini, D.M., McIntyre, T.M., Zimmerman, G.A., and Prescott, S.M. (2003). Platelet-activating factor, a pleiotrophic mediator of physiological and pathological processes. Crit Rev Clin Lab Sci 40, 643-672.

Steinberg, S.J., Dodt, G., Raymond, G.V., Braverman, N.E., Moser, A.B., and Moser, H.W. (2006). Peroxisome biogenesis disorders. Biochim Biophys Acta 1763, 1733-1748.

Stetzkowski-Marden, F., Recouvreur, M., Camus, G., Cartaud, A., Marchand, S., and Cartaud, J. (2006). Rafts are required for acetylcholine receptor clustering. J Mol Neurosci 30, 37-38.

Stoll, C., Dott, B., Roth, M.P., and Alembik, Y. (1989). Birth prevalence rates of skeletal dysplasias. Clin Genet 35, 88-92.

Styger, R., Wiesmann, U.N., and Honegger, U.E. (2002). Plasmalogen content and beta-adrenoceptor signalling in fibroblasts from patients with Zellweger syndrome. Effects of hexadecylglycerol. Biochim Biophys Acta 1585, 39-43.

Swinkels, B.W., Gould, S.J., Bodnar, A.G., Rachubinski, R.A., and Subramani, S. (1991). A novel, cleavable peroxisomal targeting signal at the amino-terminus of the rat 3-ketoacyl-CoA thiolase. EMBO J 10, 3255-3262.

Taguchi, H., and Armarego, W.L. (1998). Glyceryl-ether monooxygenase [EC 1.14.16.5]. A microsomal enzyme of ether lipid metabolism. Med Res Rev 18, 43-89.

Teigler, A., Komljenovic, D., Draguhn, A., Gorgas, K., and Just, W.W. (2009). Defects in myelination, paranode organization and Purkinje cell innervation in the ether lipid-deficient mouse cerebellum. Hum Mol Genet 18, 1897-1908.

Thai, T.P., Heid, H., Rackwitz, H.R., Hunziker, A., Gorgas, K., and Just, W.W. (1997). Ether lipid biosynthesis: isolation and molecular characterization of human dihydroxyacetonephosphate acyltransferase. FEBS Lett 420, 205-211.

References

Thai, T.P., Rodemer, C., Jauch, A., Hunziker, A., Moser, A., Gorgas, K., and Just, W.W. (2001). Impaired membrane traffic in defective ether lipid biosynthesis. Hum Mol Genet 10, 127-136.

Ueda, Y., Yamaguchi, R., Ikawa, M., Okabe, M., Morii, E., Maeda, Y., and Kinoshita, T. (2007). PGAP1 knock-out mice show otocephaly and male infertility. J Biol Chem 282, 30373-30380.

Van Kempen, M.J., Vermeulen, J.L., Moorman, A.F., Gros, D., Paul, D.L., and Lamers, W.H. (1996). Developmental changes of connexin40 and connexin43 mRNA distribution patterns in the rat heart. Cardiovasc Res 32, 886-900.

Wallace, B.G. (1995). Regulation of the interaction of nicotinic acetylcholine receptors with the cytoskeleton by agrin-activated protein tyrosine kinase. J Cell Biol 128, 1121-1129.

Walter, E.I., Roberts, W.L., Rosenberry, T.L., Ratnoff, W.D., and Medof, M.E. (1990). Structural basis for variations in the sensitivity of human decay accelerating factor to phosphatidylinositol-specific phospholipase C cleavage. J Immunol 144, 1030-1036.

Wanders, R.J., Dekker, C., Hovarth, V.A., Schutgens, R.B., Tager, J.M., Van Laer, P., and Lecoutere, D. (1994). Human alkyldihydroxyacetonephosphate synthase deficiency: a new peroxisomal disorder. J Inherit Metab Dis 17, 315-318.

Wanders, R.J., Schumacher, H., Heikoop, J., Schutgens, R.B., and Tager, J.M. (1992). Human dihydroxyacetonephosphate acyltransferase deficiency: a new peroxisomal disorder. J Inherit Metab Dis 15, 389-391.

Wanders, R.J., and Waterham, H.R. (2006a). Biochemistry of mammalian peroxisomes revisited. Annu Rev Biochem 75, 295-332.

Wanders, R.J., and Waterham, H.R. (2006b). Peroxisomal disorders: the single peroxisomal enzyme deficiencies. Biochim Biophys Acta 1763, 1707-1720.

Wanders, R.J.A., and Brites, P. (2010). Biosynthesis of ether-phospholipids including plasmalogens, peroxisomes and human disease: new insights into an old problem. Clin Lipidol 5, 379-386.

Watschinger, K., Keller, M.A., Golderer, G., Hermann, M., Maglione, M., Sarg, B., Lindner, H.H., Hermetter, A., Werner-Felmayer, G., Konrat, R., et al. (2010). Identification of the gene encoding alkylglycerol monooxygenase defines a third class of tetrahydrobiopterin-dependent enzymes. Proc Natl Acad Sci U S A 107, 13672-13677.

White, A.L., Modaff, P., Holland-Morris, F., and Pauli, R.M. (2003). Natural history of rhizomelic chondrodysplasia punctata. Am J Med Genet A 118A, 332-342.

Williams, A.F., and Gagnon, J. (1982). Neuronal cell Thy-1 glycoprotein: homology with immunoglobulin. Science 216, 696-703.

Wilson, B.S., Steinberg, S.L., Liederman, K., Pfeiffer, J.R., Surviladze, Z., Zhang, J., Samelson, L.E., Yang, L.H., Kotula, P.G., and Oliver, J.M. (2004). Markers for detergent-resistant lipid rafts occupy distinct and dynamic domains in native membranes. Mol Biol Cell 15, 2580-2592.

Wilson, G.N., Holmes, R.G., Custer, J., Lipkowitz, J.L., Stover, J., Datta, N., and Hajra, A. (1986). Zellweger syndrome: diagnostic assays, syndrome delineation, and potential therapy. Am J Med Genet 24, 69-82.

Xia, Y., Gong, K.Z., Xu, M., Zhang, Y.Y., Guo, J.H., Song, Y., and Zhang, P. (2009). Regulation of gap-junction protein connexin 43 by beta-adrenergic receptor stimulation in rat cardiomyocytes. Acta Pharmacol Sin 30, 928-934.

Ya, J., Erdtsieck-Ernste, E.B., de Boer, P.A., van Kempen, M.J., Jongsma, H., Gros, D., Moorman, A.F., and Lamers, W.H. (1998). Heart defects in connexin43-deficient mice. Circ Res 82, 360-366.

Yang, H.C., Farooqui, A.A., and Horrocks, L.A. (1996). Plasmalogen-selective phospholipase A2 and its role in signal transduction. J Lipid Mediat Cell Signal 14, 9-13.

Zemski Berry, K.A., and Murphy, R.C. (2004). Electrospray ionization tandem mass spectrometry of glycerophosphoethanolamine plasmalogen phospholipids. J Am Soc Mass Spectrom 15, 1499-1508.

Zhu, D., Xiong, W.C., and Mei, L. (2006). Lipid rafts serve as a signaling platform for nicotinic acetylcholine receptor clustering. J Neurosci 26, 4841-4851.

Zoeller, R.A., Grazia, T.J., LaCamera, P., Park, J., Gaposchkin, D.P., and Farber, H.W. (2002). Increasing plasmalogen levels protects human endothelial cells during hypoxia. Am J Physiol Heart Circ Physiol 283, H671-679.

Zoeller, R.A., Morand, O.H., and Raetz, C.R. (1988). A possible role for plasmalogens in protecting animal cells against photosensitized killing. J Biol Chem 263, 11590-11596.

ACKNOWLEDGEMENTS

CURRICULUM VITAE:

Personal Data:

Name: Fabian Dorninger

Date of Birth: July 3, 1986

Place of Birth: Linz, Austria

Citizenship: Austrian

City of Residence: Vienna, Austria

Education:

1992 – 1996: Primary school (VS 30), Linz, Austria

1996 – 2004: Secondary school (Akademisches Gymnasium Linz), Linz, Austria

June 2004: Graduation with distinction

since October 2005: Studies of molecular biology, University of Vienna, Austria

since November 2009: Diploma thesis at the Section for Pathobiology of the Nervous System, Center for Brain Research, Medical University of Vienna, Austria